VAN DER MERWE, JEANETTE

EVALUATION OF METHODS FOR THE DETERMINATION OF TRACE AMOUNTS OF PHOSPHATES BY MEANS OF FLOW INJECTION SYSTEMS

MSc UP 1996

Evaluation of methods for the determination of trace amounts of phosphates by means of flow injection systems

by

Jeanette van der Merwe

Represented to partially fulfil the demands of the degree

MASTER OF SCIENCE
in the faculty of Science,
University of Pretoria
Pretoria
November 1996

Evaluation of methods for the determination of trace amounts of phosphates by means of flow injection systems

J van der Merwe

Evaluering van metodes vir die bepaling van spoorhoeveelhede fosfate deur middel van 'n vloei - inspuitsisteem

deur

Jeanette van der Merwe

Studieleier : Professor Jacobus F. van Staden

Departement Chemie,

Universiteit van Pretoria

Graad : Magister Scientiae

SAMEVATTING

'n Kort inleiding aangaande die voordele van vloei - inspuitanalise, die goeie punte van die gemodifiseerde simpleks optimiseringsmetode en die belangrikheid van die analise van fosfate op lae vlak word gegee. Teoretiese agtergrond word verskaf vir vloei - inspuitanalise, optimisering en die analise van fosfate. Die faktor en gemodifiseerde simpleks optimisering van faktore asook die evaluering van drie verskillende fotometriese metodes van fosfaatanalise met behulp van vloei - inspuitanalise is ondersoek.

Evaluation of methods for the determination of trace amounts of phosphates by means of a flow injection system.

by

Jeanette van der Merwe

Study leader : Professor Jacobus F. van Staden

Department of Chemistry

University of Pretoria

Degree : Master of Science

SYNOPSIS

A short introduction regarding the advantages of flow injection analysis, the merits of the modified simplex optimisation technique and the importance of the analysis of phosphates at low levels are given. Theoretical background is given for flow injection analysis, optimisation and the analysis of phosphates. The modified simplex optimisation of factors and the evaluation of three different photometric methods of phosphate analysis with the aid of flow injection analysis are investigated.

Acknowledgements

Hereby the author wants to express her gratitude towards:

- professor JF van Staden, her study leader, for his aid during the research and with the writing of this thesis,

- the analytical group at MINTEK, under the leadership of Graham Marshall, for their aid with the operation and installation of the FlowTEK program and for their council during the execution of the experimental work,

- Andre Scholtz, Jaco Louw and Dawid van der Merwe for the typing and graphical illustration of the thesis,

- friends and family for their aid and encouragement during the project.

CONTENTS

CHAPTER 1

INTRODUCTION

At this point in time the availability of capital in the industry in South - Africa is severely limited. This is especially true for quality control and routine analytical laboratories in factories. They are considered to be non - profitable and have to give a service with low expenditure to the particular company. Thus to cut the costs, laboratories are usually understaffed with unqualified personnel, so that automation of an inexpensive and simple kind is necessary. This environment makes flow injection analysis an ideal method of analysis.

In the industry, which is ever expanding and adapting itself to meet the changing needs of its clients it is sometimes necessary to be able to design accurate and repeatable routine analytical methods and implement them within days. If a laboratory fails in providing such methods, profits and market share will be lost.

Flow injection analysis (FIA) is also ideally suited for quick method development and implementation due to the inherent flexibility of the technique.

Therefore the possibilities of FIA, its adaption to different methods and the optimization of any particular method for a specific characteristic e.g. sensitivity in a particular concentration range, were investigated.

The field of study that was chosen was the analysis of very low concentrations of phosphate in water. Water was chosen as the environment of study because it is a resource that is necessary to sustain life. In South - Africa water is a limited resource and many of these water resources are heavily polluted. Phosphate is generally considered to be a limiting element in the growth of living organisms in water. The level of phosphate concentration above which biological growth starts is thought to be 20 $\mu g.kg^{-1}$ P [1]. This means that the level of phosphate concentration in waste water and treated sewage water that are replaced in aquatic environments such as rivers, dams and oceans, should be monitored closely, so that the level of phosphate concentration is not raised above the level at which biological growth becomes possible. This growth is undesirable because it depletes the water of oxygen which cause fish to die and can also cause problems with the water flow in dams. Organisms that can cause diseases in humans and animals also multiply in water under these conditions.

Three different methods for the analysis of phosphate at low concentrations were investigated .

They were:

1: The reduction of molybdenum blue (a complex formed between phosphate and a molybdenum reagent in acidic conditions) by stannous chloride

2: The reduction of molybdenum blue by ascorbic acid with potassium antimony tartrate as catalyst

3: The complexation of molybdenum blue by malachite green.

The reaction products in all the methods are measured photometrically. This is one of the reasons why these three methods were chosen. A photometric method has the advantage that a filter, lightsource and photomultiplier can be used instead of the expensive spectrophotometer. Advantages of these methods are that they require inexpensive and readily available chemicals, they require no sophisticated knowledge and make use of equipment that need little maintenance.

Thus, instead of expensive equipment and intricate procedures, modified simplex optimization together with basic flow injection and spectrophotometric equipment were used to obtain low detection limits of phosphate.

In order to achieve the lowest possible detection limit for a specific method an optimum combination of physical and chemical factors is needed. Of all the

optimization techniques available, the modified simplex optimization technique was the most suitable. This method needs less experiments than the one - factor - at - a - time and the factorial design methods. The responses also do not need to be statistically verified. If the response surface contains a ridge it is less likely to give false optima, which are possible with one - factor - at - a - time - methods and with the original simplex method. The modified simplex method makes use of simple calculations unlike those of the steepest ascent procedure or Evolutionary Operation [2]. Programs for the modified simplex optimization method are also available.

Of all the factors that could interfere with the accurate analysis of orthophosphate, only three were studied.

They were:

- the presence of the $P_2O_5^{4-}$ - ion in samples.
- the presence of the Hg^{2+} - ion in samples
- the pH of the samples

$P_2O_5^{4-}$ was investigated because the possibility exist that it could hydrolyze to PO_4^{3-} under the conditions of low pH and high temperature of the reactions. It would be valuable to know if only orthophosphate (PO_4^{3-}) was being determined or if other forms of P was being determined together with orthophosphate. Hg^{2+} was being investigated as a possible interference because it is sometimes used as a preservative for water samples. The effect of pH was tested to see if extra

steps in the analytical procedure might be necessary to adjust pH before samples can be analyzed.

These methods were not developed with the idea of marketing them, but with the aim of investigating the possibilities of FIA together with certain optimization techniques that could be used to determine certain ions at very low levels of concentration.

1.1 Bibliography

1. Boltz DF, Howell JA (1987) **A Volume in Chemical Analysis: A series of Monographs on Analytical Chemistry and its Applications, Volume 8, Second Edition.** Wiley-Interscience. New York.

2. Deming SN, Morgan SL (1973) **Anal. Chem. 45:** 278A

CHAPTER 2

THEORETICAL BACKGROUND ON FLOW INJECTION ANALYSIS

2.1 Introduction

The term continuous flow analysis (FIA) refers to analytical procedures in which the analyte concentration is measured without stopping the flow of a gas or liquid [1].

Flow injection analysis is an unsegmented continuous flow analysis concept. It is based on the injection of a liquid sample into a flowing carrier stream containing a suitable reagent. The injected sample forms a zone which during its transport towards a detector, disperses and reacts with the components of the carrier stream. The shape and magnitude of the resulting recorded peak reflects the concentration of the injected analyte along with kinetic and thermodynamic information of the chemical reactions taking place in the flowing stream [2].

The essential features of FIA is the following:

i) The sample is injected (or inserted) into the flow (instead of being aspirated)

ii) Controlled dispersion of the injected sample zone

iii) Reproducible timing (because neither physical nor chemical equilibrium has been attained when the signal is detected) [3]

2.2 The components of the FIA system

2.2.1 Introduction

The FIA system consist of a propelling system, an injection system, a transport and reaction system, a detection system and some kind of recording system. Figure 2.1 is a graphical representation of the components of a FIA system.

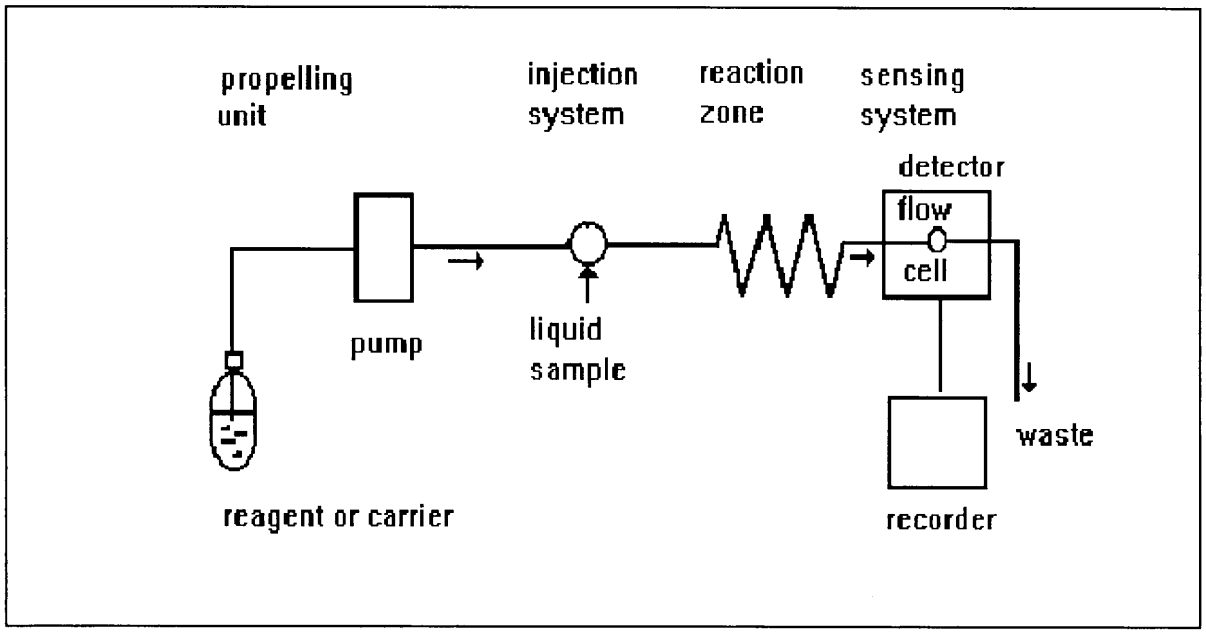

Figure 2.1 A graphical representation of the components of a FIA system

2.2.2 The propelling system

The propelling system, used to move the fluid along an FIA manifold should meet the requirements dictated by the characteristics of the FIA technique. Ideally the flow rate should be constant and perfectly reproducible in order to give a predictable residence time and a constant dispersion throughout the manifold. The flow should be pulse free. If pulses are unavoidable they should be well damped by the use of a suitable attenuator. The propelling unit can be placed at various points in the FIA system. It is usually placed before the injection system, though sometimes it is placed after the injection system for improved pulse damping. Propelling units available are peristaltic pumps, or systems in which gas pressure, a hydrostatic head or a motor driven piston burette drives the fluid through the system.

Peristaltic pumps are mostly used in FIA. A set of rollers simultaneously squeezes a number of flexible tubes arranged at right angles to the rollers, so that the successive flexions of the tubes forces various fluids through the tubes. The peristaltic pump does not offer a pulse free flow. The pulse can be dampened by inserting a damping system such as a long flexible tube after the pump through which the carrier circulates before the sample is injected, or by recirculating the waste through the pump. The tubes are made from various materials, the properties of which make them suitable for use with a specified

range of fluids [1]. For example, tygon tubing cannot be used to pump acetone, a pump tube made from natural rubber should be used.

2.2.3 The injection system

The injection system should place a volume of sample solution as a plug into the carrier stream in a reproducible manner without disturbing the flow. The sample volume injected should be adjustable. Sample withdrawal systems used in segmented flow systems is unsatisfactory since they can result in sample volume fluctuations of 3 - 4 %. This variation is not significant in continuous segmented flow analysis in which the detection reaction usually reaches equilibrium and the sample volume effects peak width rather than peak height. Although injection systems are currently the least numerous, they were the most extensively employed in the early stages of development of FIA. Therefore it is common to speak of flow injection or injection valves even though the sample is not introduced into the carrier stream by injection, but rather by the use of a carrier fluid to sweep out the solution held in a portion of tubing [1].

The type of injection system that was used in this research is the rotary valve. Figure 2.2 is an illustration of a typical valve in the filling position (i) and in the emptying position (ii). In the filling mode, the sample enters the valve through port 2, fills the loops between ports 1 and 4 and goes to waste through port 3. At the same time the carrier stream enters the valve through port 6 and passes out

through port 5. In the emptying mode, port 6, through which the carrier enters the valve, is connected internally with port 1, sweeping the sample plug towards the detector through ports 4 and 5, while the sample flows into the valve through port 2 and is sent to waste through port 3.

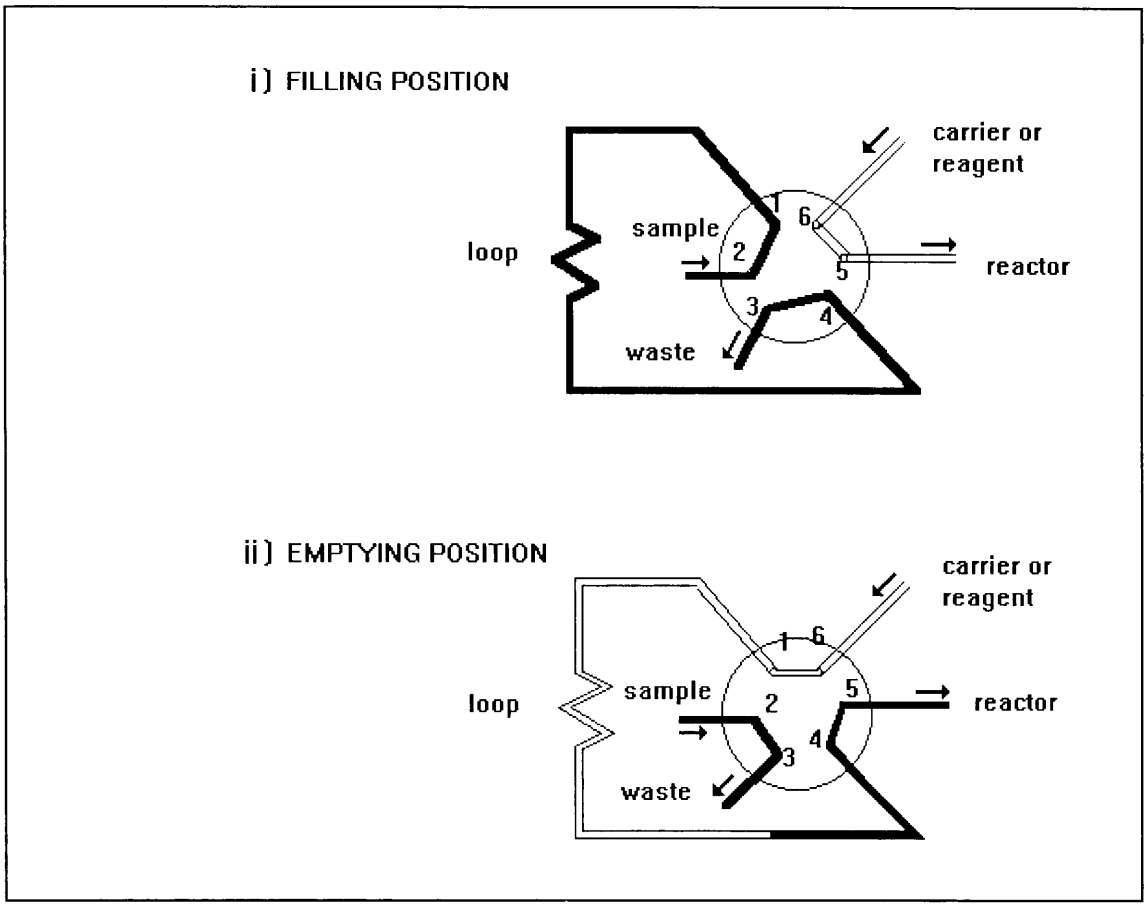

Figure 2.2 An illustration of an injection system in the filling position (i) and in the emptying position (ii)

This type of valve gives high reproducibility in injected volume, rapidity and easy manual operation as well as automation.

2.2.4 Transport and reaction systems

The components of the transport and reaction systems are intended both to carry the flowing stream along the manifold (allowing a potential reaction to develop to a suitable extent) and to interconnect the various parts making up the working system.

2.2.4.1 Tubing

Transport tubing are made from small bore tubing, the diameter being 0.1 to 2 mm. The material from which the tubing is made should be chemically inert and insensitive to temperature change. Teflon, polyethylene and polypropylene are most commonly used, but they are permeable to oxygen which is a problem when strong reductants are used or air - catalyzed oxidations are used. Teflon and polyethylene might cause problems when used in certain determinations requiring low detection limits because of the potential contamination introduced by peroxides and oxidants from these materials [1].

2.2.4.2 Connectors

The pieces of tubing are connected to one another and to the different components of the system by means of connectors. Connectors can be teflon or perspex blocks into which several holes were drilled and threaded. A threaded

fitting connects one of the ends of a piece of tubing to the block. The distance between the ends of the tubes brought together by the connector should be as small as possible in order to minimize dead volume, since this acts as a small mixing chamber, resulting in increased tailing. Aged or heat - damaged tubing might not fit so securely to connectors and can cause leakages. Connectors are employed both for merging and splitting of streams.

2.2.4.3 Reactors

Reactors are units of the transport system acting on the residence time and the sample plug and endowing the sample plug with the required characteristics for measurement by the detection unit. A reactor can simply be a length of tubing located between the injection and sensing units. It can also be tubing helically wounded around a cylinder, the diameter of the cylinder determining the size of the coils. The reactor can also be a length of tubing filled with chemically inert or active material, then called a packed reactor. The chemically active material can be ion exchange resins, oxidants or reductants and enzymes. Higher pressures are required when such reactors are used due to the higher flow resistance [1].

When slow reactions must be used, the necessary long tubes and therefore greater dispersion leads to loss of sensitivity and / or loss of sampling frequency. This problem is solved by the use of a single bead string reactor. This is a tube with a string of glass beads (diameter 70 % of the inner diameter of the tube)

that results in low dispersion so that the length of the tube and thus the residence time can be chosen on the basis of reaction time required without the substantial loss of signal height and / or sampling frequency [4].

2.2.5 The detection system

The type of detector used in an analysis will be decided by the analyte, the detection limit of the instrument, the size of the instrument, the speed of analysis, the linearity of response over a wide concentration range and the budget.

Electrochemical, optical and enthalphimetric detectors can be used in conjunction with FIA. Optical detectors are by far the most frequently used in FIA because of the large number of species which may be monitored, either because of their intrinsic optical properties or because of optical properties introduced by reaction with a suitable substance. Photometry is the most widely used technique among optical methods. It is also the most important technique in FIA, owing to the large number of selective color forming reactions available for almost every type of compound or element. It is also the technique of detection used in this research. The sensing capacity of the photometric instrument, the noise and the light source instability are limiting factors in these methods.

In FIA the photometric cell is a flow cell. This is a U - shaped cell, illustrated in figure 2.3, and is made of silica and special optical glass (depending on the

spectral region covered), with blackened walls, carrying slits on opposite faces for the light beams to pass through.

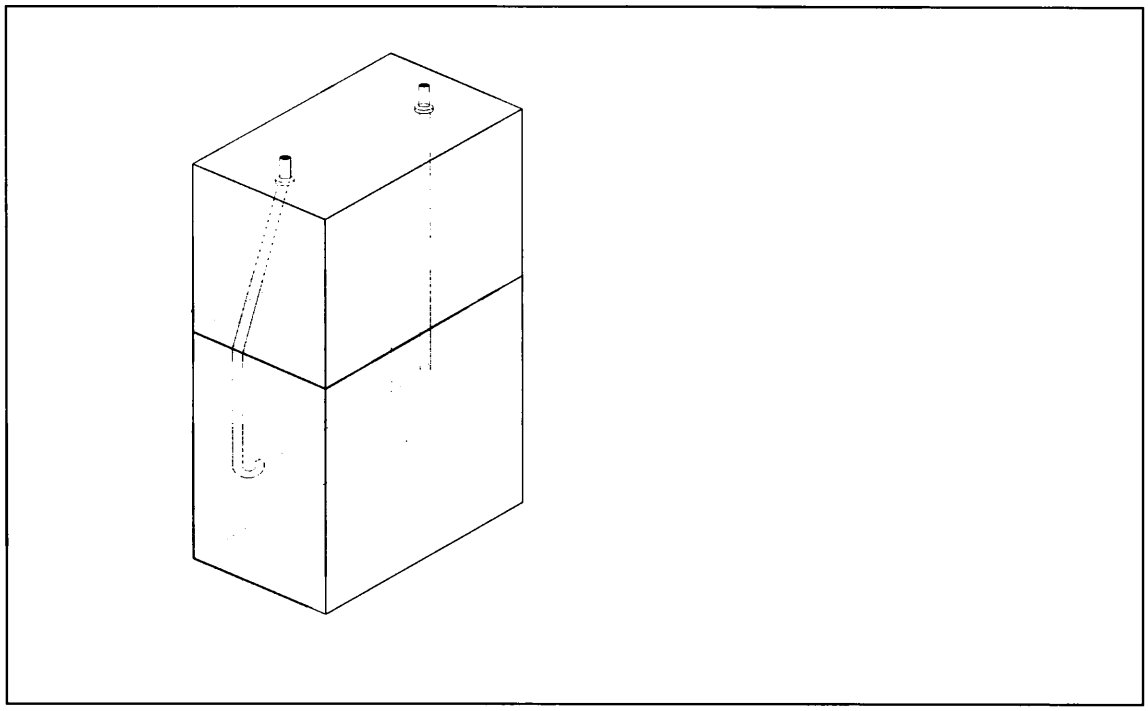

Figure 2.3 Illustration of a U - shaped flow cell

2.3 The FIA signal

The detector transduces some time-dependent property of the analyte into a continuous signal, which is commonly recorded as a peak on a recorder or microcomputer. Figure 2.4 shows the analytical signal as a function of time.

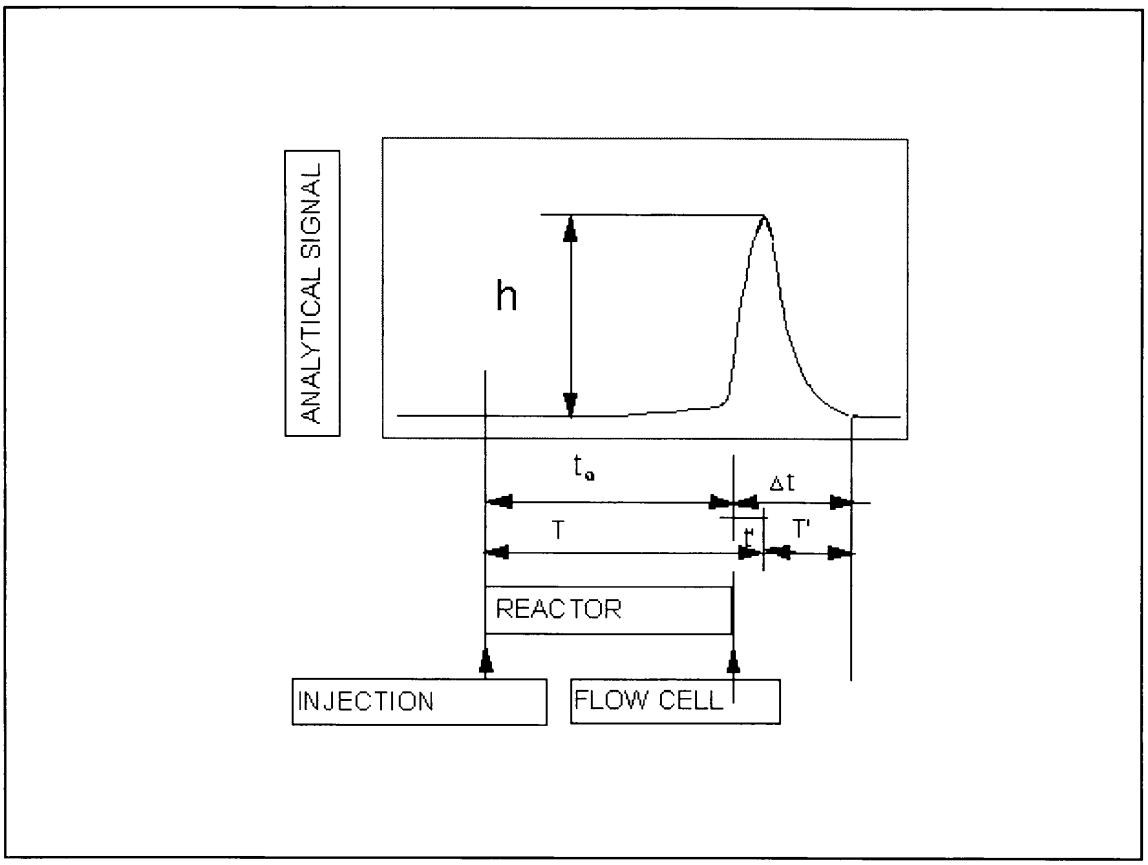

Figure 2.4 The analytical signal as a function of time

The essential features are as follows:

i) Peak height (h), which is related to the concentration of the component determined in the injected sample.

ii) Residence time (T), which is defined as the time elapsed from injection until the maximum signal is attained.

iii) Travel time (t_a), which is the period elapsed from injection to the start of the signal (1 - 2 % increase above baseline).

iv) Return time (T'), which is the period between the appearance of the maximum signal and the return to baseline.

v) Baseline - to - baseline - time (Δt), which is defined as the interval between the start of the signal and its return to the baseline. This parameter is a measure of the dispersion of the system.

The FIA signals are not Gaussian curves and therefore these parameters do not completely define the profile of the peak especially as regards its tail.

2.4 Partial dispersion as a foundation of FIA

2.4.1 General theoretical considerations

The physical foundations of FIA are related to dispersion, which is defined as the dilution undergone by a sample volume injected into the flowing stream. The dispersion is characterized by the concentration profile adopted by a zone or plug inserted into the system without stopping the flow. The analytical signal is representative of the dispersion and can be used to assess the extent of the dispersion [1].

It was first thought that the parabolic flow profile typical of laminar flow (the type of flow in the tubes) would result in rapid peak broadening and that turbulent flow was necessary for efficient mixing. The contradicting experimental fact that dilution decreased with decreasing pumping rates drew attention to the beneficial characteristics of laminar flow in FIA. The advantage of laminar flow is that it can provide a well defined sample zone, reduce reagent consumption and eliminate

the need for high pumping pressure [5]. Figure 2.5 is an illustration of turbulent and laminar flow.

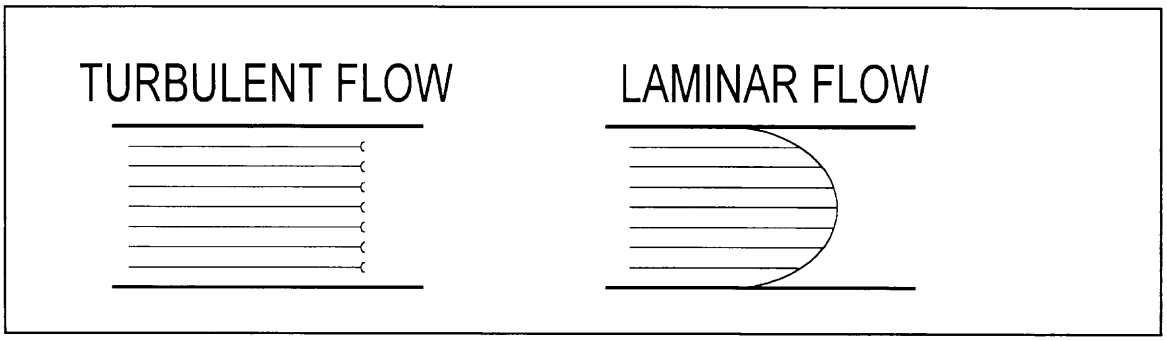

Figure 2.5 Turbulent and laminar flow

The mechanics contributing to the dispersion of the injected sample:

i) Convective transport, which is mass transfer by movement of the system as a whole [5]. This yields a parabolic velocity profile with sample molecules at the tube walls having zero linear velocity and those at the center of the tube having twice the average velocity. This impact can be serious because all measurements are made under non - equilibrium conditions.

ii) Diffusional transport which is the spontaneous process of concentration equalization [5] in the convective transport regime and consists out of axial and radial diffusion, illustrated in figure 2.6.

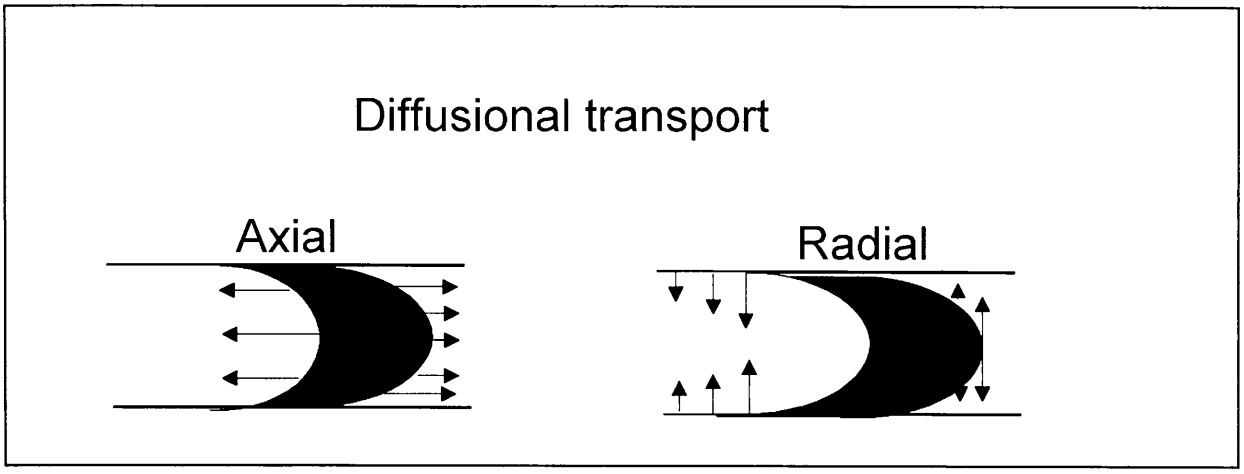

Figure 2.6 Illustration of axial and radial diffusion

Axial diffusion which is due to horizontal concentration gradients at the leading and trailing edges of the injected sample zone, contributes insignificantly to the overall dispersion, whereas radial diffusion, resulting from concentration differences perpendicular to the direction of the flow, makes an important contribution to the overall dispersion [5].

If the flow is considered to be made up of a large number of superimposed fluid cylinders traveling consecutively at different speeds, radial diffusion tends to balance concentrations in such a manner that the molecules located at the tube walls tend to move to the center, whereas those at the center travels outwards. This process is the main reason that every sample injected maintains its integrity. This motion slows down convective transport, thus hindering progressive dilution of the zone in the carrier stream [1].

iii) A third type of transport originates from density gradients but its contribution to the final dispersion is rather small since density differences between the fluid and the sample zone are generally negligible [1].

Chemical reaction can alter these forms of transport [5].

The concentration profile of a sample zone injected into a flowing stream is time dependent, as are the contributions of the various types of transport. Four different situations, together with the corresponding signals which would be obtained by detection, at different times after injection, is depicted sequentially in figure 2.7.

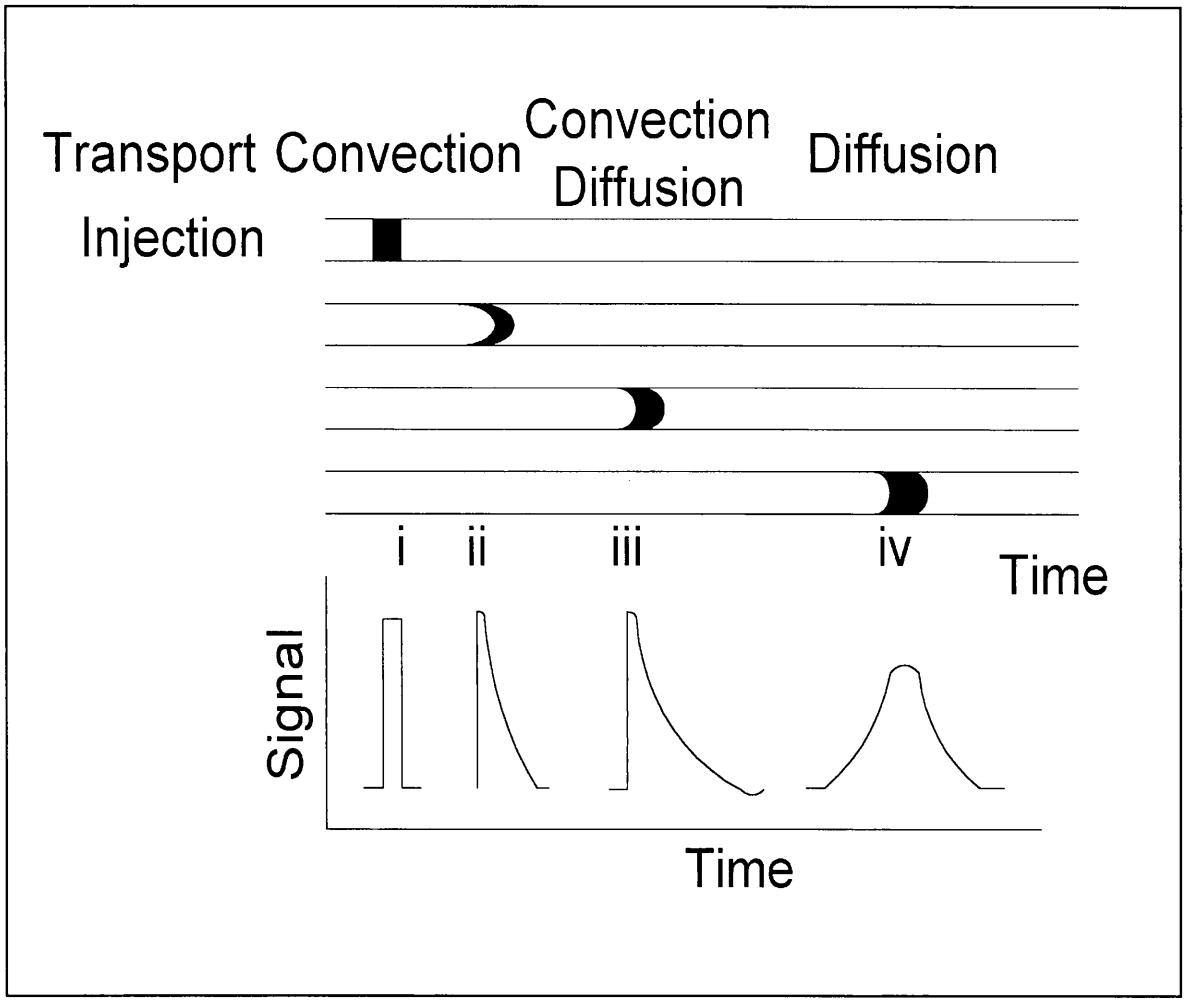

Figure 2.7 Appearance of the sample plug and corresponding signals obtained at different times after injection

Situation i) No dispersion occurs when the sample is inserted into the carrier stream. The corresponding profile is rectangular in shape. This never occurs in practice in FIA.

Situation ii) Immediately after injection convective transport is the prevailing mode of transport. The zone profile is parabolic. The recorded signal is a curve consisting of an initial vertical portion corresponding to the emergence of the molecules at the head of the parabola and a tail corresponding to the retarded portion of the sample. The parabola head travels at twice the mean velocity and therefore the travel time is given by:

$t_a = L/(2\bar{u})$

where L is the overall tube length (cm) and

$\bar{u}$ is the mean velocity ($cm.sec^{-2}$).

t_a is very short and coincides with the residence time (T). This means that t', being (Δt - T'), is zero.

$\bar{t}_r = \tau_r R^2/D$ and

$t_a = \bar{t}_r/2$,

where $\bar{t}_r$ is the mean residence time,

τ_r is the reduced mean residence time,

D is the molecular diffusion and

R is the tube radius.

For $D = 10^{-5}\ cm^2.sec^{-1}$,

R = 0.025 cm and

τ_r = 0.004,

$\bar{t}_r$ is 0.255 seconds and t_a is 0.13 seconds. This would be rather unusual under ordinary working conditions in FIA.

Situation iii) After a short time interval the contribution made by diffusion, especially of the radial type, becomes significant and competes with convective transport. The progress of the center of the injected zone is slowed down relative to the trailing portion. Both phenomena occurs simultaneously. The signal has a nearly vertical portion with a significant t' and a tail marking the return to baseline. Such profiles corresponds to reduced mean residence times of between 0.1 and 0.6 and hence for travel times from 3.12 to 18 seconds.

Situation iv) If the travel time is long enough, the contribution of radial diffusion may exceed that of convective transport. The profile of the injected zone is then much more compact, although the distortion due to the higher linear velocity of the molecules at the center of the tube is still present. The signal peak shape is practically Gaussian and therefore fulfills the condition that the time needed to pass through the detector (Δt) is twice the difference between the residence time and the travel time:

$t' = T - t_a = \Delta t/2$ and

$T = L/\bar{u}$

Such symmetrical peaks are seldom obtained since they require very long travel times or very low flow rates. They would arise when τ_r becomes much greater than 0.8 and result in a t_a of >> 25 seconds [1,6].

If the residence time is expressed in terms of the theoretical volume of the system and the volumetric flow rate:

$\bar{t}_r = \pi R^2 L/q$

where q is the flow rate,

then under the usual conditions in FIA (q = 1 ml/min and 50 cm < L < 200 cm or q = 3 ml/min and 150 cm < L < 500 cm) transport is governed by a combination of convection and diffusion processes.

Dispersion of the sample plug increases with increasing residence time until certain experimental conditions which, if exceeded, do not yield further increases in dispersion.

2.4.2 Theoretical models of dispersion

The relationships between the geometric and hydrodynamic parameters of the FIA assembly (flow - rate, reactor length, etc.) and the characteristics defining

the signal (travel -, residence - and baseline - to - baseline times and peak height) are what these mathematical models are attempting to describe. This should permit a more accurate optimization of the system. It is not an easy task to define the contribution of elements such as the injection operation, connectors or the geometry of the flow cell to the dispersion. It is accepted that the derivation of mathematical expressions fully describing the sample concentration (signal) as a function of time, have not yet been accomplished.

These quantitative relations have a narrow range of application and the optimization of a given FIA manifold is usually accomplished only through experimentation. They are not usually applicable to systems with several channels or mixing points or separation devices. However, these expressions establish concrete relationships which are highly valuable for the experimental operations involved in the optimization process [1].

2.4.2.1 Taylor's model

Taylor's model is described by the following expressions:

$C = (m/R^2) \times 1/(4\pi Dt) \times \exp[-(x-L)^2/(4Dt)]$

$C = C_o V_i/(q\sigma(2\pi)^{½} \times \exp[(t - \bar{t}_r)^2/(2\sigma^2)\ ]$

where C is the concentration of the sample at a given time,

m is the injected solute mass ($m = C_o V_i$),

σ is a parameter corresponding to the standard deviation characteristic of a Gaussian distribution,

x is the axial distance from the injection point,

t is the time after injection,

C_o is the initial concentration of the injected sample and

V_i is the volume of the injected sample

This model is only applicable if the injected volume is practically negligible compared to the reactor volume ($\tau_r >> 0.07$) and only holds for low flow rates and very long reactors (which helps to compensate for radial concentration changes and favour the prevalence of diffusion phenomena). Thus this model is not applicable under normal FIA conditions [1,5].

2.4.2.2 The tanks - in - series model

This model is analogous to the description of liquid chromatography in terms of theoretical plates. It relies on the assumption that the fluid flow passes sequentially through a large number (N) of mini chambers in which stirring is perfect (instantaneous mixing). The mathematical expression is:

$$C = 1/(\bar{t}_r)_N \times [t/(\bar{t}_r)_N]^{N-1} \times 1/(N-1)! \times \exp[-t/(\bar{t}_r)_N]$$

$(\bar{t}_r)_N$ being the mean residence time of an element of fluid in a given tank. It is assumed that the concentration of the monitored species is constant throughout each tank. The model is questionable if mixing chambers are not used or if the hypothetical situation represents a rather small number of tanks. The model is

successful in the description of a large - dispersion system generated by a well - stirred mixing chamber. A small number of tanks should result in skewed concentration time profiles while a large number of tanks would result in Gaussian type profiles [1,5].

2.4.2.3 The general model

The expression which take into account convective and diffusional transport and therefore best describes the overall physical phenomena is:

$$D(\delta^2C/\delta l^2 + \delta^2C/\delta r^2 + \delta C/r\delta r) = \delta C/\delta t + u_o(1-r^2/R^2)\delta C/\delta l$$

where l is partial tube length,

u_o is maximum velocity and

r is the partial tube radius.

This expression is derived by applying a mass balance to a differential element of volume in the fluid and takes into account axial and radial concentration gradients, as well as flow profiles under a laminar flow regime.

The left - hand side corresponds to diffusional transport, the first term within the brackets accounting for axial diffusion (dependence of C on l) and the other two terms for radial diffusion (dependence of C on r).

The first term on the right - hand side correspond to build - up of matter, which occurs in a non - steady regime. The second term accounts for the contribution from convective transport for which the velocity profile is parabolic in shape.

For this equation Taylor provided simple solutions for two extreme conditions:

i) When changes in concentration caused by convective transport takes place so rapidly that molecular diffusion can be neglected and dispersion is determined by convective transport alone.

ii) When convective transport is slow compared to molecular diffusion [5].

Other than for these two extreme conditions the general model can only be solved by numerical solutions. This has been done by Painton and Mottola [7], who developed a numerical model based on a basic dispersion equation modified by simultaneous consideration of the chemical effect introduced by a chemical reaction taking place as the sample plug disperses. This computer simulation provides a better fit to the experimental signal than the Taylor model, but fails to provide good predictions of the tail of the signal. The reason for this being departure of experimental conditions from the ideal. A better fit is obtained with the help of empirical correction factors reflecting the geometrics of the system, including that of the flow cell.

2.4.3 Practical definition of the dispersion

The description of all mass transfer processes and chemical collisions requires complex models lacking in simplicity. Empirical parameters which are inadequate to describe the complexity of the dispersion as a whole but are relatively easy to

extract from experimental data, and despite their inadequacies, may be used as practical guiding in method development [5].

The dispersion at the detector of a sample injected into the flow, is given by the position and shape of the analyte signal band. The peak is characterized by :

i) travel time (t_a)

ii) baseline - to - baseline - time (Δt)

iii) coordinates of the band maximum (T, C_{max})

2.4.3.1 Ruzicka's dispersion coefficient

Ruzicka defined the dispersion coefficient as the ratio of the concentration before (C_o) and after (C) transport through a given FIA system:

D = C_o/C and

$\mathbf{D}_{max} = C_o/C_{max}$ at the signal maximum,

where **D** is the dispersion coefficient,

$\mathbf{D}_{max}$ is the dispersion coefficient at the signal maximum and

C_{max} is the concentration of the sample at the signal maximum.

Since there is generally a direct relationship between the property used for detection (e.g. absorption), the magnitude of the transduced signal recorded and the concentration of the sample or its reaction product, the dispersion coefficient can be determined from the ratio of the height of the signal found in the absence

of dispersion (i.e. for continuous flow of the undiluted sample) to that of the FIA signal:

$\mathbf{D}_{max} = k_0 h_0/(k_1 h_{max})$

where h_0 is the height of the signal found in the absence of dispersion

h_{max} is the height of the FIA signal and

k_0 and k_1 are proportionality constants.

k_0 and k_1 are identical if the signal height is linearly related to concentration over the range considered. Dispersion always exceeds unity. The greater the dispersion the flatter the resulting curve [1].

2.4.3.2 Vanderslice's expressions

Extensive numerical methods for the solution of the diffusion convection equation have been used by Vanderslice *et al* [6] to obtain analytical expressions for the travel time (t_a) and baseline - to - baseline - time (Δt_B) which give their dependence on experimental parameters. The initial expressions did not take into account the dependence of t_a and Δt_B on either concentration or detector sensitivity. It was noted from the theoretical curves that as the initial concentration of the bolus was varied, Δt_B was proportional to a factor f and t_a varied in proportion to its reciprocal, $1/f$. f can be expected to vary under reciprocal conditions from 0.5 to 1.0. Thus, the equations are:

$t_a = (109\ a^2 D^{0.025}/f)(L/q)^{1.025}$

$\Delta t_B = (35.4a^2 f/D^{0.36})(L/q)^{0.64}$

where a is the tube radius.

Thus, dispersion can be deducted from the experimentally determined parameters D, a, L, q and f [6].

2.4.4. The influence of various factors on the dispersion

The overall dispersion within an FIA system can be considered as the sum of the dispersions originating in the four main parts of the system:

$\mathbf{D} = \mathbf{D}_{injection} + \mathbf{D}_{transport} + \mathbf{D}_{detector} + \mathbf{D}_{connectors}$

$\mathbf{D}_{injection}$ is the dispersion due to the sample volume and geometric aspects of the injection system. $\mathbf{D}_{transport}$ includes contributions of the reactor geometry and the flow rate. This is the most significant contribution to the overall dispersion. $\mathbf{D}_{detector}$ is the contribution of the flow cell geometry (shape and dimensions) to the dispersion. $\mathbf{D}_{connectors}$ is the contribution of the connectors to the dispersion.

The greater the sample volume the smaller the dispersion coefficient. The dispersion coefficient decreases with increasing flow rate. The dispersion coefficient increases with increasing reactor length and with increasing tube diameter.

When the reactor tube is coiled helically the centrifugal force originating from the circulation of a fluid through the tube results in a radial type flow. At low flow

rates the centrifugal force is not very great and the velocity profile is practically parabolic. At high flow rates the profile is completely different since molecules at the tube walls travel at a higher velocity than those at the center of the tube. Both situations result in a split circulation, symmetrical to the ideal central plane of the tube. This circulation has the same effect as radial diffusion, thus tending to decrease the dispersion. The smaller the coil diameter the smaller the dispersion.

Knotted reactors is a length of tubing which is knotted from end to end. This reduces the dispersion. The reason is an intensification of the dispersion - reducing effect introduced by coiling, since in effect knots are very tight coils.

Single bead string reactors consists of ordinary Teflon tubes packed with tiny glass beads having diameters that are 60 - 80 % of that of the tube. The effect of these beads is to increase radial dispersion, which reduces the dilution of the sample and therefore the dispersion [1].

2.4.5 The contribution of chemical kinetics to dispersion

The dispersion coefficient is inadequate to define conditions for FIA involving a chemical reaction. Hence the considerations above only apply to injecting a sample like a dye into a system and measuring one of its properties. It is incorrect to consider dispersion as a purely physical phenomena when chemical

reaction takes place in the system, especially since measurements are made under non - equilibrium conditions. A chemical reaction may modify the dispersion coefficient in two ways:

i) When a property of the reaction product is measured, then the chemical contribution results in a decrease in the practical dispersion. The higher the reaction rate constant, the smaller is **D**.

ii) When a property of one of the reactants which diminishes with time is measured, the chemical contribution increases the dispersion coefficient. The higher the reaction rate constant the larger is **D**. Painton and Mottola [8] studied this effect. They compared the signals obtained from the injection of a dichromate solution into an aqueous stream of equal pH, where dispersion would be purely physical, to the signals obtained from the injection of a dichromate solution into an aqueous stream also containing L - ascorbic acid, which would cause a chemical reaction (the consumption of dichromate), affecting the dispersion of the sample. The pH of the aqueous stream was also decreased to increase the rate of the chemical reaction. The lower the pH, the faster the reaction rate, the higher was the contribution of the chemical reaction to the overall dispersion. The chemical reaction also decreased the return time because the probability for effective collision seemed to be greater in the tail than in the leading front.

As stated before, Painton and Mottola [7] studied the chemical contribution to the dispersion by modifying the general equation governing convective - diffusional transport. An extra term:

$-k(C)^n$

was introduced to account for the decrease in concentration of the measured product, where k is the rate constant of the reaction and

n is the order of the reaction.

The modified equation was then treated as a pair of simultaneous equations and solved by applying the alternating direction implicite finite distance approximation approach. The equations are:

$\delta C/\delta t = D(\delta^2 C/\delta l^2 + \delta^2 C/\delta r^2 + \delta C/r\delta r) - u_o(1-(r^2/R^2))\delta C/\delta l$

$\delta C/\delta t = -k(C)^n$

In computer simulated curves a straight line relationship was found to exist between the time at the peak maximum and the assumed rate coefficient. The rate coefficient in the chemical kinetics term seems to change in an oscillating pattern which reflects the fact that the physical dispersions in the three regions (leading region, central region and trailing region) differ from one another.

2.5 Bibliography

1. Ruzicka J, Hansen EH (1988) **Flow injection analysis, Second Edition**. John Wiley. New York.
2. Kowalski BR, Ruzicka J, Christian GD (1990) **Trends Anal. Chem. 9:** 8

3. Ruzicka J, Hansen EH (1982) **Talanta 29:** 157

4. Reijn JM, Van der Linden WE, Poppe H (1981) **Anal Chim. Acta. 123:** 229

5. Painton CC, Mottola HA (1983) **Anal Chim. Acta. 154:** 1

6. Vanderslice JT, Stewart KK, Rosenfeld AG, Higgs DJ (1981) **Talanta 28:** 11

7. Painton CC, Mottola HA (1984) **Anal Chim. Acta. 158:** 67

8. Painton CC, Mottola HA (1981) **Anal Chim. Acta. 53:** 1713

CHAPTER 3

THEORETICAL BACKGROUND ON OPTIMIZATION

3.1 Introduction

In this chapter the problem of determining optimum conditions in chemical investigations is discussed, together with the modified simplex optimization technique used in this study.

3.2 Stating the problem

The problem of experimental attainment of optimum conditions is defined as follows: A response η is supposed dependent on the levels of k quantitative factors x_1, x_2, ..., x_k, capable of exact measurement and control. Thus for the u^{th} combination of factor levels:

(u = 1,....., N),

$\eta = \varphi(x_{1u}, \ldots\ldots, x_{ku})$,

Owing to unavoidable uncontrolled factors, the observed response y_u varies in

repeated observations, with mean η_u and variance σ^2. In the whole k - dimensional factor space, there is a region R bounded by practical limitations to change in the factors, which we call the experimental region. The problem is to find, in the smallest number of experiments, the point (x_1^o,....., x_t^o,....., x_k^o) within R at which y is a maximum or a minimum [1].

3.3 The proposed solutions

3.3.1 The sure way

A sure way of finding optimum conditions would be to explore the whole experimental region. In practice this would have to be done by carrying out experiments on a grid of points extending through R, and would in principle be possible. For a response surface of given complexity there must exist a grid of minimum density to allow adequate approximation, but it is easy to show that the number of points on such a grid would usually be far too large. A shorter method is therefore required [1].

3.3.2 The - one - factor - at - a - time - method

The sequential single - factor approach requires all factors but one to be held constant while a univariate search is carried out on the factor of interest. Figure

3.1 shows the isoresponse contours as a function of two factors x_1 and x_2, for a hypothetical analytical chemical system.

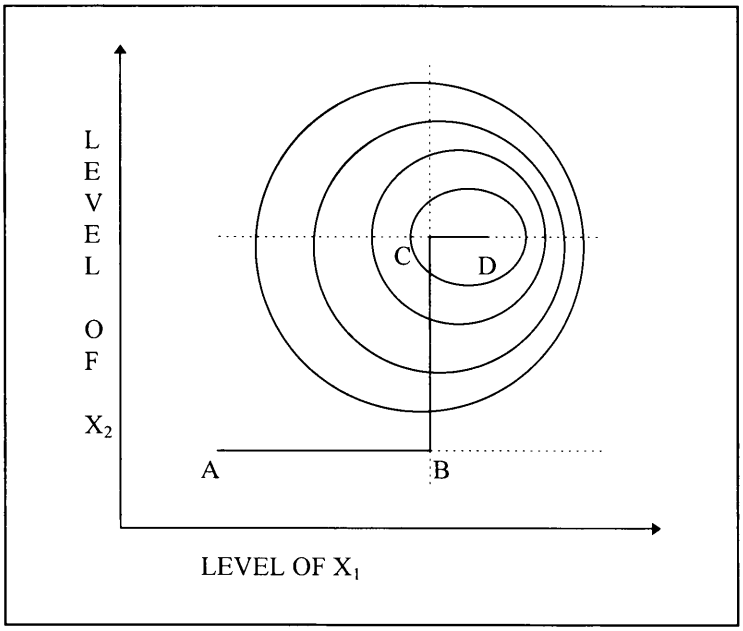

Figure 3.1 The - one - factor - at - a - time - method

The variable x_2 is fixed initially and the variable x_1 is varied along line segment AB and its extensions. An optimum response is obtained at point B. The optimized factor is now held constant and a different factor is searched. The variable x_1 is then held constant at its optimized level while the variable x_2 is varied along the line segment BC and its extensions until a new optimized response is obtained at point C. In general, one cycle of varying the factors is not sufficient to precisely define the optimum. An interactive approach is often used. In figure 3.1, the first search in the second cycle would take place along line

segment CD and its extensions would stop at point D, which is closer to the true optimum than either of the optima obtained in the previous cycle [2].

The single factor procedure is unsatisfactory when the response surface contains a ridge. Ridges are known to occur frequently in chemical systems and result from a non - independence of the chosen factors. The reason for the non - independence of the factors can be seen when it is remembered that factors like time, temperature, pressure, concentration, etc., are only regarded as natural variables because they happen to be quantities that can be conveniently measured separately. The behavior of the system could be described more economically by a more fundamental variable that can not be measured directly; for example the frequency of a particular type of molecular collision will often be a function of two or more natural variables like temperature, concentration or time. For this reason many combinations of natural variables may correspond to the best level of a fundamental variable [3]. Application of the single - factor approach to the response surface containing a ridge in figure 3.2 illustrates this problem. Holding x_2 constant and varying x_1 along the line segment AB and its extensions will find a single - factor optimum at B. However, additional experiments varying x_2 wile holding x_1 constant will indicate that the optimum value for x_2 is also at B. The presence of the ridge will not be detected by this strategy and B will be falsely accepted as the true optimum [2].

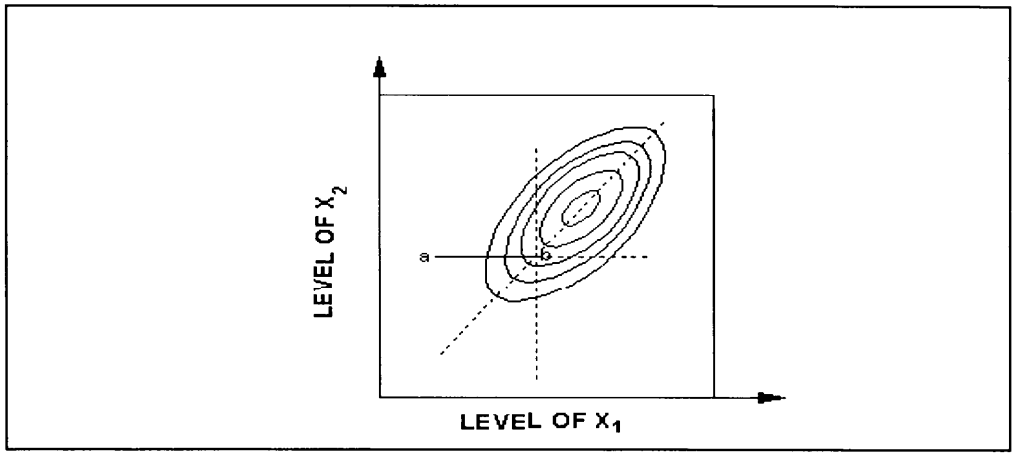

Figure 3.2: Failure of single factor method on a response surface containing a ridge

3.3.3 Factorial design

A factorial arrangement is where each level of one factor are combined with each level of a second factor [4]. A set of comparisons are selected among the experimental results that allow the evaluation of the main effects as well as the interaction effects among factors [2].

Factorial design has a few deficiencies when used for the purposes of optimization. They are :

(i) If a factor is continuous then the results are highly dependent on the choice of levels tested. The levels of the factors might be set too close together in which case the effect might not be statistically significant or too far apart in which case the optimum might be missed entirely.

(ii) The factorial design can explore either a small region comprehensively and give an indication of the direction in which to move and conduct new experiments or it can explore a large region superficially and give an optimum known so imperfectly that further experiments would still be required [2].

3.3.4 The steepest accent method

On response surfaces that contain ridges, if the factors are changed together in the direction of the axis of the ridge then improvement is possible even though no improvement is possible by changing any single variable [3].

The object is then to proceed from a point O in the k-dimensional space to a point P at a distance r from O, at which the gain in response is a maximum. This is shown in figure 3.3. O is made the origin so that the response there is $\varphi(O)$ and the response at P is $\varphi(P) = \varphi(x_1.....x_k)$. Since OP is equal to r,

$r^2 = \sum x_t^2$ .....t = 1, 2, ….,k (1)

$\varphi(P) - \varphi(O)$ is required to be a maximum subject to condition (1). If Lagrange's method of undetermined multipliers is used, the following function can be constructed:

$\Psi = \varphi(P) - \varphi(O) - 0.5\mu\sum x_t^2$ (2)

The required maximum is where $\partial\psi/\partial x_t$ are all zero. This is at the point where K equations are satisfied. These equations are:

$\mu x_t = \varphi_t(P) \qquad t = 1,2,.....k \qquad (3)$

($\varphi_t(P)$ denotes that the function is differentiated with respect to x_t and the value then inserted at P.) From equation (1) and (3):

$\mu = \pm\{\sum[\varphi_t(P)]^2\}^{0.5}/r \qquad (4)$

These equations show that for P to be the point (at a distance r from O) at which the gain is maximum, the coordinates at P must be proportional to the first order derivatives at P (assumed not all zero). This means that the point of maximum gain will be one of the points at which a hypersphere radius r and center O touches a contour surface. The derivatives at P are usually unknown. If it is assumed that φ can be represented about the origin by its Tailor series in which terms of degree greater than d are ignored, then derivatives at P can be expressed in terms of those at O by the equation:

$\varphi_t(P) = [D_t\sum\{(D_1x_1 + D_2x_2 + \ldots + D_kx_k)^s/S!\}]\varphi(O) \qquad (5)$

Formulae which specify the coordinates of the point P of maximum gain distance r from O may now be obtained by substituting equation (5) in equation (3) and choosing μ so that the solutions of (3) give a maximum. If second and higher degree terms may be ignored in the region considered, then there is K equations:

$\mu x_t = \varphi_t(O) \qquad t = 1,2, \ldots k. \qquad (6)$

These are the equations of steepest accent or greatest slope from O. By varying the factors in proportion to their first order derivatives at O, movement is in a direction at right angles to contour planes assumed to be locally parallel and equidistant. If the first order derivatives at O can be determined, they may be

used to move to a better response at P [1]. Figure 3.3 illustrates, for two factors x_1 and x_2, the steepest accent approach along the path O'P'.

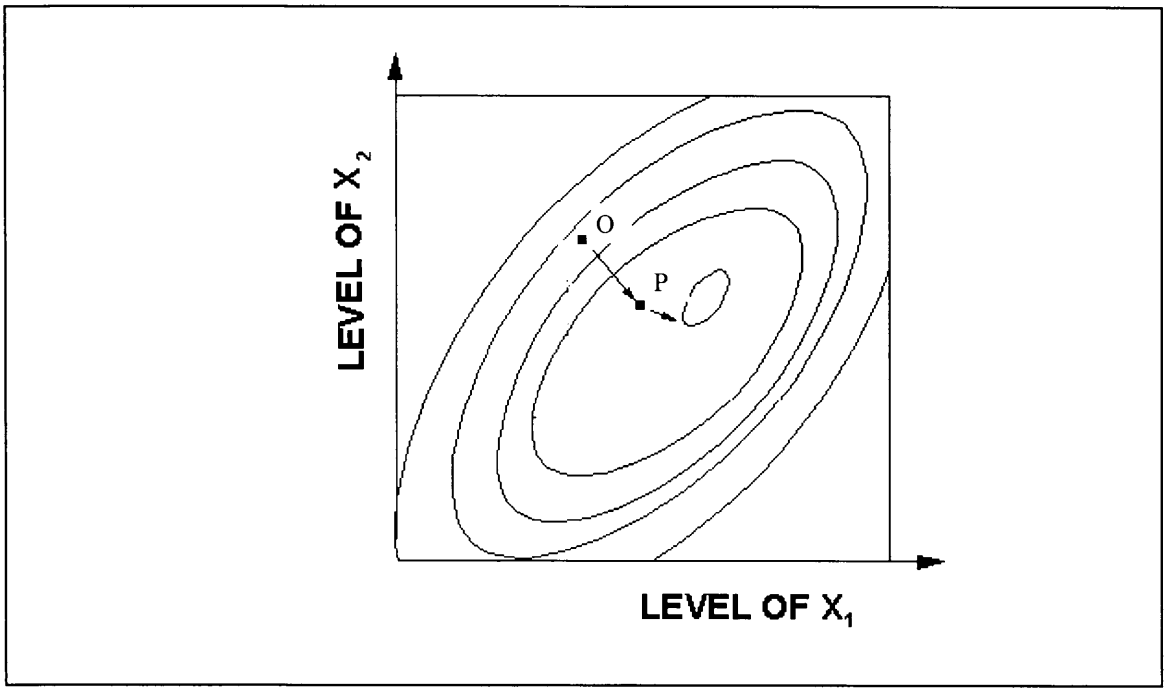

Figure 3.3 The steepest ascent path.

If the derivatives could be determined without experimental error it would be possible by successive application of the steepest accent formula (6) to move to points of higher and higher response until eventually a stationary point was reached. Because of experimental error, the more successfully the derivatives is reduced, the more difficult it would become in the next set of experiments to determine them with sufficient accuracy to proceed further. Therefore the steepest ascent technique is employed to move from a point remote from a

stationary value at which the surface slopes are large to a point closer to it at which they are small compared with the experimental error [1].

This steepest ascent procedure forms the foundations of the Evolutionary Operation method (EVOP), the atomization of which led to simplex optimization.

3.3.5 Evolutionary operation

Evolutionary operation is a method of process operation that has a built-in procedure to increase production. An experiment (usually a factorial experiment) is run within the range of operability of a process as it is currently running. It is assumed that the factors to be adjusted are measurable and can be changed a little without disturbing production quality. Data on the response are gathered at the various points of an experimental design. When one set of data has been collected at all the points, one cycle is completed. One cycle is usually not sufficient to detect any shift in the response, so a second cycle is made. This process continues until a change in the mean shows up as significant when compared to a measure of experimental error. The estimate of error is obtained from the cycle data. After a significant increase in yield has been detected, one phase is completed. At this point a decision is usually made to change the basic operating conditions in a direction that should improve the yield. Several cycles may be necessary before a shift can be detected [4].

3.3.6 Simplex optimization

The simplex optimization method sprang originally from considerations of how Evolutionary operation might be made automatic. Two problems were posed:

(i) Could a procedure be devised which would more rapidly approach and attain optimum conditions, and

(ii) Could the calculations and decisions be so formalized and simplified that they could be executed automatically by a digital computer [4].

The basic design of the technique is the regular simplex in k dimensions, k being the number of factors or variables under study. A simplex is a geometric figure defined by a number of points equal to one more than the number of dimensions of the space. A simplex in two dimensions is a triangle and a simplex in three dimensions is a tetrahedron. The series can be extended to higher dimensions, but the simplexes are not easily visualized. The dimensions or parameters to be varied are chosen by initial factorial experiments. Single experiments are carried out to determine the responses at points which forms the vertices of the first simplex. The objective of the sequential simplex optimization method is to force the simplex move to the region of optimum response. The simplex is moved preferably after each observation, the reasons being:

(i) Drift in measuring instruments may give the appearance of a moving optimum, even when the true optimum does not change. It is possibly

worthless to base changes on observations which have ceased to be relevant by the time the decision to move is made.

(ii) A false move will be made only when the real effects are obscured by observational errors, i.e. when the effects are small relative to such errors. Provided any resultant changes in operating conditions are small comparable with the changes in the basic design, no great harm will be caused by such a false move. There will certainly be no lasting harm if the decisions taken can be continuously reviewed and corrected in the light of fresh data. The greater any adverse effect the more rapidly will it be detected and eliminated [4].

Since it is possible, by adding just one further point, to complete a new simplex on any face of the original simplex chosen, movement can be made into an adjacent simplex in the direction of steepest ascent. This means proceeding from the center of the simplex out through that face of the simplex which is opposite to the point corresponding to the lowest observation.

An example of a simplex optimization procedure is given below:

Figure 3.4 is a two-dimensional simplex superimposed on a contour diagram of isoresponse lines of a function of two variables (factors). A,B and C is response values of factor 1 and factor 2. A move is made to the connecting simplex that is achieved by rejecting the least desirable response of the original response of the original simplex and replacing it with its mirror image across the hyperface of the two remaining points.

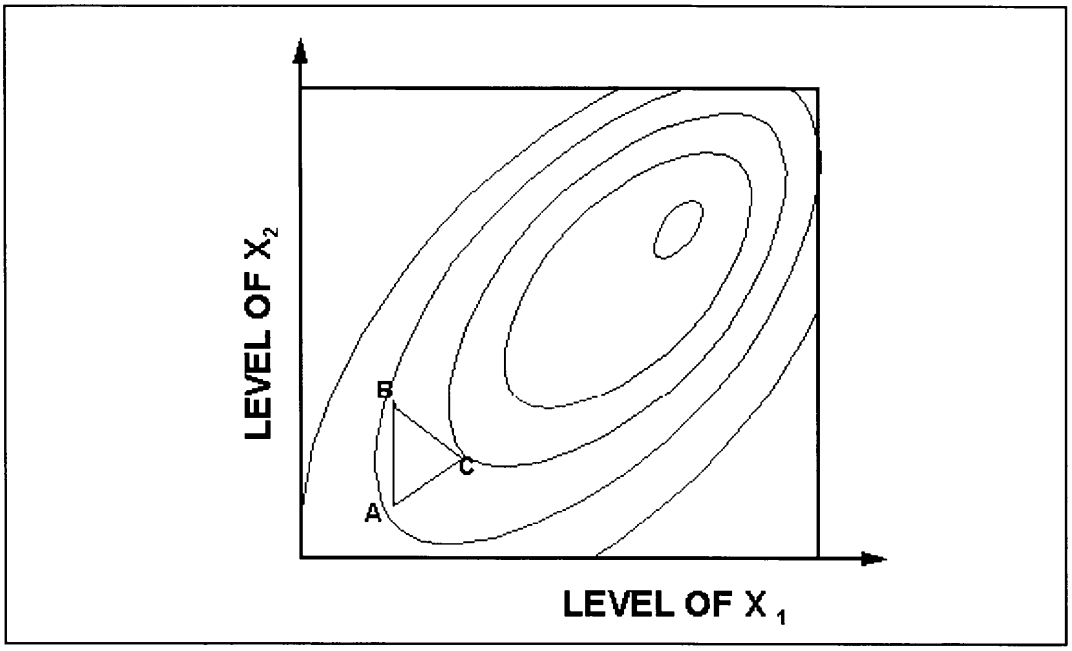

Figure 3.4 A simplex in two dimensions

In figure 3.5 three moves from ABC to DEF is shown. In the original simplex A had the lowest response and was rejected, leaving B and C. Reflection of A in the hyperface of BC created D. An experiment is carried out with factors 1 and 2 at levels determined by coordinates at point D. The response is higher than the response at B or C. C is rejected and reflection gives the new simplex BDE. An experiment is carried out at point E and a response obtained. B is rejected because it is the lowest response and reflected to F to give the fourth simplex EDF [5].

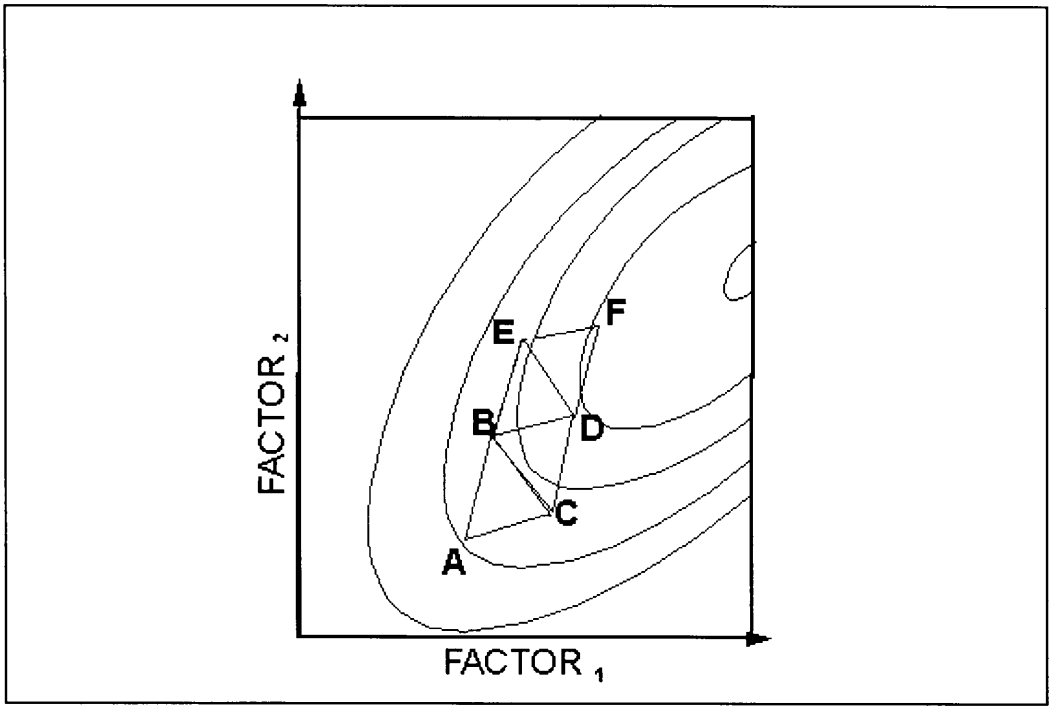

Figure 3.5 Three simplex moves from ABC to DEF

For a k - dimensional simplex with coordinate vectors

$P_1, P_2, \ldots, P_j, \ldots, P_k, P_{k+1}$ (7)

elimination of the least wanted response P_j gives the symmetry axis

$P_1, P_2, \ldots, P_{j-1}, P_{j+1}, \ldots, P_k, P_{k+1}$ (8)

with centroïed

$\bar{S} = (1/k)(P_1 + P_2 + \ldots + P_{j-1} + P_{j+1} + \ldots + P_k + P_{k+1})$ (9)

The new simplex is defined as the symmetry axis together with a new corner point P_j^* that is the reflection of the rejected corner point P_j over the centroïed $\bar{S}$.

$$P_j^* = \bar{S} + (\bar{S} - P_j) \qquad (10)$$

If the reflected point gives the lowest response in the new simplex the second lowest response in the new simplex is rejected. If a corner point has not been rejected for k+1 simplexes, the experiment corresponding to that point is repeated. If the high response was because of an error, a re - evaluation of the response at that point corrects the mistake and eventually eliminates that point. If a reflected corner point falls outside the boundaries of the factors a highly undesirable response is designated to it. This will bring the next simplex back to within the boundaries. When an optimum is reached the simplex moves in a circle as is shown in figure3.6.

The thickpacking of triangles makes it obvious when an optimum is reached in the case of two factors but with tetrahedra and polyhedra of higher dimensions it is not always obvious when an optimum is reached. This is one limitation of the sequential simplex technique. A second limitation is that there is no provision for acceleration. It is also possible to obtain a false optimum on a ridge when using this technique [5]. To overcome these problems a modification of the original simplex procedure by Nelder and Mead is used.

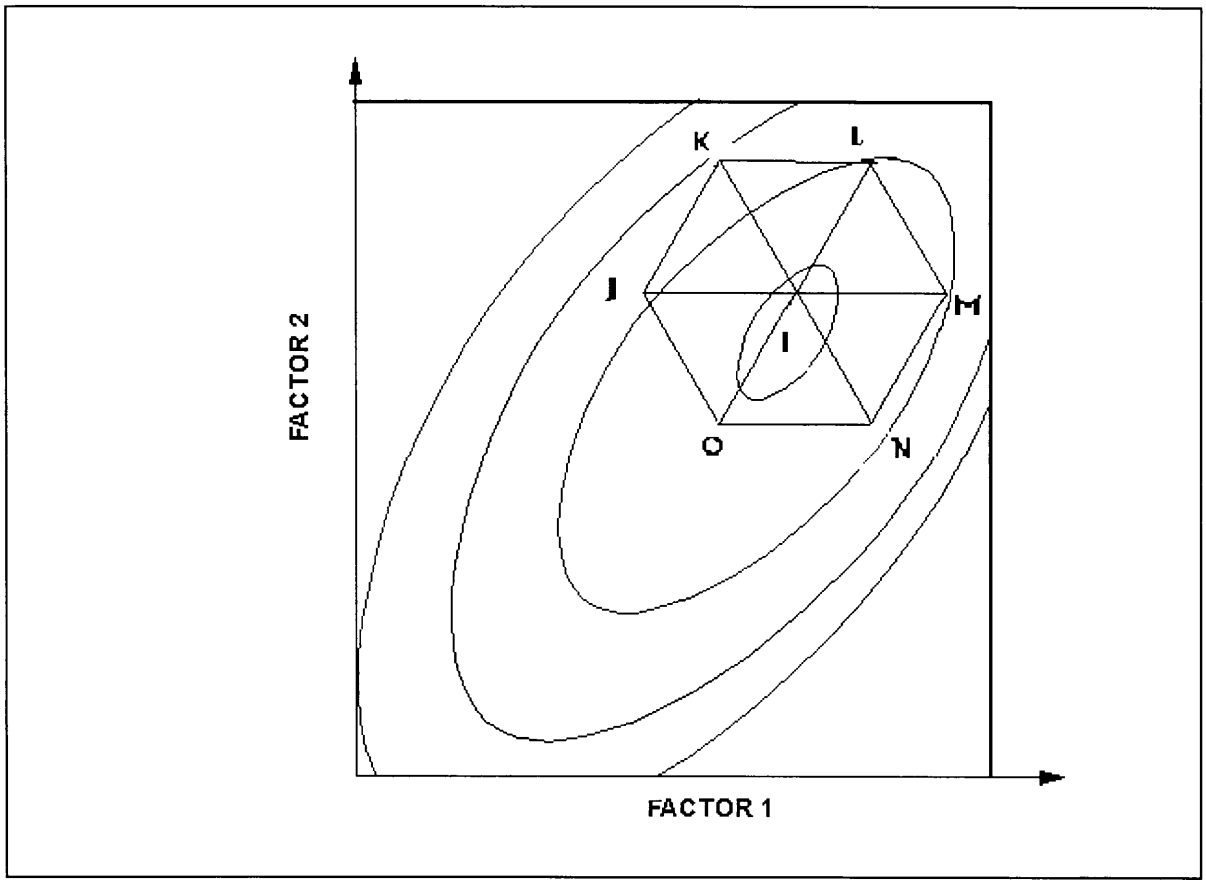

Figure 3.6 Circular movement of simplex when optimum is reached

3.3.7 The modified simplex method

A modification by Nelder and Mead of the original simplex procedure involves two new operations, expansion and contraction, and leads to a clear indication of when a sufficiently precise optimum has been attained and has the advantage of acceleration and adaptation to the specific response surface [5].

Figure 3.7 shows the starting simplex BNW. B is the best response, W the worst response and N the second best response. $\bar{S}$ is the centroïed of the symmetry axis BN. Reflection of W across BN gives point R

$P_r = \bar{S} + (\bar{S} - P_w)$

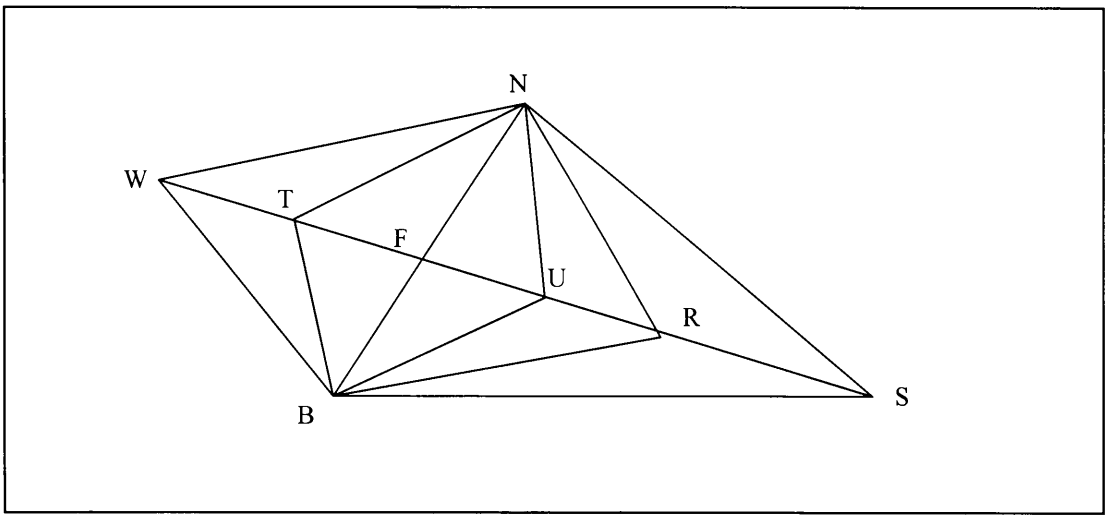

Figure 3.7 Three possible modified simplex movements

There are three possibilities available depending on the response at point R.

The possibilities are:

i) The response at R is better than the response at B. This means that movement is in the right direction and warrants further investigation. Thus the segment WR is expanded:

$P_s = \bar{S} + \gamma(\bar{S} - P_w)$

where γ is the expansion coefficient ($\gamma > 1$).

The response is evaluated at point S. If S is better than B, the new simplex is BNS. If S is worse than B, the new simplex is BNR.

ii) The response at R is not better nor worse than the response at B. There is no need for expansion or contraction and the new simplex is BNR.

iii) The response at R is less desirable than the response at N. Movement is in the wrong direction and contraction in this direction is desirable.

If the response at R is less desirable than the worst previous corner point (W) then the new contracted simplex should be at T which is closer to W than to R.

$P_t = \bar{S} + \beta(\bar{S} - P_w)$

where β is the contraction coefficient and $0 < \beta < 1$.

If the response at R is not less desirable than the lowest previous corner point (W), then the new contracted simplex is at U which is closer to R than to W:

$P_u = \bar{S} + \beta(\bar{S} - P_w)$

The simplex is stopped when the size of the steps becomes smaller than a previously determined size e.g. when the response differences become close to the value of the indeterminable error [5].

In contrast to factorial design experiments, the number of experiments required in the simplex method does not increase rapidly with the number of factors. Therefore all factors thought to have a bearing on the result should be included in the optimization [2].

To verify that the result obtained in the simplex optimization do represent an optimum, univariate mapping about the optimum can be done. This shows the effect on the response on changing one factor while holding all other factors constant at their optimum level [2].

The mathematics involved in modified simplex optimization are a great deal less complicated than the mathematics of the steepest ascent method.

3.3.8. Bibliography

1. Box GEP, Wilson KB (1951) **J.R. Statist. Soc.,B 13:** 1
2. Morgan SL, Deming SN (1974) **Anal. Chem. 46:** 1170
3. Box GEP (1954) **Biometrics 10:** 16
4. Hicks CR (1982) **Fundamental Concepts in the Design of Experiments. Third Edition.** Holt, Rinehart and Winston, Inc. New York.
5. Deming SN, Morgan SL (1973) **Anal. Chem. 45:** 278A

CHAPTER 4

THEORETICAL BACKGROUND ON PHOSPHORUS AND PHOSPHATE ANALYSIS

4.1 The occurrence of phosphorus

The determination of traces of orthophosphate ions is one of the most widely applied analysis, despite the fact that phosphorus occurs only to the extent of about 0.12 % in the lithosphere [1].

Phosphorus occurs in minerals in the fully oxidised state namely phosphate and is found dissolved in natural waters as a result of weathering of the minerals and soil erosion [2].

Phosphate compounds, particularly "super phosphate" $Ca(H_2PO_4)_2$ are used in fertiliser for agricultural and domestic fertilisation, where the phosphates are carried into surface waters with storm run - off and to a lesser extent with melting snow. The determination of phosphate in soils, in plant food and in feeds is important in studying plant growth, nutrition and the fertility of soils [1].

Phosphates are often added to boiler feed water for the prevention of scale formation and the embrittlement of boilers. The phosphate precipitates calcium ions as hydroxy

apatite, $3Ca_3(PO_4)_2.Ca(OH)_2$, which does not form boiler scale. Hard water can also be softened by treatment with sodium hexameta phosphate, $Na_6P_6O_{18}$, which sequesters the calcium by the formation of a chelate complex, thereby preventing the consumption of soap by the calcium ions. The extensive use of phosphates in soaps or detergents has led to serious problems in water pollution [1].

Phosphorus is found in ferrous metallurgical products because of the occurrence of phosphates in iron ore and in the limestone used as a flux. High concentrations of phosphorus in steel causes embrittlement. Industrial electroplating uses sodium ortho phosphates, tripolyphosphates and pyrophosphates in cleaning operations [1].

Phosphorus is essential for bone formation. Calcium mono hydrogen phosphate, $CaHPO_4$, is often added to foods as a mineral supplement. Phosphorus compounds, such as creatine phosphate, are presumably involved in muscle contraction and in the utilisation of carbohydrates. Phosphates also play an important role in buffering the blood at the proper pH value. Organic phosphates are formed primarily by biological processes. They are contributed to sewage by body wastes and food residues, and also may be formed from orthophosphates in biological treatment processes or by receiving water biota. A number of organic phosphates are utilised commercially. Triphenyl phosphate is a plasticizer, and tricresyl phosphate is an additive for gasoline. Many organophosphorus pesticides such as parathion, malathion, ethion and thimet are used quite extensively [1].

Phosphorus is essential to the growth of organisms and is considered to be one of the

limiting nutrients in most fresh water aquatic ecosystems. Thus, the discharge of raw or treated wastewater, agricultural drainage, or certain industrial wastes to that water may stimulate the growth of photosynthetic aquatic micro - and macro - organisms in nuisance quantities [3,4].

The determination of the phosphate content of water is, therefore, a highly significant determination in detecting contamination and in controlling water treatments and industrial waste disposal systems.

4.2 The different forms of phosphorus and its transformations

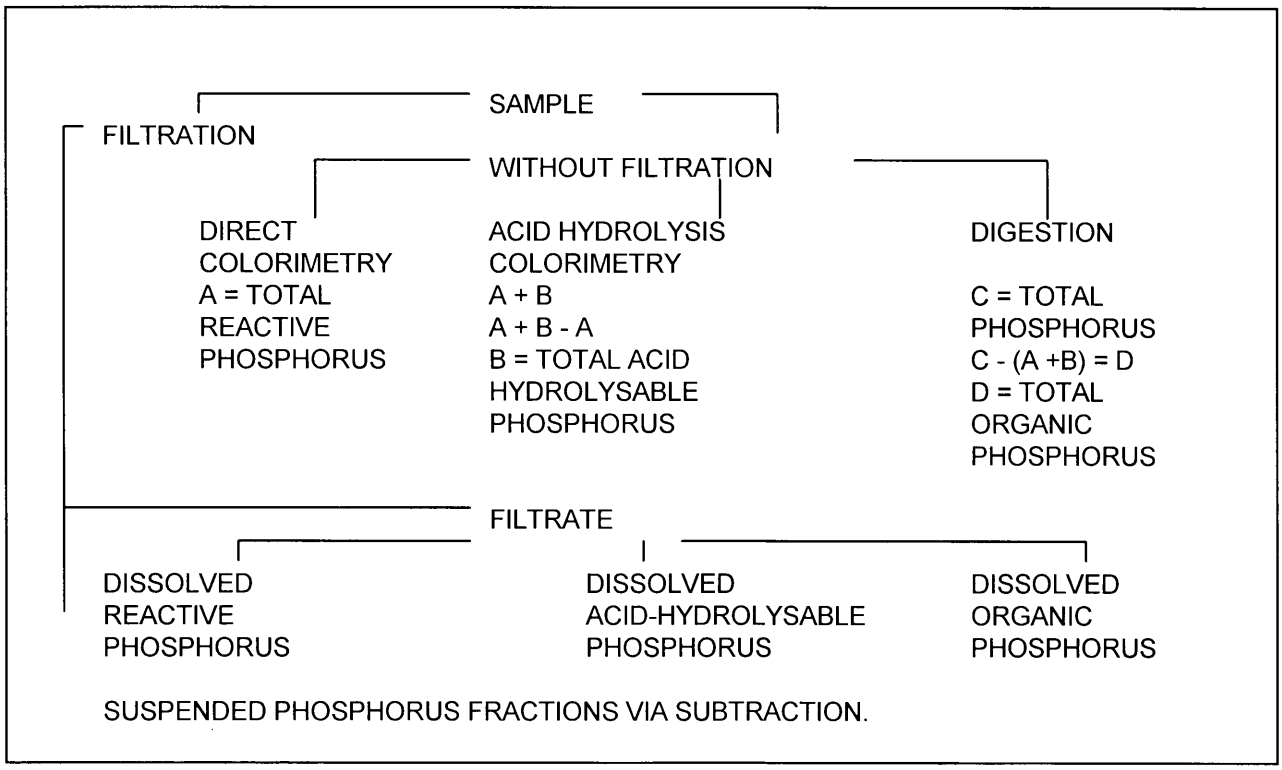

Figure 4.1 A schematic diagram of the various forms of phosphorus.

The separation of phosphorus into its various forms is defined analytically. Filtration through a 0.45 μm membrane filter separates dissolved from suspended forms of phosphorus.

No claim is made to the separation, it is merely a convenient and reliable analytical technique designed to make a gross separation. Figure 2.1 is a schematic diagram of the various forms of phosphorus and how they are obtained [3].

Changes can occur in the commonly measured phosphorus fractions in the field before samples are preserved. Studies showed that only total phosphorus concentrations showed no significant change. The other phosphorus fractions decreased with time. Total dissolved phosphorus (TDP) decreased by 28 % to 45 %, total reactive phosphorus (TRP) decreased by 33 % to 40 % and dissolved reactive phosphorus (DRP) decreased by 36 % to 58 %. If phosphate is adsorbed on the walls of the sample container then total phosphorus concentrations will also decrease. Biological activity, the formation of insoluble phosphates and absorption into particulate material are the likely reasons for the decrease in TDP, TRP and DRP. Biological action is known to cause the formation of colloidal and high molecular mass phosphorus compounds [4]. Hydrolytic scission of pyrophosphate and tripolyphosphate is thermodynamically favourable and yields orthophosphate as the eventual product. However the rates of conversion can be slow. Among the physical, chemical and biochemical factors that influence the rate of hydrolytic breakdown of the condensed phosphates are temperature, pH and enzymatic activity. In addition, metal - ion complexing of the condensed phosphates (Ca^{2+},Mg^{2+}) appears to affect

hydrolysis rates. The presence of bacteria, algae and enzymes causes a significant increase in the rate of condensed phosphate degradation. Half lives of tripolyphosphate or polyphosphate in distilled water are in the order of 4000 to 5000 days. The hydrolysis rates in natural lake and river waters are 100 to 1000 times faster [2]. TDP an DRP required the sample to be filtered. Filtrations it self may contribute to a change in the phosphorus concentrations measured in these fractions. Filter papers can retain soluble phosphorus, they also have only a nominal pore size (only 70 % 0.45 μm pore size) and during filtration, filter cakes can form, changing the effective pore size. Algal cells can also lyse when water is filtered under pressure releasing phosphorus into solution. These factors may increase the variability of phosphorus measurements requiring filtration. Thus only total phosphorus measurements could be made with any validity unless water samples are filtered immediately upon collection [4].

Field acidification to pH 1.0 is frequently a convenient technique for preventing biological uptake of phosphorus during sample transit and storage. Sulphuric acid should be used for acidification, since nitric acid can cause discoloration later and hydrochloric acid is volatile. If samples are acidified in the field only total phosphorus and total soluble phosphorus fractions can be determined on unfiltered and filtered splits [5].

Total phosphorus is useful for predicting Algal biomass, while TRP, TDP, DRP give an indication of the phosphorus immediately available to algae and to predict Algal growth rates [4].

Sea water samples were examined for the effects of storage on nutrients [6]. For phosphate analysis it was found that quick freezing offered an advantage over freezing because it increased accuracy and precision, provided turbid samples are filtered. Analysis must however be done within two months of collection to limit variance caused by storage. This method of sample preservation offered advantages in that it was simple and avoided the possibility of contamination or interference from the added preservatives.

The Department of Water Affairs and Forestry stated that Hg(II) could be added to preserve the samples and that the interference caused by Hg(II) could be eliminated by the addition of chloride ions [7].

4.3 The different methods of phosphate analysis

There are numerous methods available for the determination of low levels of phosphates. They range from the classical molybdenum blue method where orthophosphate reacts with molybdate ions in acidic solution to form molybdophosphoric acid, which, upon selective reduction, produces a heteropoly blue complex (maximum absorbance at (820 - 830 nm) or a molybdenum blue complex (maximum absorbance in the 650 - 700 nm region), to laser induced thermal lensing colorimetry that can be used to analyse phosphate in the parts per trillion (1.61×10^{-10} $mol.dm^{-3}$) level. Some of these methods will be discussed in the next paragraphs.

The method chosen for a specific purpose will depend on the apparatus and reagents available and the requirements of the analysis. The requirements of the analysis is the detection limit or the range of linearity needed, the amount of samples to be done, the speed of analysis required and the specific elements in the specific samples that would interfere with the method.

4.3.1 Stannous chloride as reducing agent

There is a number of reductants that could be used in the molybdybdenum blue method. One of these reductants are chlorostannous acid with hydrazine sulphate as stabiliser. With the aid of factorial design, simplex optimisation and the above mentioned reagents a method for the analysis of phosphate by FIA was developed [8]. A detection limit of 3.2 x 10^{-7} mol.dm^{-3} P (10 ppb P), a linear range from 1.3 $\times$ 10^{-6} mol.dm^{-3} to 80.7 x 10^{-6} mol.dm^{-3} and a sampling rate of 180 injections per hour were obtained. The response that was optimised (minimised) was peak width/(peak height)^2. The application was for inorganic phosphate found in surface waters.

Tecator also determined orthophosphate by the stannous chloride method and FIA [9]. They obtained a detection limit of 3.2 x 10^{-7} mol.dm^{-3} a linear range of 8.1 x 10^{-3} to 161.4 x 10^{-7} mol.dm^{-3} sample throughput of 90 injections per hour and a repeatability of 1 % rsd for 129.1 x 10^{-7} mol.dm^{-3}.

A FIA method for the determination of phosphate in surface waters with stannous chloride as reductant was developed [10]. A calibration curve that was linear between

1.6 x 10^{-6} mol.dm^{-3} and 161.4 $\times$ 10^{-7} mol.dm^{-3}, a sampling frequency of 90 injections per hour, a precision of 0.8 % at 161.4 x 10^{-7} mol. dm^{-3} and a carry over of 1 % at 161.4 x 10^{-7} mol.dm^{-3} were obtained. A detection limit was not given.

4.3.2 Ascorbic acid as reducing agent

Another type of reductant used in the molybdenum blue method is ascorbic acid with potassium antimony tartrate as catalyst. Total phosphorus was determined in an automated microbatch analyser system with the above mentioned reactants [11]. The limit of detection was smaller than 3.2 x 10^{-7} mol.dm^{-3} P and the method had a sampling rate of 6 samples per hour.

A field monitor for the determination of phosphates in natural waters was developed [12]. The monitor made use of the molybdenum blue method with reduction by ascorbic acid that was stabilised with glycerol. The response was linear over the range 0 - 6.5 x 10^{-5} mol.dm^{-3} P with a correlation of 0.9992 and a limit of detection of 3.9 x 10^{-7} mol.dm^{-3} P (2σ). The relative standard deviation was 0.9 %. The manifold was based on the "reverse" flow injection concept (reagent injection method). This characteristic prolongs the unattended time of the monitor.

An automated flow injection - stopped flow analyser was developed for the analysis of phosphates with the molybdenum blue method and reduction by ascorbic acid without antimony or glycerol [13]. The method had a sample throughput of 114 injections per hour and a relative error of 0.3 - 2.0 %. The correlation of the graph was better than

0.999 and linear between 1.6 x 10^{-4} mol.dm^{-3} P and 9.7 x 10^{-4} mol.dm^{-3} P.

4.3.3 Other reducing agents

Other reducing agents is also used in the molybdenum blue method.

A manual method for the determination of phosphate in polluted waters by solvent extraction of molybdenum blue was developed [14]. The reductant used was malonyl dihidrazide. The method was for the determination of phosphorus at sub - microgram levels. A detection limit was not given. This method was free from interference of arsenic.

Another manual method for the determination of phosphate in water samples was developed with oxalyldihidrazide as reductant [15]. No detection limit was given but the results obtained was said to correspond with results obtained from methods with ascorbic acid as reductant.

Zinc acetate at a pH of 5 was used as a reductant in the molybdenum blue method [16]. This method was suitable for the range 2 x 10^{-6} mol.dm^{-3} to 275 x 10^{-6} mol.dm^{-3} P. The sensitivity of this method was not affected by temperature or pH. The mild conditions for phosphate determination employed in this method were unique in making it suitable for the assay of orthophosphate in the presence of labile organo phosphates. A highly labile phosphate, carbamyl phosphate, was only 0.8 % hydrolysed if this method was employed at a temperature of 2°C and a pH of 5.

4.3.4 Dyes as complexing agents

A different way to determine orthophosphate is to form a complex between phosphomolybdate and a dye.

A method to determine phosphate with the dye malachite green was developed [17]. The ion - association complex was (Malachite green)$_3$[PO_4(Mo_3O_9)$_4$] and it was measured at 650 nm. The sampling rate was 40 samples per hour and the detection limit several parts per billion (nmol.dm^{-3}).

Malachite green was also used as complexing agent in a method in which segmented flow analysis was combined with a dialysis system [18]. This method was developed to determine low levels of phosphate in 0.01 mol.dm^{-3} $CaCl_2$ - extractions of soils with high phosphate fixing capacities. The detection limit of the system was lower than 6.5 x 10^{-8} mol.dm^{-3} P. The dialysis system removed organic constituents as well as macromolecular chains of silicate that arose when silicic acid was protonated in acidic medium and H_2O subsequently released.

Another dye that can be used is Rhodamine B [19]. Phosphate was reacted with molybdate ion and Rhodamine B in an acid medium and yielded a complex measured at 586 nm. The calibration curve was linear up to a concentration of 3.9 x 10^{-5} mol.dm^{-3} P with a correlation 0.9998. For a phosphate concentration of 6.5 x 10^{-7} mol.dm^{-3} the relative standard deviation was 0.13 %. The detection limit for a signal to noise ratio of 3:1 was found to be 3.9 x 10^{-7} mol.dm^{-3} P. The sampling frequency

achieved was 55 samples per hour.

A manual method was developed in which Alizarin red sulphonate was used as a dye to complex with the phoshomolybdate complex [20]. The complex that formed at a pH of 6.6 was (PO_4^{3-})(alizarinred sulfonate) in the relation 1:3. The concentration range was 9.7 x 10^{-7} mol.dm^{-3} P to 1937.1 x 10^{-7} mol.dm^{-3} P. No detection limit was given.

Manual methods were developed for the spectrophotometric determination of phosphate using the reaction between phosphomolybdate and resazurine and phosphomolybdate and p - rosolic acid [21]. With resazurine as dye a linear range of 6.5 x 10^{-7} to 25.8 x 10^{-7} mol.dm^{-3} P was obtained and the relative standard deviation was 2.08 % for 19.4 x 10^{-7} mol.dm^{-3} P. With p - rosolic acid as dye a linear range of 6.5 x 10^{-7} to 51.7 x 10^{-7} mol.dm^{-3} P and a relative standard deviation of 1.95 % for 19.4 x 10^{-7} mol.dm^{-3} P were obtained.

A method for determining phosphate based on the reaction of 12 - molybdophosphate and crystal - violet using FIA was developed [22]. A rate of 60 samples per hour and a detection limit of 6.5 x 10^{-7} mol.dm^{-3} P was achieved. The method was linear up to 1.614 x 10^{-7} mol.dm^{-3} P and the relative standard deviation of the method for 3.22 x 10^{-7} mol.dm^{-3} P was 0.69 % (n = 10). A mixing chamber was added to the FIA manifold and this improved the sampling rate of the method to 100 samples per hour and the detection limit to 3.2 x 10^{-7} mol.dm^{-3} P [23].

4.3.5 Special apparatus or detection systems

Some methods for determining phosphate at low levels of concentration involved special apparatus and / or other detection systems than the spectrophotometer.

A highly sensitive manual method was developed, involving fluorophotometry, for the determination of phosphate using the ion pair formation of molybdophosphate with the cationic dyestuff, Rhodamine 6G [24]. This ion pair was collected on a membrane filter made of cellulose nitrate, the pH adjusted, and filtered through the membrane filter under suction. The membrane filter and ion pair were dissolved into methyl cellusolve. The fluorescence intensity was measured at 555 nm and excitation at 535 nm. The correlation coefficient for the calibration graph was 0.999. The detection limit was 3.2 x 10^{-9} mol.dm^{-3} P (0.1 ppb) and the relative standard of deviation was 1.6 % for 3.2 x 10^{-3} mol.dm^{-3} P (n = 12).

Neutron activation and solvent extraction of phosphorus with dialkyltin dinitrates were used for the determination of phosphorus [25]. This manual method was used to separate phosphorus from large amounts of aluminium, iron and zirconium. The limit of detection for this method was 3.2 x 10^{-8} mol. dm^{-3} P.

A FIA method was developed with chemiluminescence detection for the enzymatic determination of inorganic phosphate [26]. Purine nucleoside phosphorylase, xanthine oxidase and urate oxidase were immobilised on controlled - pore glass beads. Hydrogen peroxide released by the enzymatic reactions of phosphate and inosine in a

carrier buffer was detected by the luminol - microperoxidase system in a flow cell. The detection limit was 1 x 10^{-8} mol.dm^{-3} P (0.3 ppb P). The calibration graph was linear over the range 1 x 10^{-7} mol.dm^{-3} P to 50 $\times$ 10^{-7} mol.dm^{-3} P and the reproducibility was 1.75 % at 2 x 10^{-7} mol.dm^{-3} P.

A manual method was developed in which the laser induced thermal lensing effect was applied to molybdenum blue colorimetry in the measurement of phosphate [27]. An Ar^+ laser pumped rhodamine 101 laser was used as the heat and probe source. The signal from a silicon photocell with a 1 mm^2 photosensitive surface, which was used as a laser radiation detector, was processed with an inexpensive computer. The detection limit was 1.6 x 10^{-10} mol.dm^{-3} P (5 parts per trillion). The method was applied to the determination of phosphate in sea water and lake water.

Mixtures of phosphates were separated with HPLC on an ion exchange column, using a magnesium tartrate buffer. An ICP was used as a selective detector by observing emissions at 214.9 nm. The detection limit for orthophosphate was 1 x 10^{-6} mol.dm^{-3} P [28].

A long capillary cell (LCC) was used as a detector for the determination of phosphate with the classical molybdophosphate blue technique [29]. The radiation source was a near infrared light - emitting diode and a siliconphototransistor was used as a detector. The capillary cell was 0.6 m long but the instrument was compact and easy to use in the field and laboratory. The detection limit was 1 x 10^{-9} mol.dm^{-3} P (30 parts per trillion), determined from twice the standard deviation of the blank. The relative

standard deviation was 6 % and the working range 1×10^{-9} - 500 x 10^{-9} mol.dm^{-3} P.

A technique was developed for determining phosphorus as orthophosphate in water by a spectrophotometric method involving flow injection coupled with solvent extraction. The ion associate formed between molybdophosphate and malachite green was extracted into benzene - 4 - methylpentan - 2 - one (1 + 2 V/V) and the absorbance was measured at 630 nm. The sampling rate was 40 samples per hour and the detection limit 3.2 x 10^{-9} mol.dm^{-3} P (0.1 ppb) [30].

4.4 Bibliography

1. Boltz DF, Howell JA (1987) **A Volume in Chemical Analysis: A series of Monographs on Analytical Chemistry and its Applications, Volume 8, Second Edition.** Wiley-Interscience. New York
2. Mellor JW (1931) **A Comprehensive treatise on inorganic and theoretical chemistry, Volume 8.** Longmans, Green and Co. London.
3. Greenberg AE, Conners JJ, Jenkins D (1980) **Standard Methods for the Examination of Water and Waste water, Fifteenth Edition.**
4. Lambert D, Maher W, Hogg I (1992) **Wat. Res. 26:** 645
5. Stauffer RE (1983) **Anal. Chem. 55:** 1205
6. Macdonald RW, McLauglan FA (1982) **Wat. Res. 16:** 95
7. Personal communication with Prof JF van Staden. University of Pretoria, Department of Chemistry.
8. Janse TAHM, Van der Wiel PFA, Kateman G (1983) **Anal. Chim. Acta. 155:** 89

9. Tecator 1983 ASN 60-01/83

10. Pauer JJ, Van Vliet HR, Van Staden JF (1988) **Water SA. 14:** 125

11. Dong S, Dasgupta PK (1991) **Talanta 38:** 133

12. Worsfold PJ, Clinch JR, Casey H (1987) **Anal. Chim. Acta. 197:** 43

13. Georgiou CA, Koupparis MA (1991**) Journal of automatic chemistry 13:** 199

14. Chuabe MA, Gupta VK (1983) **Analyst. 108:** 1141

15. Salem FB (1991) **Water, Air, and Soil Pollution. 60:** 27

16. Bencini DA, Wild JR, O'Donovan GA (1983) **Anal. Biochem. 132:** 254

17. Motomizu S, Wakimoto T, Toei K (1983) **Talanta 30:** 333

18. Novozamsky I, Van Dijk D, Van der Lee JJ, Houba VJG (1993) **Commun. Soil. Sci. Plant anal. 24:** 1065

19. Mas F, Estela JM, Cerda V (1990) **Water, Air, and Soil Pollution. 52:** 359

20. Abdallah AM, Khalifa ME, Akl MA (1991) **Anal. Chim. Acta. 251:** 207

21. Hassan SM, Salem FB (1987) **Analytical Letters. 20:** 1

22. Burns DT, Chimpalee D, Chimpalee N, Ittipornkul S (1991) **Anal. Chim. Acta. 254:** 197

23. Burns DT, Chimpalee N, Harriott M (1992) **Fresenius J. Anal. Chem.342:** 734

24. Kan M, Nasu T, Taga M (1991) **Anal. Sci. 7:** 87

25. Yakovlev YV, Kolotov VP (1981) **Zhurnal Analiticheskoi Khimii. 36:** 1534

26. Kawasaki H, Sato K, Ogawa J, Hasegawa Y, Yuki H (1989) **Anal. Biochem. 182:** 366

27. Fujiwara K, Lei W, Uchiki H, Shimokoshi F, Fuwa K, Kobayashi T (1982) **Anal. Chem. 54:** 2026

28. Morita M, Uehiro T (1981) **Anal. Chem. 53:** 1997

29. Ormaza - Gonzalez FI, Statham PJ (1991) **Anal. Chim. Acta. 244:** 63

30. Motomizu S Oshima M (1987) **Analyst. 112:** 295

CHAPTER 5

EXPERIMENTAL PROCEDURE

5.1 Introduction

All the methods were optimised and evaluated according to the same procedure. Flow injection systems were constructed that were similar to systems reported in the literature. Reagents were also made with constitutions similar to those obtained from literature. These conditions were used to start the experimentation. One factor was changed at a time, while the others were kept constant. This allowed assessment of the individual effects of the different factors. Based on these results it was decided which factors would be included in the simplex optimization. Factors not included in the simplex optimization were optimised at this stage. After the modified simplex optimization were completed a single stage one - factor - at - a - time optimization were done to improve the response or verify that an optimum were reached. When the optimization were completed the methods were evaluated. The characteristics of the method that were evaluated were linearity, recovery, detection limit, repeatability, carry - over and interferences.

This chapter contains a short description of the three methods, the experimental apparatus that were used, the optimization procedure for the three methods and the

evaluation procedures that were used.

5.2 Experimental apparatus

A peristaltic pump (10 revolutions per minute) and pump tubing from Technicon were used as the propelling unit. A Vici rotary injection valve with the option of changing the sample loop volume was used as the system of injection. Figure 2.2 in chapter 2 depicts the Vici rotary valve used and also the pathways that the samples and carrier stream followed through the valves and the loop during injection and refilling.

Technicon and Teflon tubing of various internal diameters were used for the construction of the reactors. Technicon or Teflon tubing were coiled around 0.01 m diameter glass rods to serve as reactors. A water bath with a thermostat were used to control the temperature at which the reactions took place. A 8625 UV - VIS spectrophotometer with a Hellma - type flow through cell (depicted in figure 2.4 in chapter 2) were used as the detector system. A computer with a colour screen, together with a computer programme, FlowTEK, and an interface, supplied by MINTEK, were used to receive and interpret the signal from the spectrophotometer and also to control the injection valve. The arrangement of the apparatus can be seen in figure 2.1 in chapter 2.

5.3.Glassware, reagents and standards

The reagents used were all analytical grade reagents. Doubly distilled water was used

throughout the experiments. Glassware used were washed with phosphate-free detergent and left overnight in diluted HCl. Before being used, the glassware were thoroughly rinsed with doubly distilled water. Volumetric flasks used were grade A. A stock - solution of 3.29 x 10^{-3} mol.dm^{-3} phosphate - P was made by drying KH_2PO_4 at 110 °C for two hours and by dissolving 0.4394 g of this KH_2PO_4 in 1 dm^3 distilled water. The stock solution was kept in a fridge that was maintained above freezing point. A hundred fold dilution of the stock solution was made each day from which the required standards were made. The standards, their concentrations and the dilutions used to prepare the standards are given in table 5.1. No mercury chloride was added to the stock solution or standards since it appeared that mercury affected the signals.

5.4 Description of the methods

5.4.1 Stannous chloride as reducing agent

An aqueous sample containing orthophosphate ions was injected via an injection valve into a carrier stream. The carrier stream was then joined with another stream carrying an acidic ammonium molybdate solution. The analyte and reagent were mixed while passing through a reaction coil to form a heteropoly acid. A third stream carrying stannous chloride and hydrazinium sulphate was merged with the stream carrying the heteropoly acid and then passed through a second reaction coil in which the heteropoly acid was reduced to molybdenum blue. The reaction coils were emersed in a water bath. The final reaction product passed through a flow cell in a spectrophotometer and then through a back pressure coil to waste. The signal was

recorded by a computer. The flow injection system was illustrated in chapter 6, figure 6.9. An interface connected the computer with the spectrophotometer and also the computer with the injection valve. These instruments are discussed in chapter 2.

5.4.2 Ascorbic acid as reducing agent

The second method was similar in construction to the first method. The differences between the two methods were that the reducing agent in the second method was ascorbic acid and that a catalyst, potassium antimony tartrate, was added to the ammonium molybdate reactant to increase the speed of the reaction. The system is portrayed in chapter 6, figure 6.24.

5.4.3 Malachite green as complexing agent

In the third method the sample was injected into the first stream with which a second stream carrying all the reagents was combined. The reagents, ammonium molybdate and malachite green in an acidic environment, reacted with the phosphate - ion to form the ion - association complex (malachite green)$_3$[$PO_4(Mo_3O_9)_4$]. The system is shown in chapter 6, figure 6.44.

5.5 Preliminary optimisation

5.5.1 Stannous chloride as reducing agent

In order to test the effects of the different factors on the response of the signal an

original flow injection system was built that operated with original reagents. The original system had the physical characteristics of systems used by other researchers [1,2] and reagents that were similar to reagents suggested by Tecator [3]. The wavelength was originally set at 690 nm.

The physical factors that could not be changed continuously were optimised by keeping all other factors constant and by changing only that specific factor. This included internal diameter of the reactor tubing and internal diameter of the sample loop. The diameter was chosen to fit the Vici valve perfectly and also to give minimal length of tubing per sample volume injected. Temperature and wavelength were optimised at this stage since their effects were dramatic and to include them in the simplex optimization could complicate the procedure unnecessarily.

The pump tube size of the carrier stream was optimised at this stage in order to simplify the simplex optimisation. The reason was that the response increased with increasing pump tube size of the carrier stream. The pump tube size was limited only by a too high pressure in the system.

The concentration of hydrazinium sulphate appeared not to have an effect on the response and was not included in the simplex optimization. However, without hydrazinium sulphate, the stannous chloride reagent became cloudy after a few days. All other factors were tested for their effect on the response by varying only that factor and keeping the other factors constant at no specific level. If a factor (other than the factors mentioned above) had an effect on the response, it was included in the

simplex optimization. Therefore reagent pump tube sizes, sample loop volume, reactor length and the concentrations of the stannous chloride, the ammonium molybdate and the sulphuric acid were included in the simplex optimization. These tests also established the minima and maxima values of the levels of the factors.

5.5.2 Ascorbic acid as reducing agent

The physical appearance of the original system and the original reagents' concentrations were based on the articles of other researchers [4]. Sample loop diameter and reaction tube diameter were kept the same as for the stannous chloride method. Wavelength and temperature were optimised at this stage. Since response increased with antimony concentration and pH and the solubility of antimony in solution decreased with increasing pH, a compromise had to be made between antimony concentration and pH. The amount of ammonium molybdate in the reagent was also optimised since the effect of the molybdate reagent on the response levelled off after a certain level of concentration. The wetting agent, sodium laurel sulphate, influenced the pH and thus caused cloudiness in the reagent. For this reason it was not included in the reagent. Thus antimony tartrate, sulphuric acid and ammonium molybdate were combined in one reagent and optimised before the start of the simplex optimization. The ascorbic acid concentration in the second reagent was also optimised before simplex optimisation since response did not increase noticeably after a certain level of concentration was reached. Therefore only the pump tube sizes, the sample volume and the reaction coil length were included in the simplex optimization.

5.5.3 Malachite green as complexing agent

The physical construction of the initial flow injection system as well as the reagent concentrations used were based on the work done by Motomiza et al. [5]. The internal diameters of the sample loop and reactor tubing were kept as with the other two methods. The temperature and the wavelength were optimised at this stage. The type and amount of wetting agent were also optimised at this stage. Ethanol, poly vinyl chloride and sodium laurel sulphate were tested as potential wetting agents. The amount of sulphuric acid contained in the carrier stream was also optimised before simplex optimization. The other physical factors and the concentrations of the other reagents were also tested for their effect on the response and included in the simplex optimization. The colour reagent containing the malachite green, sulphuric acid, ammonium molybdate and ethanol were filtered through a 0.45 μm filter before use.

5.6 Optimisation of the methods

5.6.1 Stannous chloride as reducing agent

Since seven factors were optimised by the modified simplex optimization technique, eight co - ordinates were chosen randomly within the boundaries determined by the preliminary investigation.

Experiments were made and responses were obtained for these eight co - ordinates. The values of the factors constituting the eight co - ordinates together with the

responses obtained for each co - ordinate and the boundaries for the various factors were entered into a computer that calculated, with the aid of a modified simplex optimization programme, the first simplex move. The different factors were then set at the levels of the co - ordinates obtained from the programme, an experiment executed and a response obtained. Since stannous chloride took a long time to stabilise, a reagent was made containing a stannous chloride concentration equal to the maximum boundary value and a sulphuric acid concentration near the minimum boundary. This meant that the reagent contained 2.00 x 10^{-3} mol.dm^{-3} $SnCl_2.2\ H_2O$ and 0.68 mol.dm^{-3} H_2SO_4. The reagent also contained 1.54 x 10^{-2} mol.dm^{-3} $N_2H_6SO_4$. For each simplex move 0.1 dm^3 of reagent were needed. Therefore a dilution was made from the stock reagent to satisfy the stannous chloride concentration of the co - ordinate calculated by the computer. The amount of $N_2H_6SO_4$ was added that was needed to make the final concentration of the reagent 1.537 x 10^{-2} mol.dm^{-3} $N_2H_6SO_4$ The amount of H_2SO_4 needed to make the final concentration of the reagent 0.68 mol.dm^{-3} H_2SO_4 was also added. $(NH_4)_6\ Mo_7O_{24}.4\ H_2O$ dissolved easily and was made fresh for each simplex move in the required concentration. This reagent was 0.004 % in the wetting agent sodium laurel sulphate. The acid concentration of the ammonium molybdate reagent was also obtained from the co - ordinates of the simplex move calculated by the computer programme.

The response of the first simplex move was entered into the computer and the co - ordinate of the second simplex move was obtained from the computer. The factors were then set at the levels of the co - ordinates obtained from the computer for the second simplex move, an experiment executed and a response obtained. This

response was entered into the computer and the co - ordinates for the third simplex move obtained. This procedure continued until the optimum was reached as explained in chapter 3. Optimization was restarted twice due to replacement of the spectrophotometer and the replacement of the lightsource in the spectrophotometer. Each time that optimization were restarted the co - ordinates of the eight best responses were used as the new original simplex.

When the optimum was reached the co - ordinate point with the highest value was chosen and the values of the factors were used to build a flow injection system on which a one - factor - at - a - time optimization was done. This optimisation also included optimization for baseline drift and ghost peaks.

5.6.2 Ascorbic acid as reducing agent

Since it was decided to optimise five factors with the modified simplex optimization technique, six co - ordinates were chosen randomly within the boundaries determined by the preliminary experiments. Optimization was continued and concluded as with the stannous chloride method. Since only physical parameters were optimized by the simplex optimization method, the molybdate reagent was prepared beforehand as described in section 5.5.2 and prepared fresh once a week. The ascorbic acid reagent was prepared fresh each day.

5.6.3 Malachite green as complexing agent

Optimization was done as with the other two methods. Simplex optimization was restarted once due to changes in the interface. The eight previous best responses' co - ordinates were used to form the new original simplex. The colour reagent was made new for each simplex move.

5.7 Evaluation

5.7.1 Linearity

For each test of linearity a new set of standards were made up from the stock solution. A second dilution of the stock solution was first made of 0.010 dm^3 stock solution into 1 dm^3 distilled water. From this second dilution a specific volume was added with a burette into a 0.1 dm^3 volumetric flask and made up to the mark with water. The volumes that were used to make a certain standard is depicted in table 5.1

TAVLE 5.1 The volume stock solution used in the standards and the concentrations of the standards

NO OF STANDARD	STANDARD		VOLUME OF SOLUTION THAT IS 3.229 X 10^{-5} $mol.dm^{-3}$ P in dm^3
	$mol.dm^{-3}$	$\mu g.kg^{-1}$ (ppb)	
1	0	0	0.0000
2	6.457×10^{-8}	2	0.0002
3	1.614×10^{-7}	5	0.0005
4	3.229×10^{-7}	10	0.0010
5	6.457×10^{-7}	20	0.0020
6	1.614×10^{-6}	50	0.0050
7	3.229×10^{-6}	100	0.0100
8	4.843×10^{-6}	150	0.0150
9	6.457×10^{-6}	200	0.0200
10	1.291×10^{-5}	400	0.0400
11	2.583×10^{-5}	800	0.0800

Each standard was injected five times and the average response (absorption) is stipulated against the concentration of the standard. A curve is fitted on the graph with the aid of a calculator and the correlation is calculated.

5.7.2 Recovery

The absorption of a real sample of tap or bore whole water was determined. Occasionally the samples had to be diluted because it were out of the linear range of the methods. From the absorption of the real sample and the equation describing the graph and the dilution factor used the concentration of phosphate in the sample was determined. The same sample was then spiked with a known amount of phosphate and the absorbance of this determined. From the phosphate concentration of the unspiked sample, the dilution factor and the amount of phosphate added it was determined what phosphate concentration to be expected. From the absorbance of

the spiked sample and the dilution factor and the equation describing the graph the concentration of the spiked sample is obtained. Thus recovery as a percentage was obtained as follows:

$$\text{Percentage Recovery} = \frac{C_2 \times DF}{[(C_1 \times DF) + C_A]} \times \frac{100}{1} \qquad (5.1)$$

where C_1 was the concentration of the unspiked sample,

C_2 was the concentration of the spiked sample,

C_A was the concentration of the added phosphate and

DF was the dilution factor.

The three methods were not tested on the same real sample to compare accuracy. The reason for this was that the orthophosphate concentration in a real sample, if untreated, does not remain stable for more than four hours. The reason for this was discussed in chapter 2.2.This is not long enough to analyse the sample on one flow - injection system, disassemble that system, assemble the next flow injection system, condition it and analyse the sample. Mercury(II) was not added because of the interference it caused with the methods.

5.7.3 Detection limit

The lowest standard or a blank were injected 15 times and the standard deviation (σ) of the 15 responses determined. The detection limit was then the value of the Blank + 3σ which was converted from absorption units into concentrations.

5.7.4 Repeatability

Repeatability was determined by repeating a low standard 15 times and calculating the standard deviation (σ). Repeatability was then the average (x) value of the 15 responses plus or minus the standard deviation. Thus repeatability was $x \pm \sigma$ which was converted into concentration units.

5.7.5 Carry over

Standard number 5 were injected 5 times and an average concentration determined. Standard number 9 were then also injected 5 times and the average determined. Immediately after standard number 9 stand number 5 was injected again 5 times and the average determined. The calculation was then done as follows:

$$\text{Percentage Carry - over} = \frac{X5_2 - X5}{X9} \times \frac{100}{1} \qquad (5.2)$$

Where X5 was the average concentration of the first set of injections of standard number 5, $X5_2$ was the average concentration of the second set of injections of standard number 5 and

X9 was the average concentration of the set of injections of standard number 9.

5.7.6 Interferences

Interferences was determined by spiking a specific standard with different concentrations of the interference in question and determining what the effect was on the peak height or shape. If there was no effect on the peak shape and the difference in peak height was less than 2 % it was considered that the specific interference does not affect the method at that concentration. Amount of interference present was expressed as n (interference): n (phosphate - P) where n were the amount of moles of the ion in question. The interferences that were investigated were Hg(II), P_2O_5, and pH.

5.8 Bibliography

1. Janse TAHM, Van der Wiel PFA, Kateman G (1983) **Anal. Chim. Acta. 155:** 89
2. Pauer JJ, Van Vliet HR, Van Staden JF (1988) **Water SA. 14:** 125
3. Tecator 1983 ASN 60-01/83
4. Worsfold PJ, Clinch JR, Casey H (1987) **Anal. Chim. Acta. 197:** 43
5. Motomizu S, Wakimoto T, Toei K (1983) **Talanta. 30:** 333

CHAPTER 6

RESULTS AND DISCUSSION

6.1 Stannous chloride as reductant

6.1.1 Preliminary optimization of the physical factors

The smaller the internal diameter of the reaction coils, the higher the response. This agrees well with the theory of dispersion [1]. Coils with an internal diameter of 0.64 mm gave a higher response than coils with an internal diameter of 0.76 mm. Coils with an internal diameter of 0.51 mm was not used because of possible pressure problems [2].

The internal diameter of the sample loops was chosen as 1 mm since smaller internal diameter loops did not fit easily on the valve and would result in uncomfortably long loops.

A temperature of 30°C was chosen because lower temperatures gave lower responses, possibly due to the slower rate of the chemical reaction at lower temperatures. The fact that the reaction product was measured in this case would

cause the practical dispersion to decrease due to the chemical reaction. The practical dispersion would decrease even more at higher reaction rates. This effect is the opposite of that studied by Painton *et al* [3] and discussed in Chapter 2 paragraph 2.4.5. Higher temperatures than 30°C gave worse responses that were less repeatable. This could be due to the increased number of air bubbles in the system caused by the raised temperature or from the possible increased destabilisation of $SnCl_2$, also because of the raised temperature. The results are illustrated in figure 6.1. Absorbancies are given in units of length since measurements were made with a chart recorder.

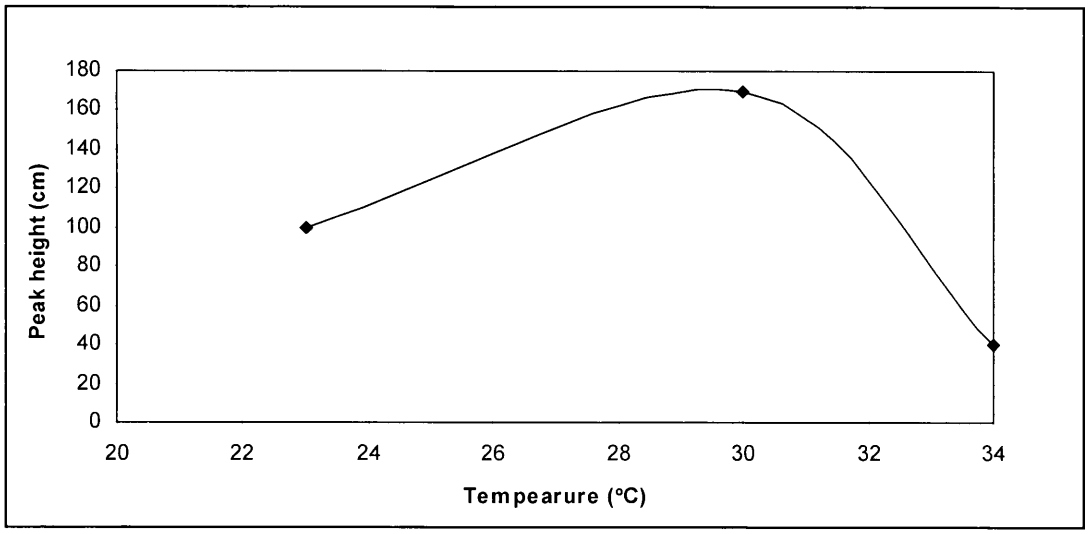

Figure 6.1: The effect of temperature on peak height

The wave length at which optimum peak height was detected was 690 nm. The response as a function of the wave length is shown in figure 6.2.

An increase in the pump speed of the carrier stream caused the peak height to increase. Therefore the maximum value of 3.9 $cm^3.min^{-1}$ was chosen as the optimum value. This agreed well with the theory of dispersion [1]. Figure 6.3 depicts the peak height as a function of the pump speed of the carrier stream.

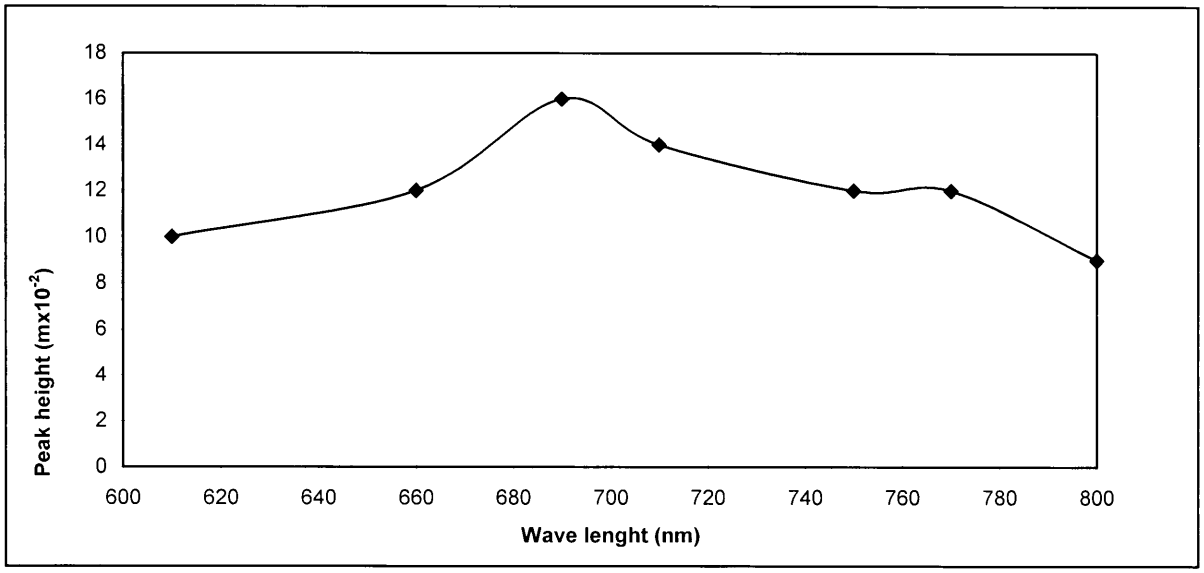

Figure 6.2: The effect of wave length on peak height

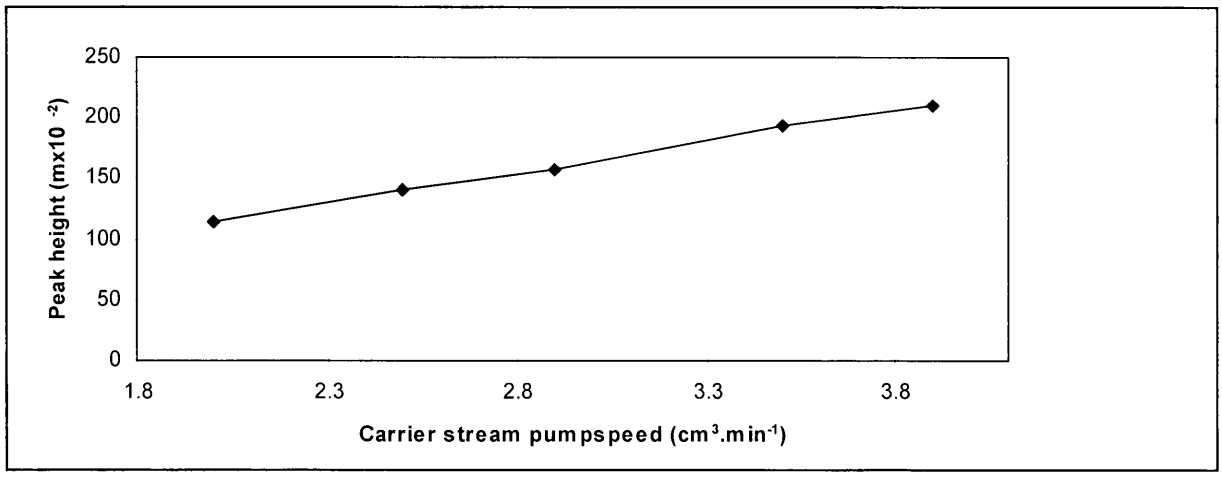

Figure 6.3: The effect of carrier stream pump speed on peakheight

The pump speed of the molybdenum reagent (R1) appeared to give a maximum response at about 0.42 $cm^3.min^{-1}$. The lower response at pump speeds below 0.42 $cm^3.min^{-1}$ might be due to less chances of collision between analyte and reagent, since the concentration of the reagent is less. Lower responses at higher pump speeds could be due to a pH effect or an effect of mixing that somehow increased dispersion. This information is depicted in figure 6.4. This factor was left to be optimised during simplex optimization.

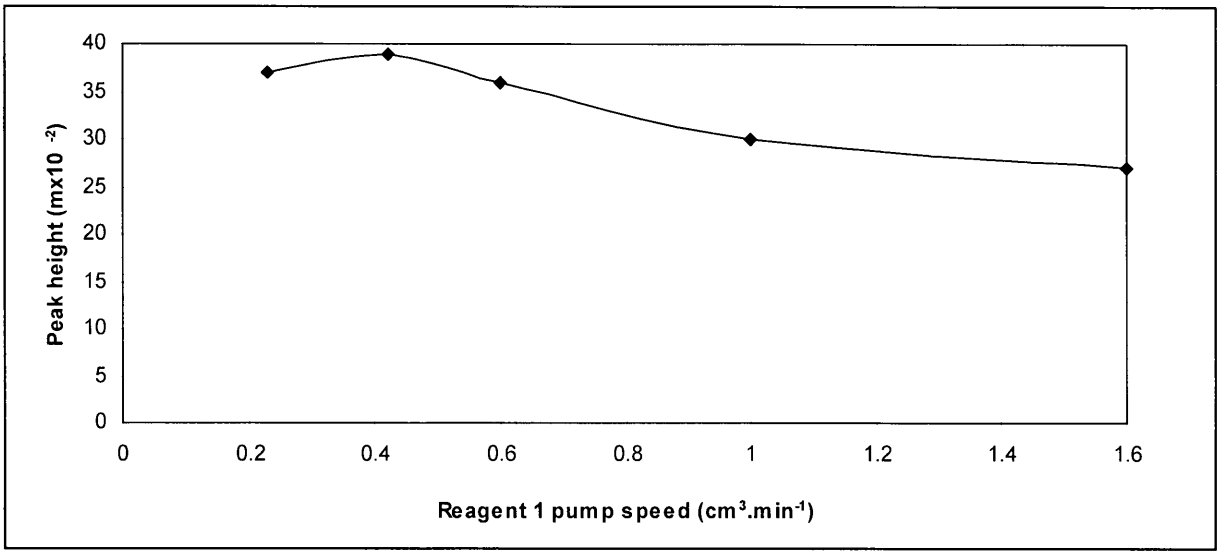

Figure 6.4: Effect of the pump speed of the molybdenum reagent on the peak height

The peak height as a function of the pump speed of the stannous chloride reagent (R2) is illustrated in figure 6.5. The response seems to be higher for lower pump speeds. The reason for the shape of this curve might be the same as the reason for the shape of the curve of the molybdenum reagent. This factor was also optimised during simplex optimization.

An increase of the pump speed of the sample stream caused the peak height to increase, but only marginally. The pump speed of the sample stream is therefore set at 2.5 $cm^3.min^{-1}$. This information is outlined in figure 6.6.

The length of the coil that was used for the reaction between the molybdenum reagent and the analyte was kept at 0.30 m when it was found to have little influence on the peak height.

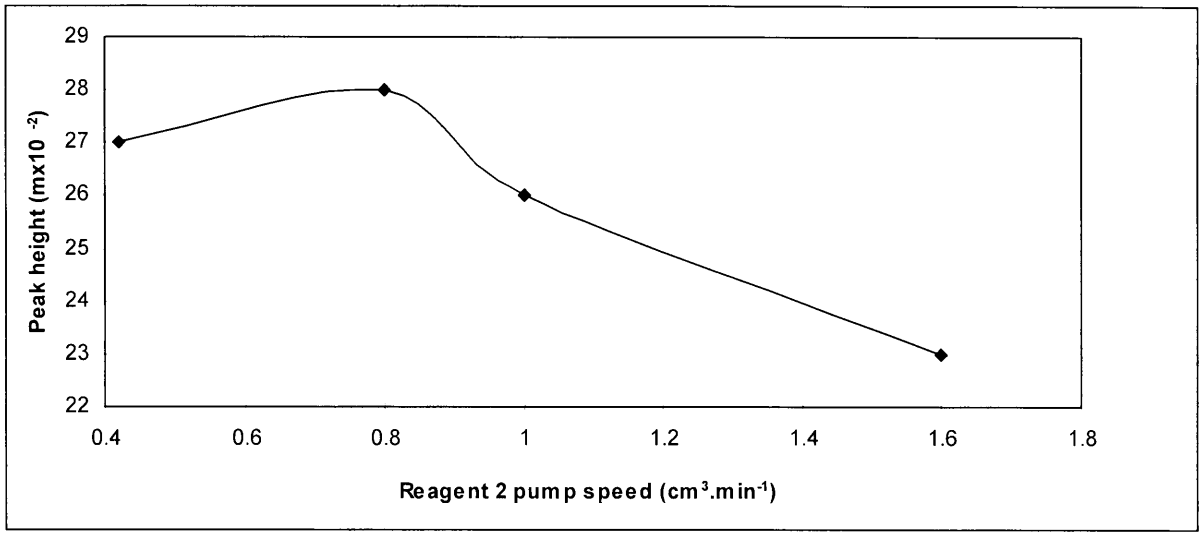

Figure 6.5: The effect of the pump speed of the stannous chloride reagent on the peak height

The length of the second coil that was used for the reduction reaction was found to decrease the response with increasing coil length. This agreed well with the theory of FIA in that the dispersion would increase with increased path length [1]. This information is illustrated in figure 6.7. The coil length was included in the simplex optimization.

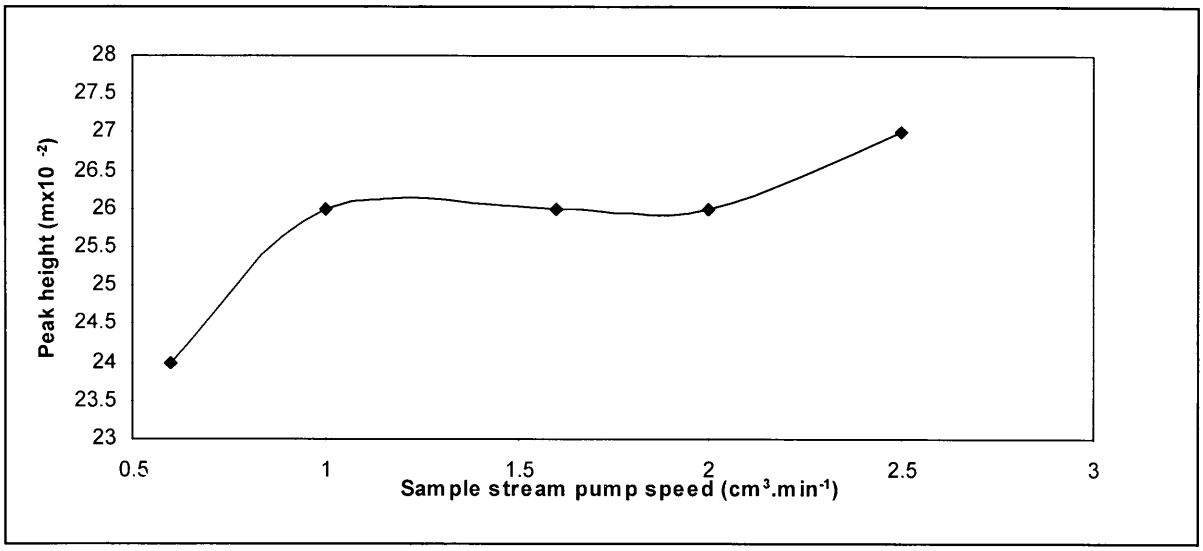

Figure 6.6: The effect of the sample stream pump speed on peak height

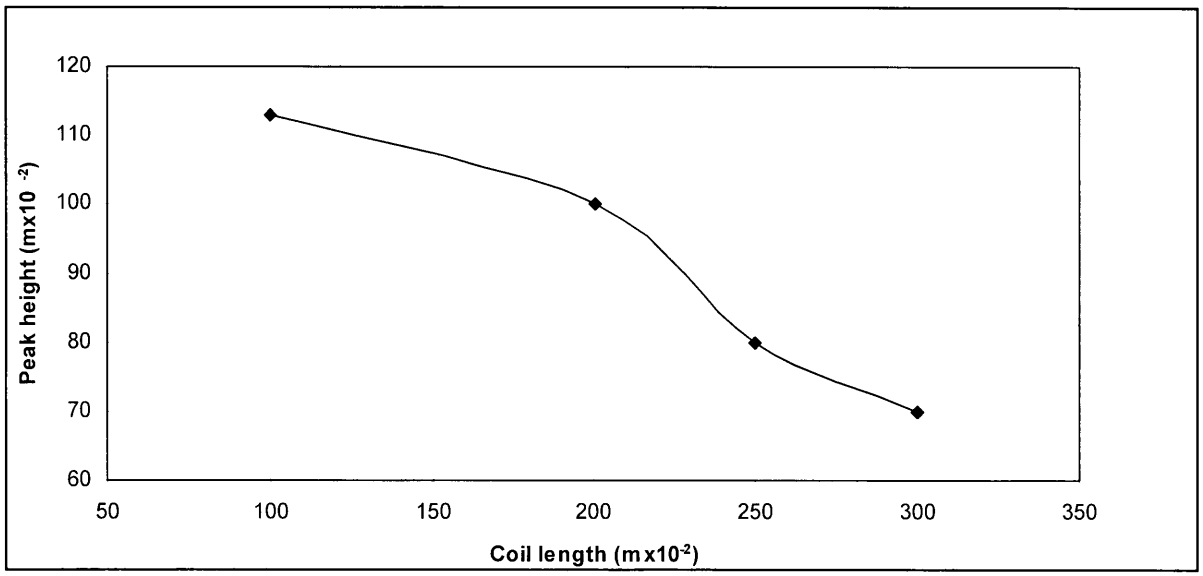

Figure 6.7: The effect of coil length on peak height

The peak height increased with the volume of the sample. This is consistent with the theory of FIA [1]. No maximum was obtained. This relationship is illustrated in figure 6.8. The volume of the sample loop was included in the simplex optimization.

6.1.2 Preliminary optimization of the chemical factors.

The effect of the concentration of hydrazinium sulphate was tested at various levels of stannous chloride concentration. The hydrazinium sulphate concentration had no noticeable effect on the peak height. However if it was not included in the stannous chloride reagent, that the reagent became turbid within a few days, much sooner than the hydrazinium sulphate containing reagents. A concentration of 1.537×10^{-2} $mol.dm^{-3}$ hydrazinium sulphate ($N_2H_6SO_4$) was chosen.

Ethanol in the carrier stream decreased the signal and therefore only doubly distilled water was used in the carrier stream.

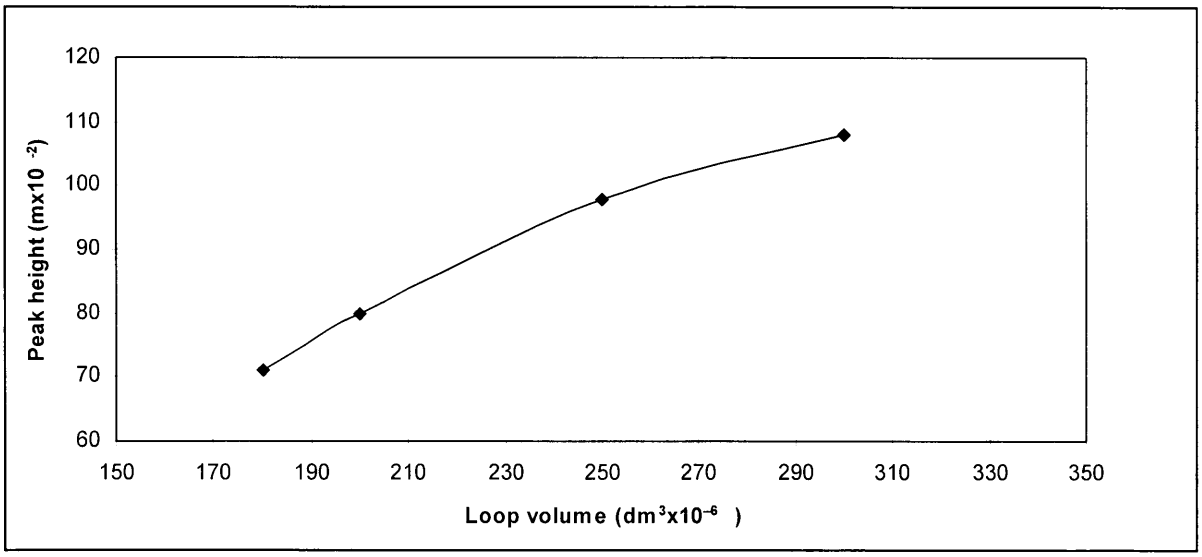

Figure 6.8: The effect of loop volume on peak height

Increased sulphuric acid concentration decreased the response, but an acidic environment is necessary for this chemical reaction, therefore the sulphuric acid

concentration was optimised in the simplex optimization. (The sulphuric acid concentration was kept constant in the stannous chloride reagent and varied in the molybdic acid reagent, so that the one would not cancel the effect of the other.)

Increasing the stannous chloride concentration in the reagent increased the peak height. However the stannous chloride concentration could not be allowed to be near saturation. If this was the case the cell walls and tubing coated dark blue immediately. The stannous chloride concentration was optimised during the simplex optimization.

Peak height increased with an increase in molybdenum concentration. Therefore the molybdenum concentration was optimised in the simplex optimization.

6.1.3 Simplex optimization

The co - ordinates of the original simplex, together with the boarder values of each factor and the response obtained is given in table 6.1 and the simplex optimization in table 6.2.

The simplex optimization was stopped because it seemed that a pattern was occurring in the co - ordinates. The seventh simplex move was taken as the optimum since it had the highest response.

Table 6.1 The co -ordinates of the original simplex and the boarder values of the factors

	No	coil length (m)	loop volume $\times 10^{-6}$ (dm^3)	pump speed R1 ($cm^3 min^{-1}$)	pump speed R2 ($cm^3 min^{-1}$)	concentration Mo* $\times 10^{-3}$ ($mol.dm^{-3}$)	concentration Sn* $\times 10^{-3}$ ($mol.dm^{-3}$)	concentration H* ($mol.dm^{-3}$)	response absorbance
minimum		0.10	20	0.01	0.01	0.809	0.00	0.00	
maximum		5.00	500	3.00	3.00	24.273	2.00	5.600	
	1	2.00	350	0.50	0.50	8.019	1.000	0.450	0.5156
	2	1.90	340	0.55	0.55	7.929	0.900	0.443	0.3723
	3	2.10	330	0.60	0.60	7.767	0.800	0.458	0.3369
	4	1.80	320	0.65	0.65	7.606	0.720	0.466	0.4094
	5	2.20	310	0.70	0.70	7.444	0.640	0.473	0.2873
	6	1.70	300	0.75	0.75	7.282	0.560	0.481	0.3506
	7	2.30	290	0.80	0.80	7.120	0.480	0.488	0.3481
	8	1.60	280	0.85	0.85	6.958	0.400	0.496	0.3687

*H = H_2SO_4
*Mo = $(NH_4)_6Mo_7O_{24}.4\ H_2O$
*Sn = $SnCl_2.H_2O$

Table 6.2 The information on the simplex optimization.

No	coil length (m)	loop volume $\times 10^{-6}$ (dm^3)	pump speed R1 (cm^3min^{-1})	pump speed R2 (cm^3min^{-1})	concentration Mo* $\times 10^{-3}$ ($mol.dm^{-3}$)	concentration Sn* $\times 10^{-3}$ ($mol.dm^{-3}$)	concentration H* ($mol.dm^{-3}$)	response absorbance
1st SM	1.63	321	0.64	0.64	7.630	0.748	0.464	0.3994
2nd SM	1.59	299	0.76	0.76	7.266	0.574	0.481	0.2451
NC,F, 2nd WV	1.97	322	0.64	0.64	7.646	0.744	0.464	0.2344
3rd SM	1.34	350	0.50	0.50	2.091	0.986	0.443	0.3485
4th SM	1.32	316	0.67	0.67	7.549	0.718	0.470	0.4109
5th SM	2.08	286	0.82	0.82	7.055	0.456	0.492	0.2025
NC S	1.52	334	0.58	0.58	7.840	0.854	0.455	0.4477
6th SM	1.66	346	0.52	0.52	8.034	0.966	0.447	0.5806
7th SM	1.64	369	0.40	0.40	8.407	1.168	0.428	0.6514
8th SM	1.78	392	0.29	0.29	8.771	1.346	0.411	0.8034
9th SM	1.44	345	0.52	0.52	8.034	0.972	0.457	0.5247
10thSM	1.66	372	0.39	0.39	8.455	1.188	0.432	0.5278
11thSM	1.45	389	0.31	0.31	8.722	1.350	0.421	0.7795
	1.48	340	0.55	0.55	7.937	0.922	0.453	

NC = negative contraction
SM = simplex move
F = failed
R = reject
W = worst
V = vertex
S = successful

6.1.4 Factor optimization

The peaks at this stage in the optimization was double humped peaks. The first hump was bigger than the second hump. The second hump was considered the response peak due to it's position and the fact that only it grew or shrank as the concentration of analyte increased or decreased. The existence of the first hump made it difficult to electronically detect the absorbance of the smaller peaks of the smaller analyte concentrations. Various authors have reported double humped peaks and have given possible reasons for their occurrence. The occurrence of a chemical reaction favours the appearance of the double peak for large injection volumes under conditions in which a single peak due entirely to physical dispersion would be obtained in the absence of a chemical reaction. This kind of double peak results from the concentration gradients induced by the chemical reaction at both interfaces. The effect of the splitting of the peak is more pronounced when the appearance of the reaction product is measured [4]. When these peaks are present where no chemical reaction is taking place, it only takes the slightest turbulence for the humps to disappear [5]. The ghost peaks disappeared after a few accidental changes which might have caused the desired changes needed to smooth the peaks out. These accidental changes happened because the factor optimization was done a few months after the completion of the simplex optimization and during reassembly of the FIA system the first merging point was accidentally shifted from after the injection point to before it. Because of pressure problems the pump speed of the carrier stream was changed from 3.9 $cm^3.min^{-1}$ to 3.5 $cm^3.min^{-1}$ and the sulphuric acid was also accidentally left out of reagent 1. Either one or all of these

changes could have caused the ghost peak to disappear. Since it was desirable not to have a ghost peak, conditions was not changed back to their simplex optimised states.

The sulphuric acid in reagent 2 was factor optimised and the optimum concentration was found to be 0.376 mol.dm^3. The stannous chloride concentration was also factor optimised and found to be 0.886×10^{-3} mol.dm^{-3}. Factor optimization of the molybdate reagent showed that even though their was an increase in peak height if the molybdate concentration was increased up to the point specified by the simplex optimization, these high concentrations lead to less repeatable results and unacceptable coating of the tube and cell walls. A molybdate concentration of 5.24×10^{-3} mol.dm^{-3} $(NH_4)_6Mo_7O_{24}.4\ H_2O$ was chosen as compromise between peak height and repeatability. The optimum values for the physical factors did not change during factor optimization.

The final flow injection system is illustrated in figure 6.9 and the final optimised values for the physical and chemical factors are given in table 6.3.

6.1.6 Evaluation

Figure 6.10 is an illustration of the graph of the absorbance as a function of the concentration of phosphate - P. The equation describing the graph is:

$y = 0.04316 + 222671x$ with r^2 equal to 0.9998.

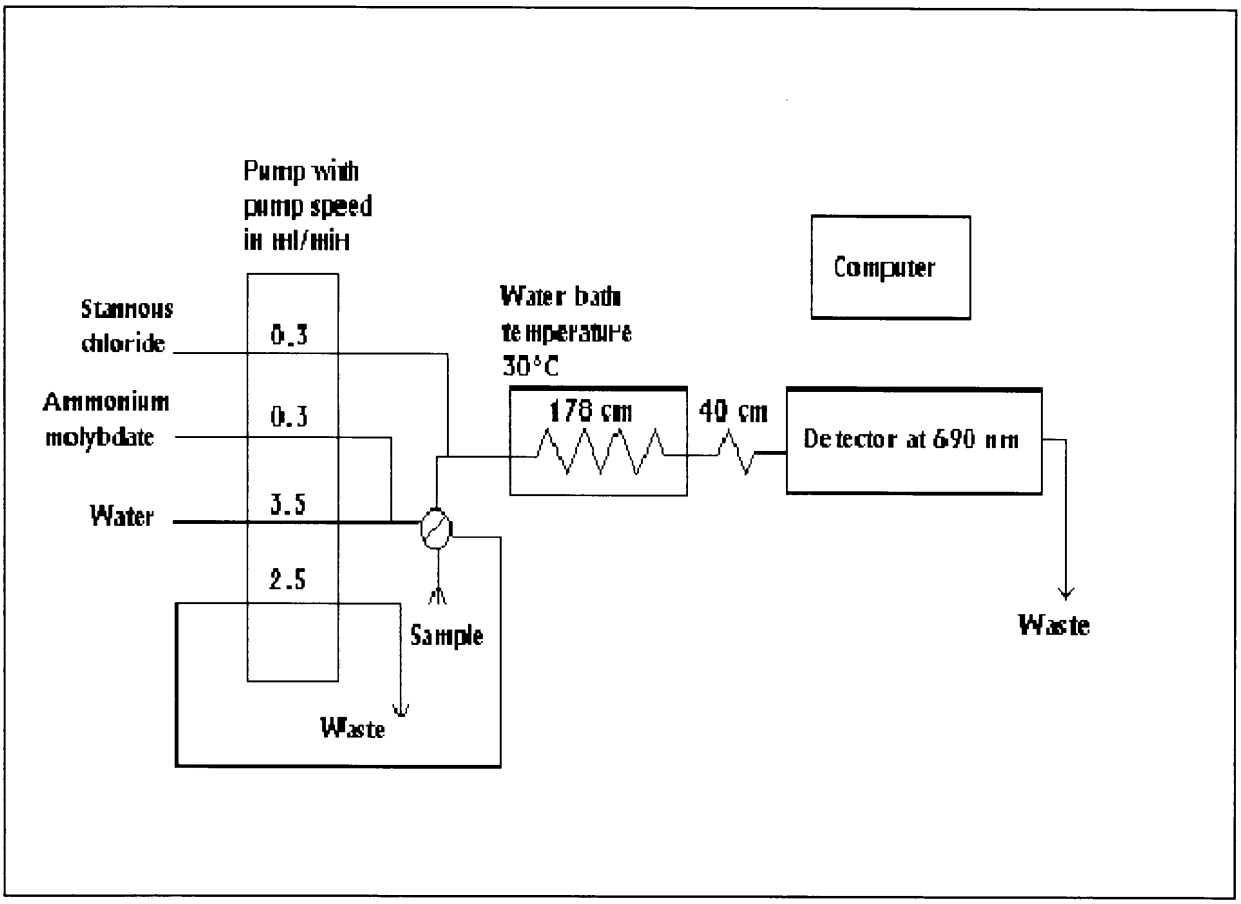

Figure 6.9 The final flow injection system

Table 6.3 The final values for some of the factors

Factor	Characteristics
Sample loop volume	392×10^{-6} dm^3
carrier	H_2O
reagent 1	5.243×10^{-3} mol.dm^{-3} $(NH_4)_6Mo_7O_{24}.4\ H_2O$ 0.004% Sodium Laurel sulphate
reagent 2	1.537×10^{-2} mol.dm^{-3} $N_2H_6SO_4$ 0.3756 mol.dm^{-3} H_2SO_4 0.8864×10^{-3} mol.dm^{-3} $SnCl_2.2\ H_2O$
Temperature	30°C

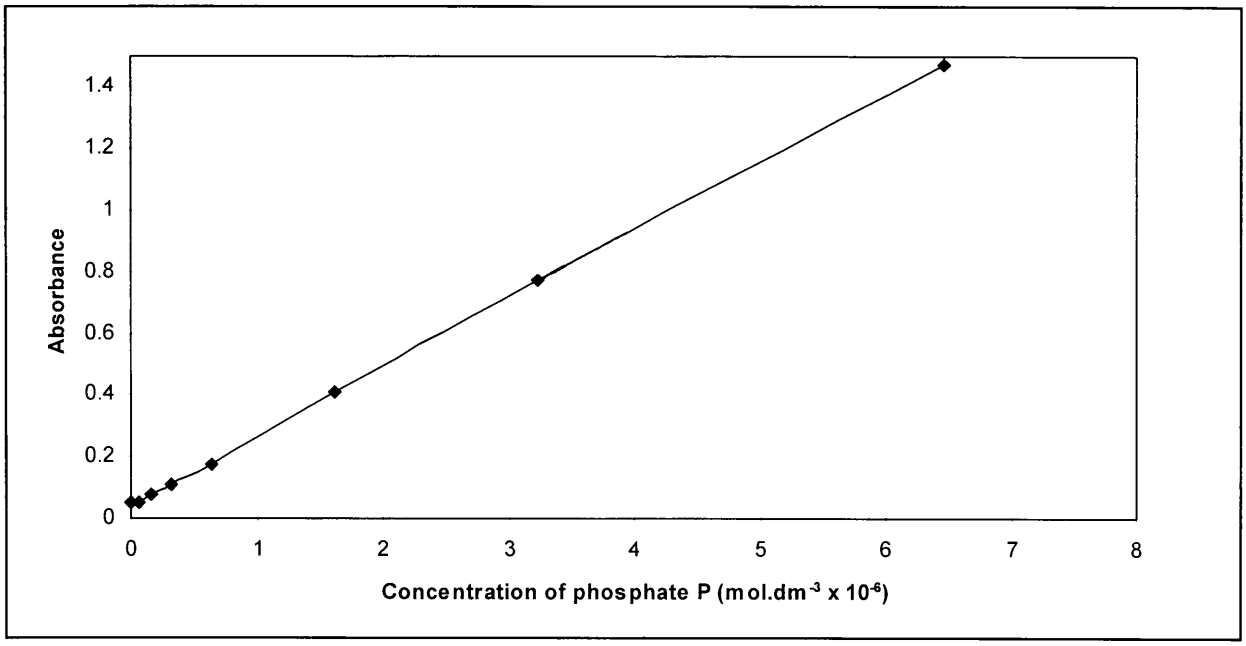

Figure 6.10. Absorbance as a function of phosphate P concentration

The evaluation of the method is given in table 6.4.

Table 6.4 The evaluation of the method

linearity	1.28×10^{-7} - 6.46×10^{-6} (4 - 200 μg.dm^{-3})
detection limit	1.28×10^{-7} mol.dm^{-3} (4 μg.dm^{-3})
recovery of 0.646×10^{-6} mol.dm^{-3} P (tap water)	98 %
recovery of 0.323×10^{-6} mol.dm^{-3} P (bore hole water)	101 %
carry over (6.457×10^{-6} mol.dm^{-3} P on 6.457×10^{-7} mol.dm^{-3} P)	1.08 %
repeatability (6.457×10^{-7} mol.dm^{-3} P)	$\pm 2.294 \times 10^{-8}$ mol.dm^{-3} (n = 47)
sample throughput	55 samples per hour

The rate of sample throughput was measured with a valve that contained one loop. This was done not to compromise on repeatability and detection limit due to slight differences in the sizes of the two sample loops. The baseline - to - baseline time of the peaks were only 45 seconds so the method could in actual fact analyse 80 samples per hour. $P_2O_5^{4-}$ and Hg(II) interfered with the analysis. pH did not interfere with the analysis.

6.2 Ascorbic acid as reductant

6.2.1 Preliminary optimization of the physical factors

For the system where ascorbic acid was the reductant 880 nm gave better response values than 690 nm.

The effect of the sample volume on the absorbance is portrayed in figure 6.11. This is consistent with the theory of flow injection [1]. This factor was included in the simplex optimization.

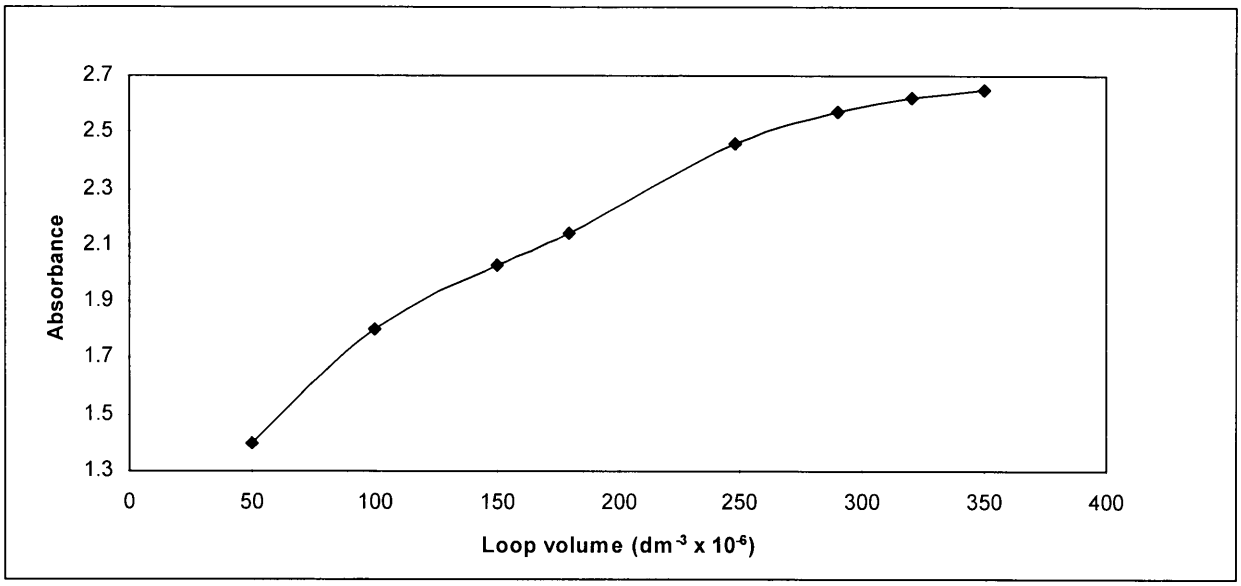

Figure 6.11: The effect of the sample volume on the absorbance

Figure 6.12 is a graph of the absorbance is a function of the coil length. The absorbance was a maximum at a coil length of around one meter. The reason for the shape of this curve was possibly that at shorter coil lengths the reaction had not proceeded far enough and at longer coil lengths the greater dispersion flattened the peaks again. This factor was included in the simplex optimization.

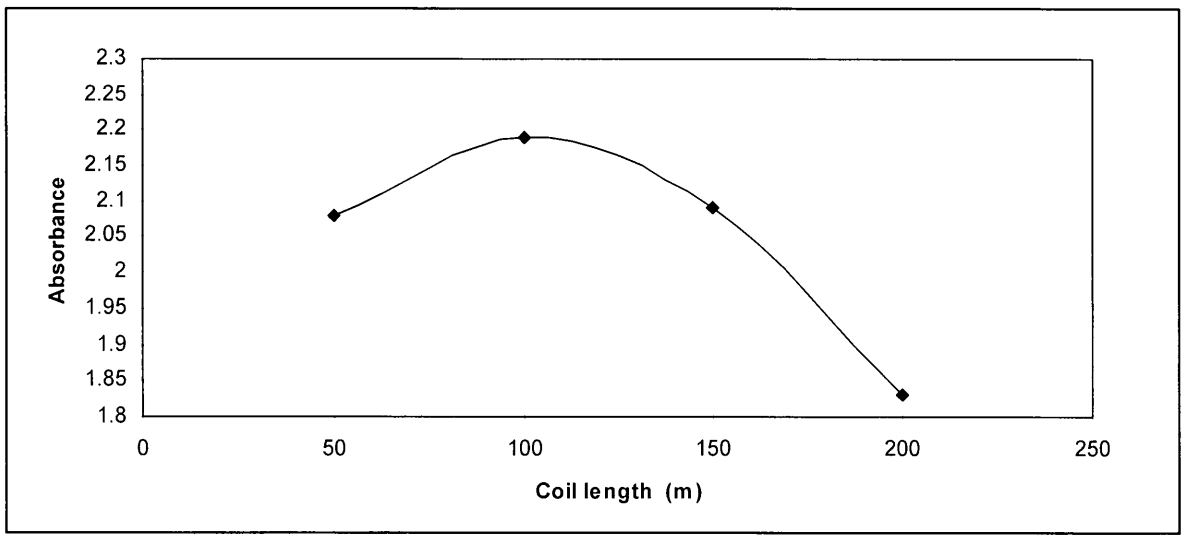

Figure 6.12: Absorbance as a function of coil length

Absorbance as a function of the pump speed of the molybdate reagent (R1) carrying stream is shown in figure 6.13. The response reached a maximum at 0.80 $cm^3.min^{-1}$. The reason for the shape of this curve was probably the same as for the first method. This factor was also optimised by the simplex optimization.

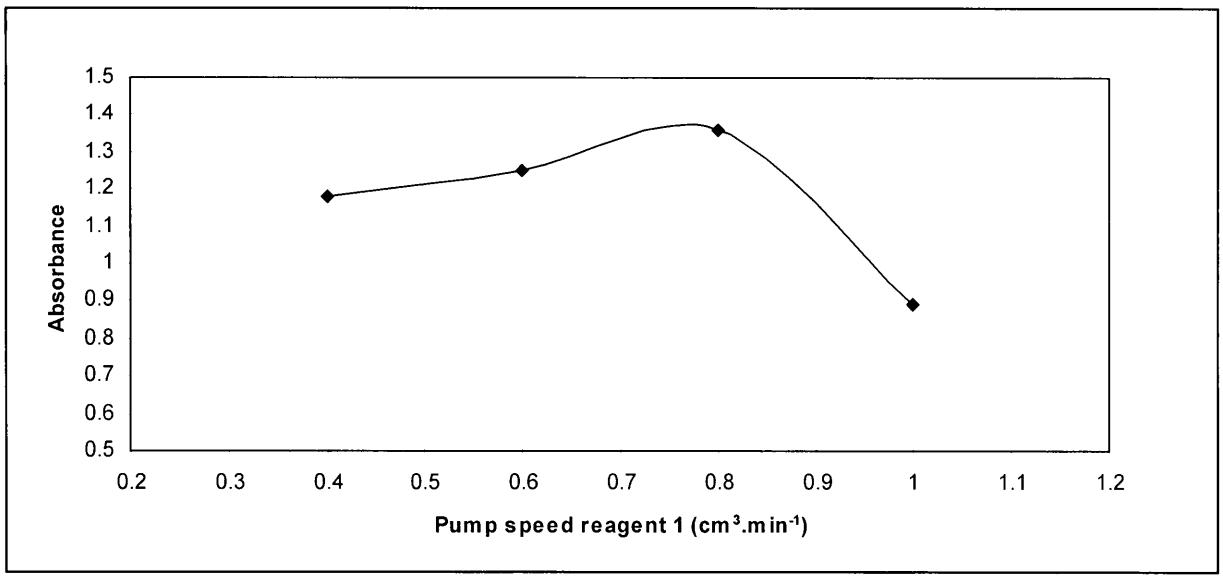

Figure 6.13: Absorbance as a function of pump speed (R1)

The effect of the pump speed of the ascorbic acid carrying reagent (R2) on the absorbance is shown in figure 6.14. The absorbance reached a maximum around a pump speed of 0.6 $cm^3.min^{-1}$ of the ascorbic acid carrying reagent. This factor was optimised during simplex optimization.

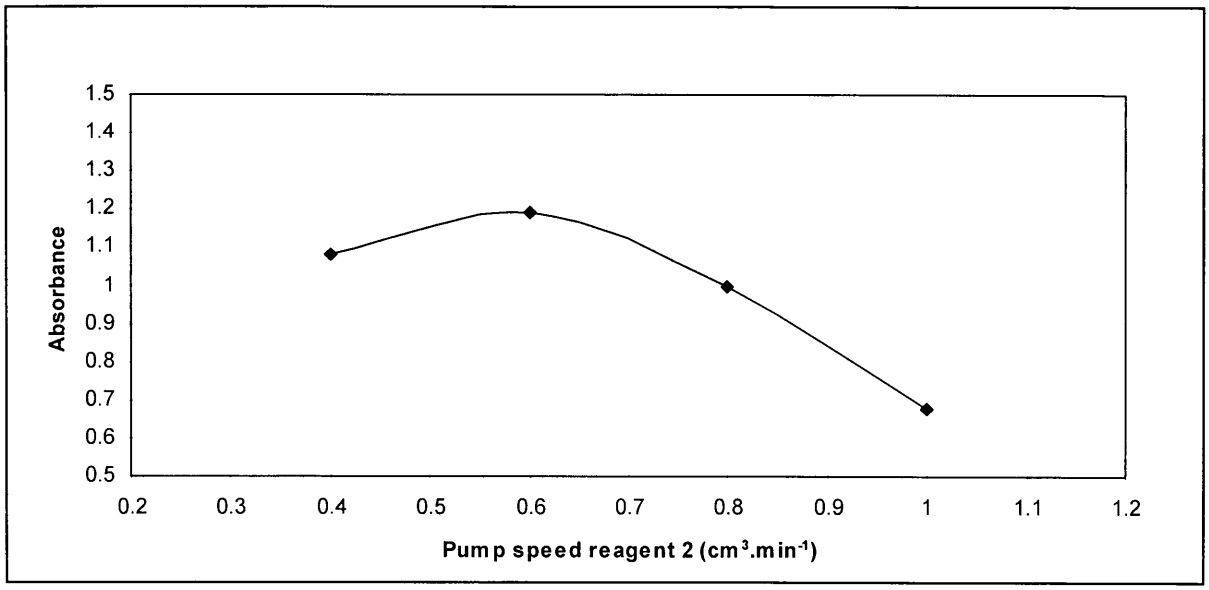

Figure 6.14: Absorbance as a function of pump speed of reagent 2 (R2)

Absorbance increased as the pump speed of the carrier stream increased. This is consistent with the theory of flow injection systems. A maximum of 3.90 cm^3. min^{-1} was taken as the optimum. Sample stream pump speed was kept at 2.50 $cm^3.min^{-1}$.

The absorbance increased with temperature up to 40°C. Beyond 40°C the absorbance decreased with increase in temperature. The reason is probably the same as for the first method. The absorbance as a function of temperature is shown in figure 6.15. The temperature was set at 40°C.

6.2.2 Preliminary optimization of the chemical factors

Experiments proved that antimony tartrate only remained in solution under very low pH conditions. Since SLS (sodium laurel sulphate) increased pH, it was not included in this method.

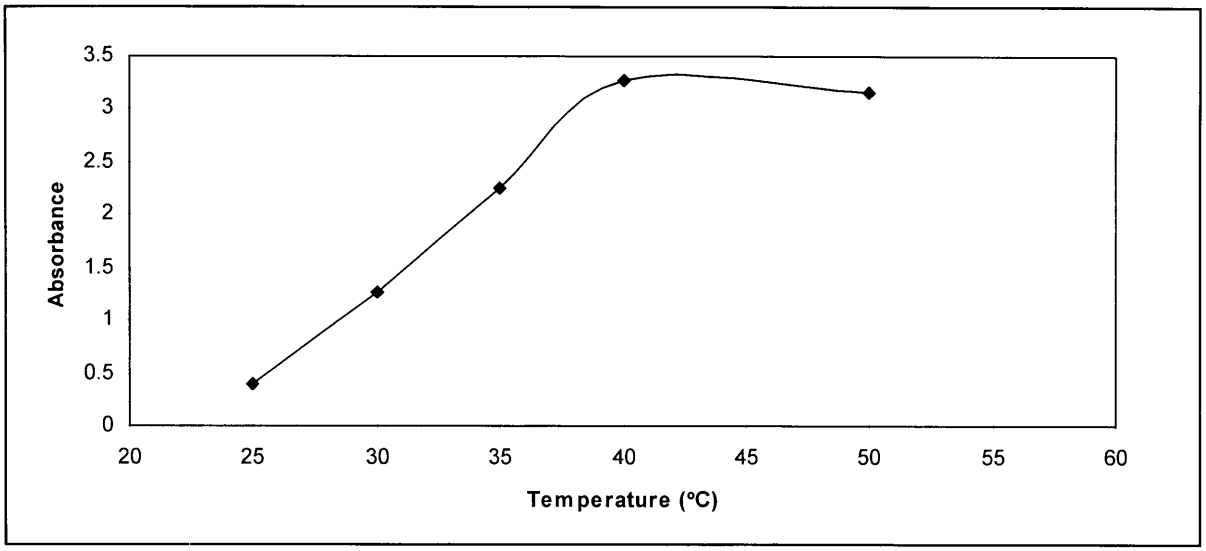

Figure 6.15: Absorbance as a function of temperature

Peak height increased as antimony tartrate concentration increased. This relationship is illustrated in figure 6.16. Peak height increased as pH increased. This is depicted in figure 6.17. For this reason the maximum amount of antimony that could dissolve in a minimum amount of acid was used to make the reagent. This was 0.30 g potassium antimony tartrate and 0.022 dm^3 H_2SO_4 in 0.5 dm^3 of H_2O, which was 1.719 x 10^{-3} $mol.dm^{-3}$ $K(Sb0)C_6H_4O_6$ and 0.8264 $mol.dm^{-3}$ H_2S0_4. There was little increase in peak height above 5 g $(NH_4)_6Mo_7O_{24}.4\ H_2O$ in 0.5 dm^3. Thus this reagents' final concentration in $(NH_4)_6Mo_7O_{24}.4\ H_2O$ was 8.09 x 10^{-3} $mol.dm^{-3}$. $K(SbO)C_6H_4O_6$, H_2SO_4 and $(NH_4)_6Mo_7O_{24}.4\ H_2O$ was combined in reagent 1. Figure 6.18 is a graph of absorbance as a function of molybdate concentration.

Increasing the ascorbic acid concentration increased the peak height up to an ascorbic acid concentration of 50 g per 0.5 dm^3 (0.5678 $mol.dm^{-3}$) after which peak height did not increase significantly with increasing ascorbic acid concentration. Figure 6.19 is a graph of absorbance as a function of ascorbic acid concentration.

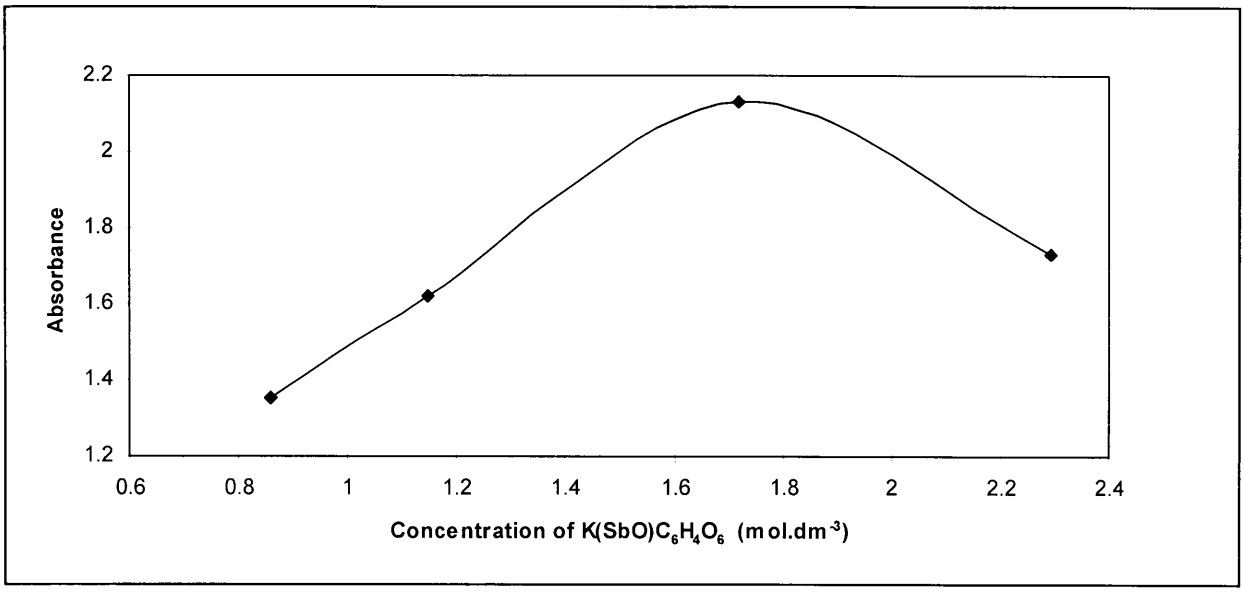

Figure 6.16: Absorbance as a function of antimony concentration

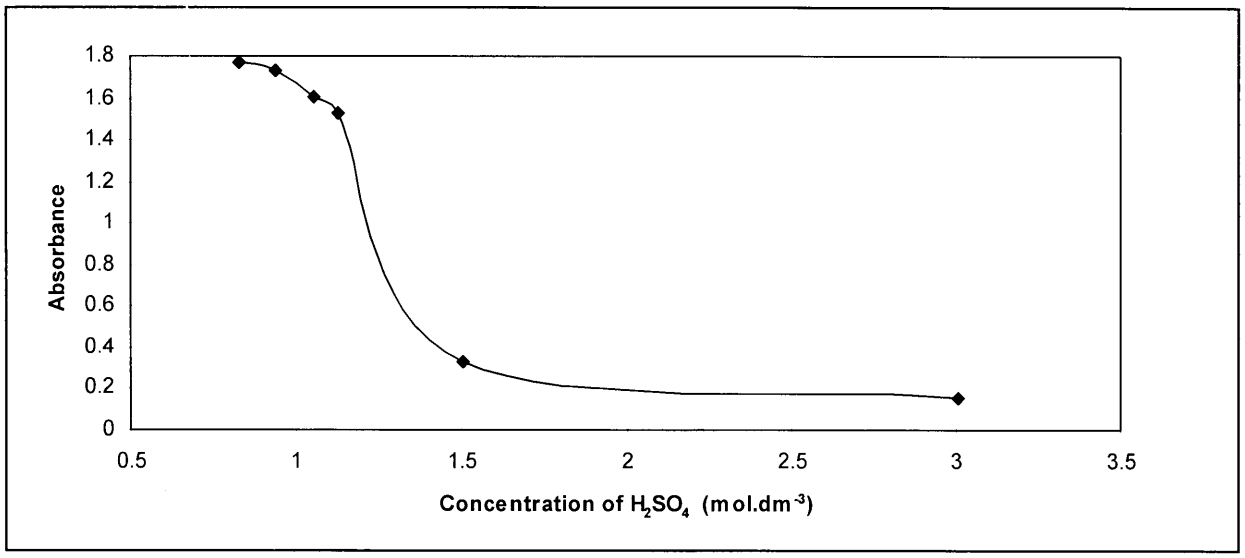

Figure 6.17: Absorbance as a function of pH

6.2.3 Simplex optimization

Table 6.5 contains the co - ordinates of the original simplex and the boundary conditions of the factors. Table 6.6 contains the information on the simplex

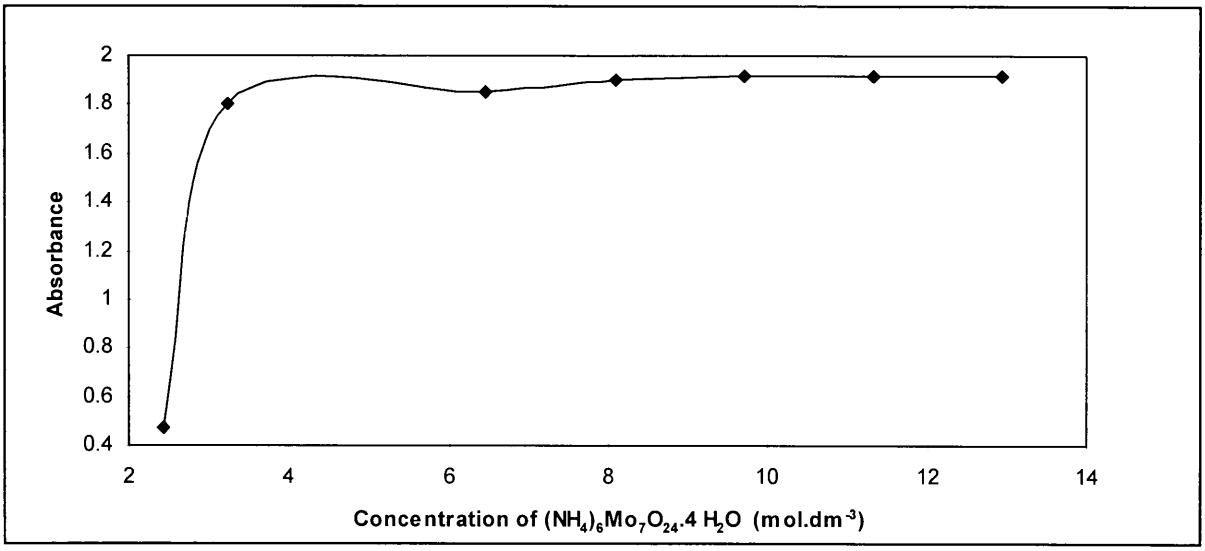

Figure 6.18: Absorbance as a function of molybdate concentration

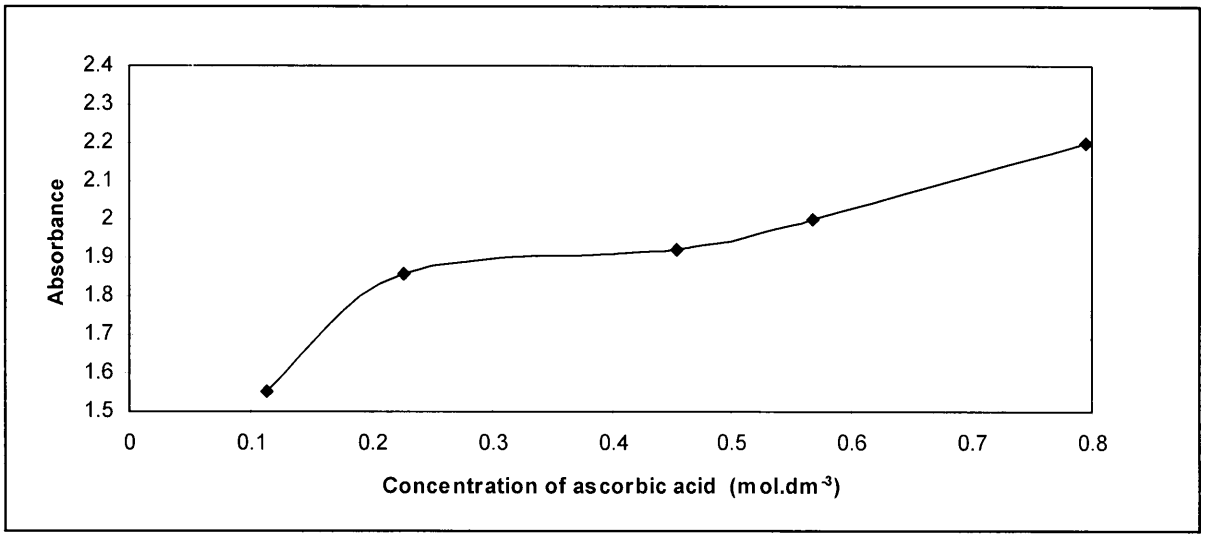

Figure 6.19: Absorbance as a function of ascorbic acid concentration

optimization. Simplex optimization was stopped when there was no longer any significant change in the values of the factors or the responses. The negative contraction marked with the asterisks, just after the 30th simplex move, was taken as the optimum co - ordinates.

Table 6.5 The co - ordinates of the original simplex and the boundary conditions of the factors

	NUMBER	COIL LENGTH m	LOOP VOLUME x 10^{-6} dm^3	PUMP SPEED REAGENT 1 $cm^3.min^{-1}$	PUMP SPEED REAGENT 2 $cm^3.min^{-1}$	RESPONSE ABSORBANCE
minimum maximum		0.01 5.00	20 500	0.03 3.90	0.3 3.90	
	1 2 3 4 5	1.00 0.50 0.55 0.75 0.40	100 110 120 130 150	0.47 0.42 0.60 0.32 0.65	0.52 0.32 0.65 0.42 0.60	0.8325 0.6067 0.8418 0.7744 0.9458

Table 6.6 The simplex optimization

TYPE OF SYMPLEX MOVE (SM)	CIOL LENGTH m	LOOP VOLUME $X10^{-6}$ dm^3	PUMP SPEED REAGENT 1 ($cm^3.min^{-1}$)	PUMP SPEED REAGENT 2 ($cm^3.min^{-1}$)	RESPONSE ABSORBANCE
1st SM	0.85	140	0.60	0.78	0.9258
2nd SM	0.65	125	0.84	0.85	0.8413
3rd SM	0.23	168	0.88	0.92	0.7197
NC	0.81	117	0.57	0.62	0.8608
4th SM	0.65	139	0.37	0.47	0.8917
5th SM	0.81	153	0.50	0.58	0.9815
EXP Symp.	0.93	169	0.44	0.55	1.0493
6th SM	0.61	182	0.46	0.58	1.1211
EXP Symp.	0.51	214	0.41	0.55	1.2529
7th SM	0.70	198	0.68	0.77	1.0810
8th SM	0.42	226	0.49	0.46	1.1380
9th SM	0.88	254	0.36	0.57	1.3657
EXP Symp.	1.12	306	0.22	0.55	1.3642
10th SM	0.32	277	0.53	0.63	1.2720
11th SM	0.38	287	0.21	0.35	0.7188
NC	0.62	221	0.56	0.66	1.2027
12th SM	0.75	257	0.44	0.74	1.2457
13th SM	0.62	281	0.30	0.59	1.2598
14th SM	0.42	256	0.36	0.42	1.1809
NC	0.67	256	0.42	0.66	1.3320
15th SM	0.73	320	0.40	0.67	1.4095
EXP Symp.	0.84	372	0.39	0.73	1.4412
16th SM	0.74	300	0.55	0.71	1.3505
17th SM	1.24	314	0.33	0.70	1.2915
POS.C	1.01	305	0.38	0.69	1.3385
18th SM	1.07	359	0.42	0.68	1.3888
19th SM	0.75	337	0.48	0.66	1.4010
20th SM	0.82	430	0.56	0.82	1.5412

TYPE OF SIMPLEX MOVE(SM)	COIL LENGTH m	LOOP VOLUME x 10^{-6} dm^3	PUMP SPEED REAGENT 1 (cm^3 min^{-1})	PUMP SPEED REAGENT 2 ($cm^3.min^{-1}$)	RESPONSE ABSORBANCE
21st SM	1.00	450	0.38	0.73	1.5641
22nd SM	0.64	437	0.49	0.79	1.5682
EXP Symp.	0.42	475	0.52	0.84	1.4924
23rd SM	0.79	380	0.47	0.71	1.5242
24th SM	0.78	475	0.56	0.80	1.6098
25th SM	0.80	414	0.48	0.75	1.5347
26th SM	0.82	482	0.51	0.82	1.5686
27th SM	0.81	492	0.41	0.75	1.6119
28th SM	0.52	493	0.60	0.84	1.4864
NC	0.88	461	0.44	0.76	1.5596
29th SM	0.75	456	0.47	0.78	1.5140
30th SM	0.96	494	0.45	0.77	1.4715
NC	0.80	465	0.47	0.78	1.5713
31st SM	0.90	464	0.43	0.76	1.5042
Check 7th SM	0.70	493	0.54	0.81	1.5213
32nd SM	0.79	486	0.51	0.80	1.4349
33rd SM	0.73	480	0.47	0.75	1.5459
34th SM	0.85	464	0.41	0.73	1.4829
NC	0.74	486	0.51	0.79	1.5478
35th SM	0.83	479	0.50	0.81	1.5532
36th SM	0.87	470	0.46	0.78	1.4975

exp = expanded simplex, NC = negative contraction

6.2.4 The factor optimization

The factor optimization proved that the simplex optimization was on target. Figure 6.20 to figure 6.23 illustrates the factor optimization.

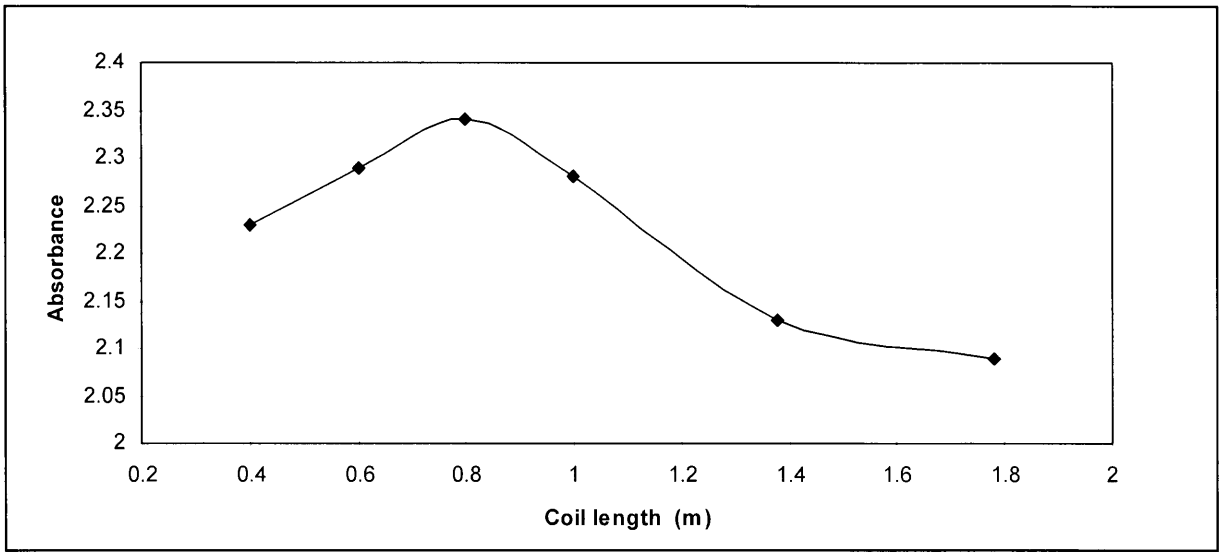

Figure 6.20 Optimization of coil length

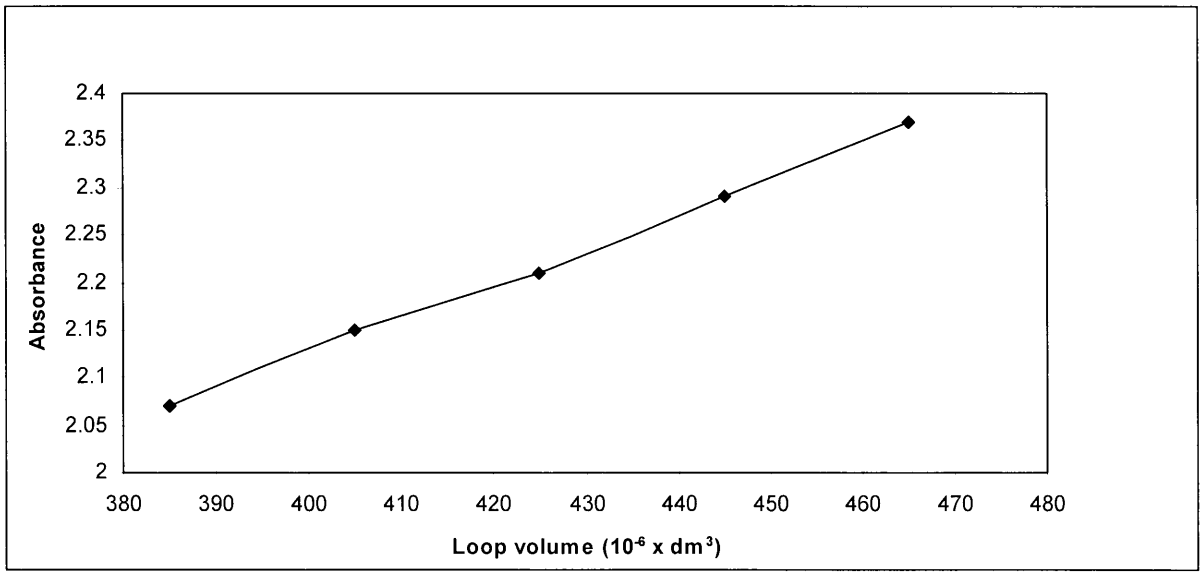

Figure 6.21 Optimization of sample volume

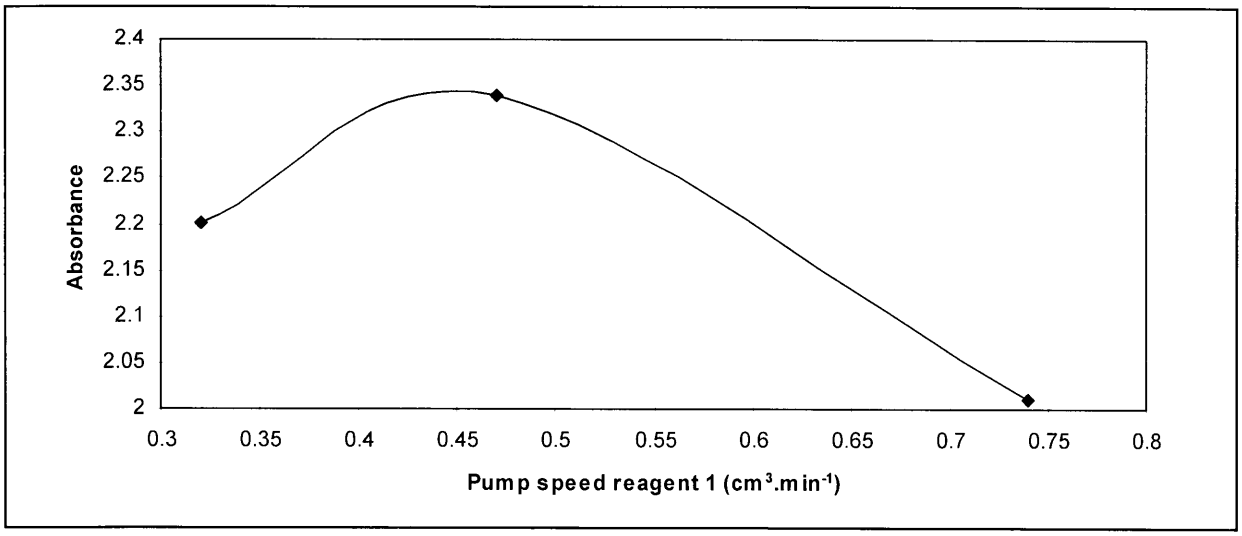

Figure 6.22 Optimization of reagent 1 pump speed

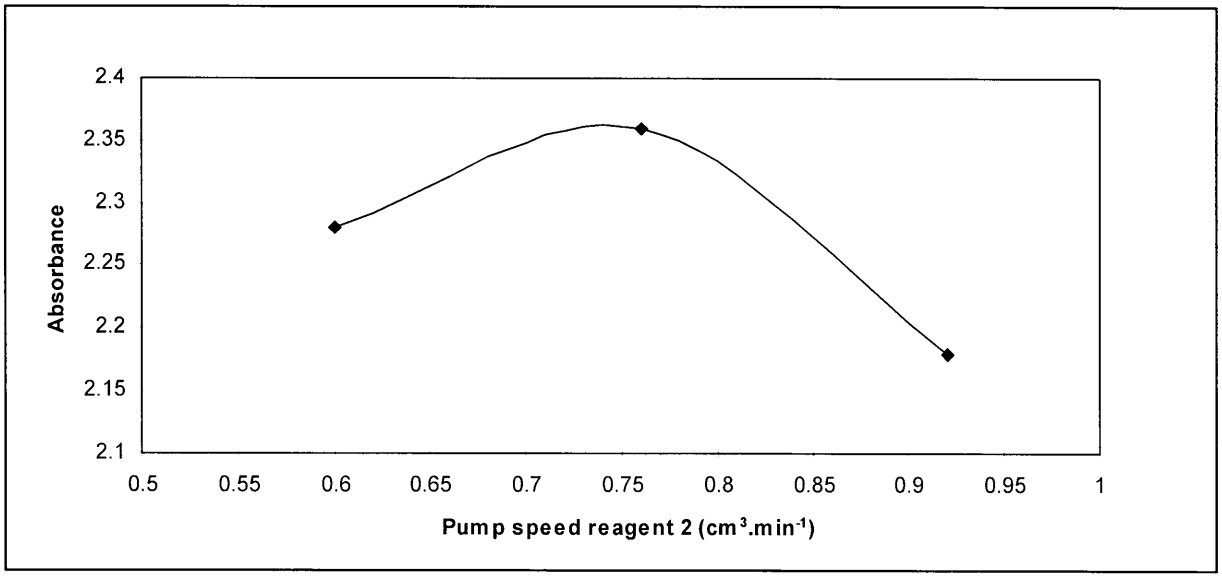

Figure 6.23 Optimization of reagent 2 pump speed

Figure 6.24 and Table 6.7 gives the final flow injection system and the final optimised physical and chemical parameters.

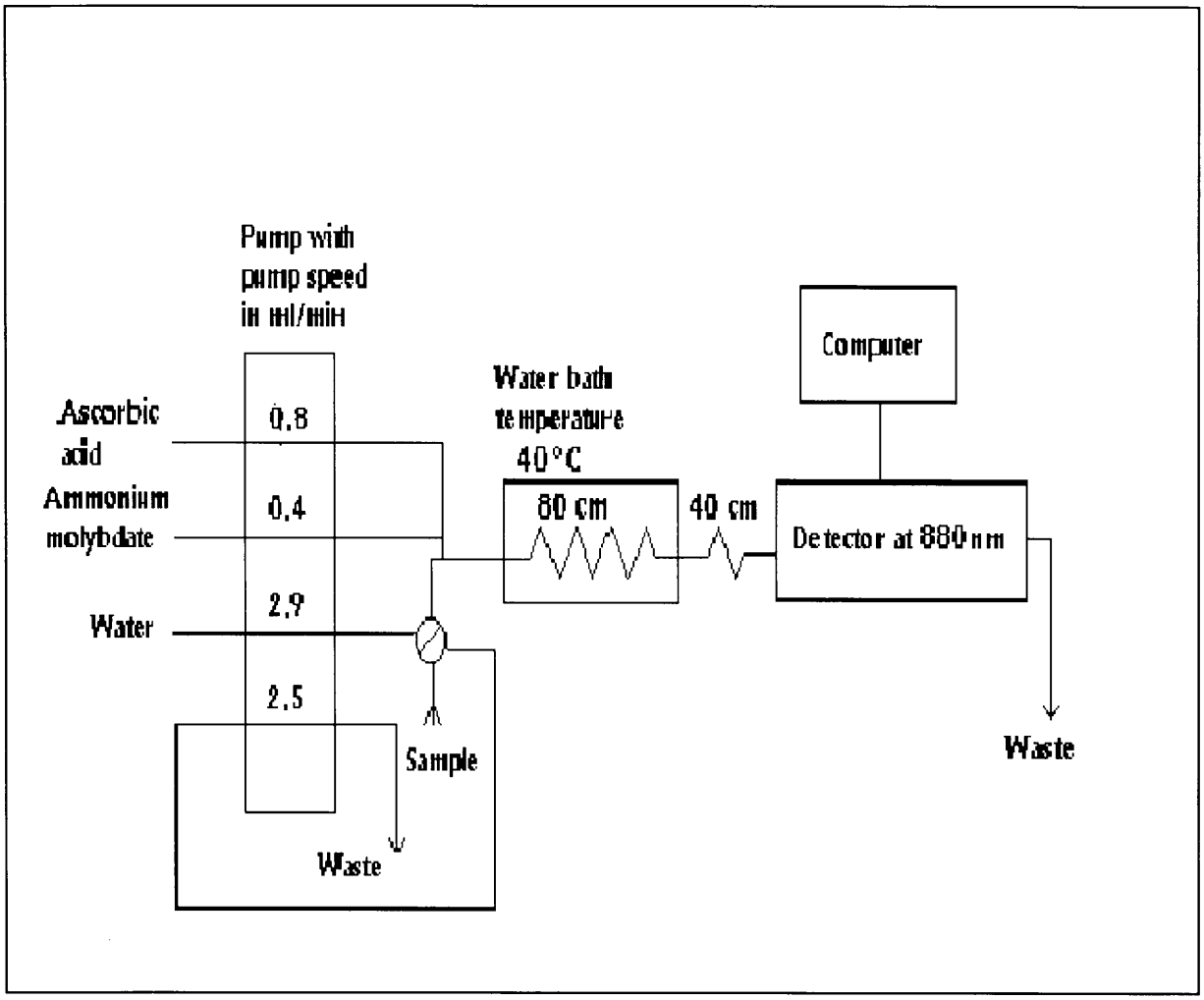

Figure 6.24: The final flow injection system

Table 6.7 The final optimised physical and chemical parameters

FACTOR	CHARACTERISTICS
TEMPERATURE SAMPLE	40°C
LOOP VOLUME	465 X $10^{-6}dm^3$
REAGENT 1	1.719 X 10^{-3} mol.dm^{-3} $K(Sb0)C_6H_4O_6$ 0.8264 mol.dm^{-3} H_2SO_4 8.91 x 10^{-3} mol.dm^{-3} $(NH_4)_6Mo_7O_{24}.4\ H_2O$
REAGENT 2	0.5678 mol.dm^{-3} ascorbic acid
CARRIER	H_2O

6.2.5 Evaluation

The method is linear between 20 x 10^{-7} mol.dm^{-3} P (50 - 400 mg.kg^{-1} P). The equation for the straight line is y = 103 706.11 x - 4.12 x 10^{-2} and the correlation coefficient is 0.994. Figure 6.25 shows the absorption as a function of phosphate - P concentration

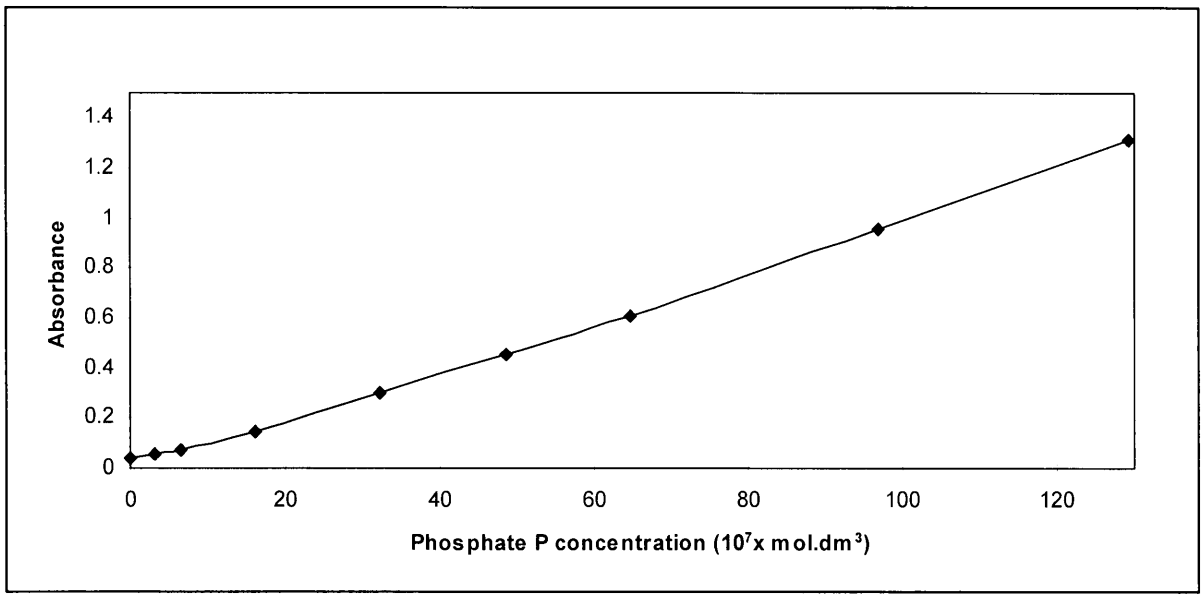

Figure 6.25: The absorption as a function of phosphate - P concentration

The detection limit was 6.6654 x 10^{-7} mol.dm^{-3} phosphate - P (17 mg.kg^{-1}). The percentage carry - over was 0.5 %. The repeatability for the 7th standard was 3.255 x 10^{-6} ± 4.876 x 10^{-8} mol.dm^{-3}. The percentage recovery for 1.614 x 10^{-6} mol.dm^{-3} phosphate - P added to tap water was 101.25 %. The sample throughput rate was 80 samples per hour.

Figure 6.26 shows the interference effect of $Na_2H_2P_2O_7$. The absorbance of the unspoiled sample is marked on the y - axis directly over 0:1 (mole ratio) added $P_2O_5^{4-}$. It appears as though hydrolysis of $P_2O_5^{4-}$ takes place to a great extent.

Hg (II) has a negative interference up to 88:1 mole ratio (Hg (II) : P) and with higher concentrations of Hg (II) the interference becomes positive. At a level of 480:1 the interference is increasing the peak height to nine times its correct value.

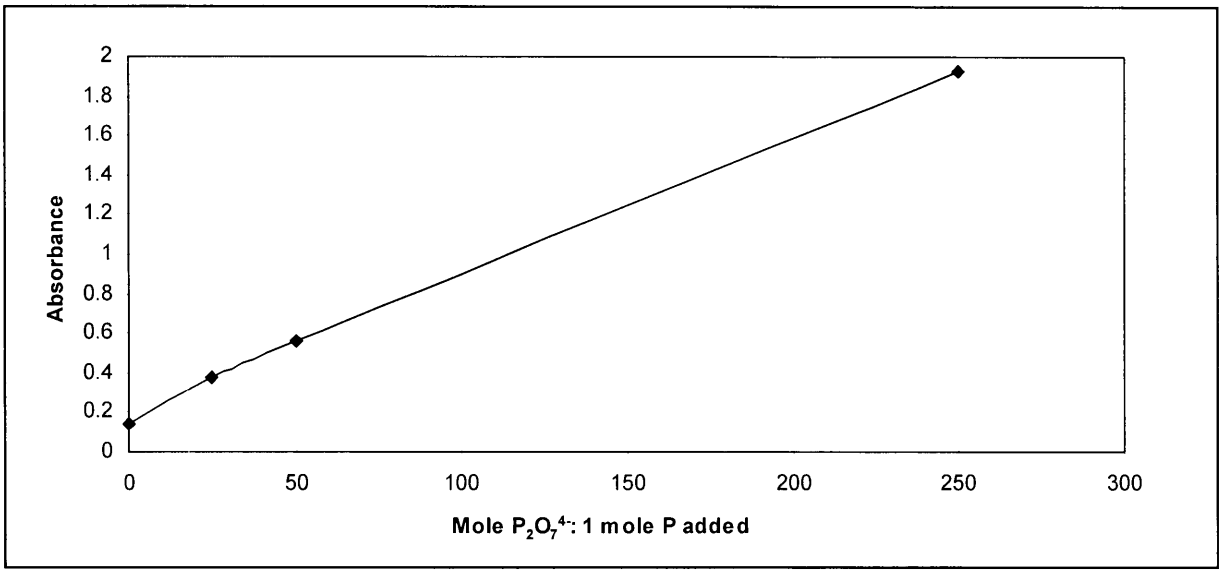

Figure 6.26: The effect of $P_2O_7^{4-}$ on the absorbance

Very low (pH 2.5) and very high (pH 9 and 10) pH values of samples causes positive interferences.

6.3 Malachite green as complexing agent

6.3.1 Preliminary optimization of the physical factors

The optimum wavelength to analyse phosphate with malachite green was found to be 640 nm.

The temperature was found to increase the peak heights when raised and 50°C was found to be the optimum temperature. The reason for this was probably that the raised temperature increased the rate of the reaction and this would decrease the practical dispersion [1]. The temperature was not raised above 50°C since such high temperatures would degrade the tubing material and this would have a negative effect on the tube fittings. The absorbance as a function of temperature is shown in figure 6.27.

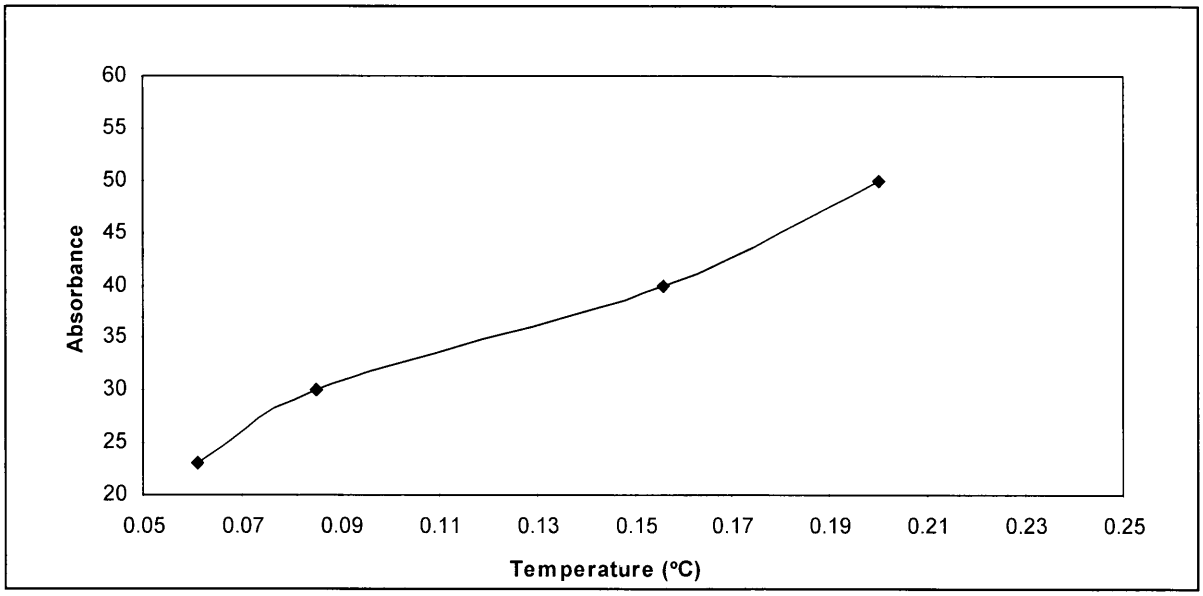

Figure 6.27: Absorbance as a function of temperature

Figure 6.28 shows absorbance as a function of sample volume. Absorbance increased with increasing sample loop volume since the practical dispersion would decrease with increasing sample loop volume. This is consistent with the theory of simplex optimization [1]. Sample loop volume was optimised during simplex optimization.

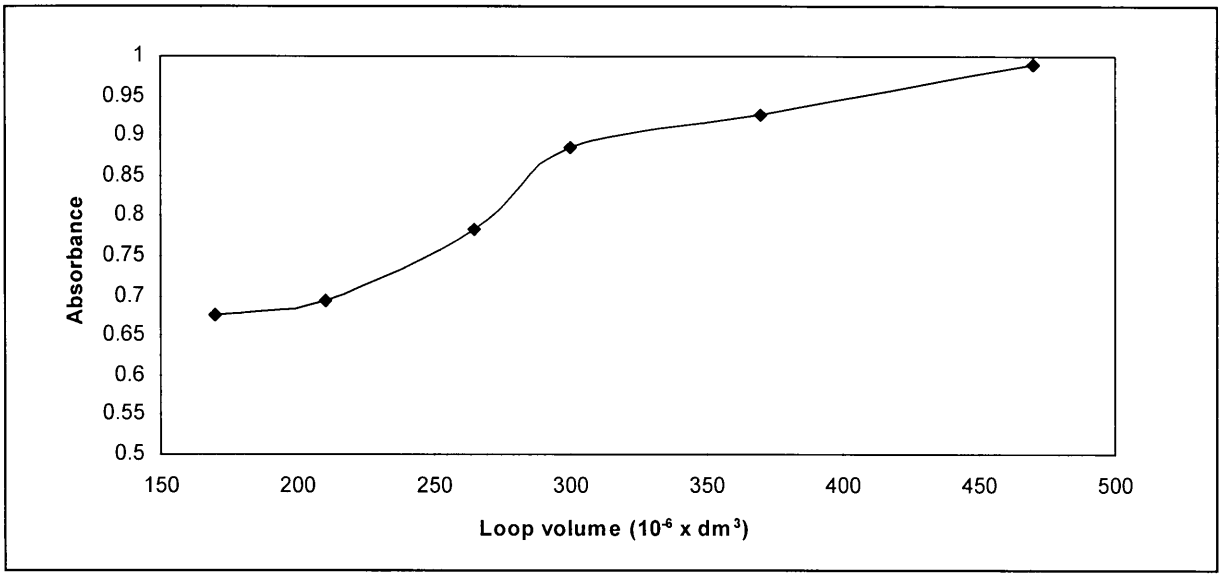

Figure 6.28: Absorbance as a function of sample volume

Peak height increased as the carrier streams' pump speed was increased, as shown in figure 6.29. A higher carrier pump speed would lead to lesser practical dispersion [1]. The pump speed of the carrier stream was included among the factors to be optimised during simplex optimization.

A shorter coil length would lead to a higher signal. This is because dispersion increase with increasing coil length [1]. The absorbance as a function of coil length is shown figure 6.30. The coil length was included among the factors to be optimised during

simplex optimization.

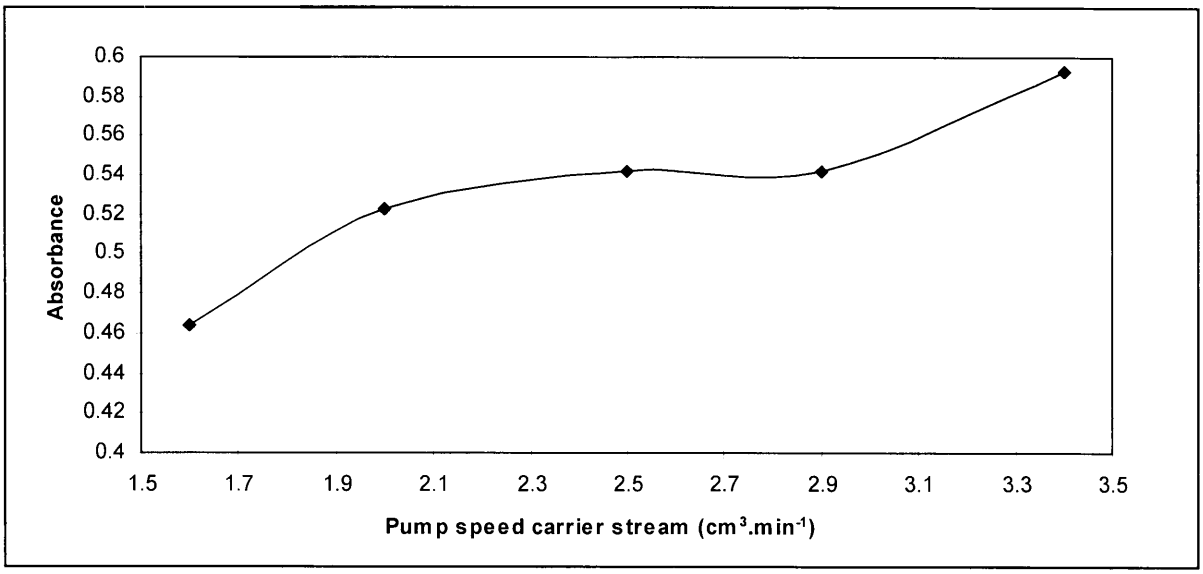

Figure 6.29: Absorbance as a function of carrier stream pump speed.

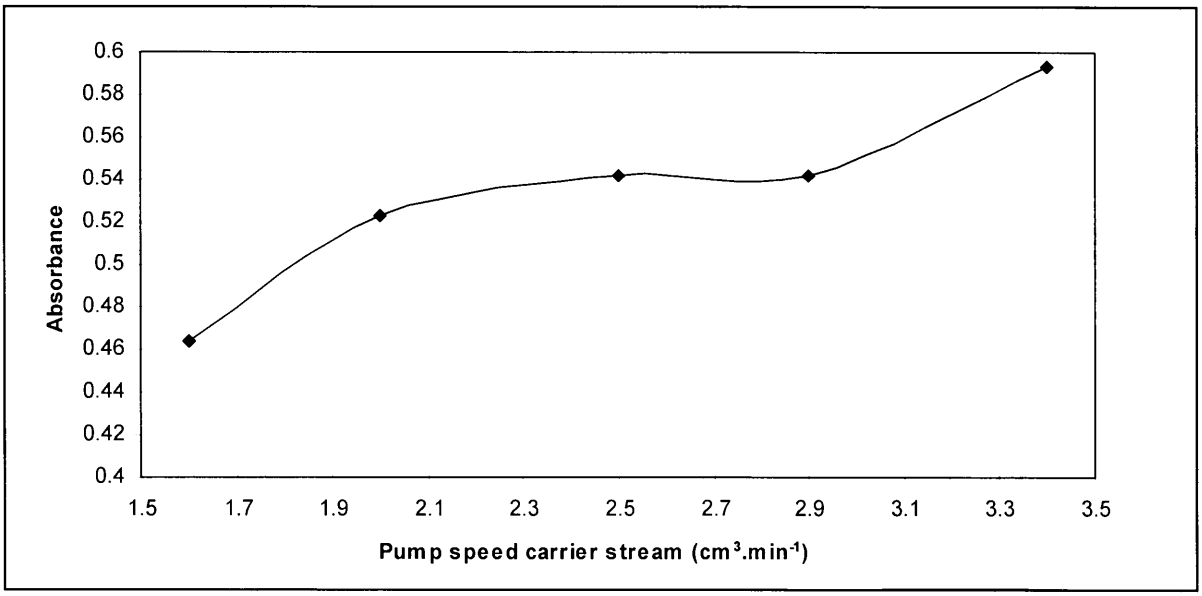

Figure 6.30: Absorbance as a function of coil length

The graph of absorbance as a function of reagent pump speed had a maximum at

0.80 $cm^3.min^{-1}$. The reason for this would be the same as for the other two methods This relationship is illustrated in figure 6.31. This factor was also optimised during simplex optimization.

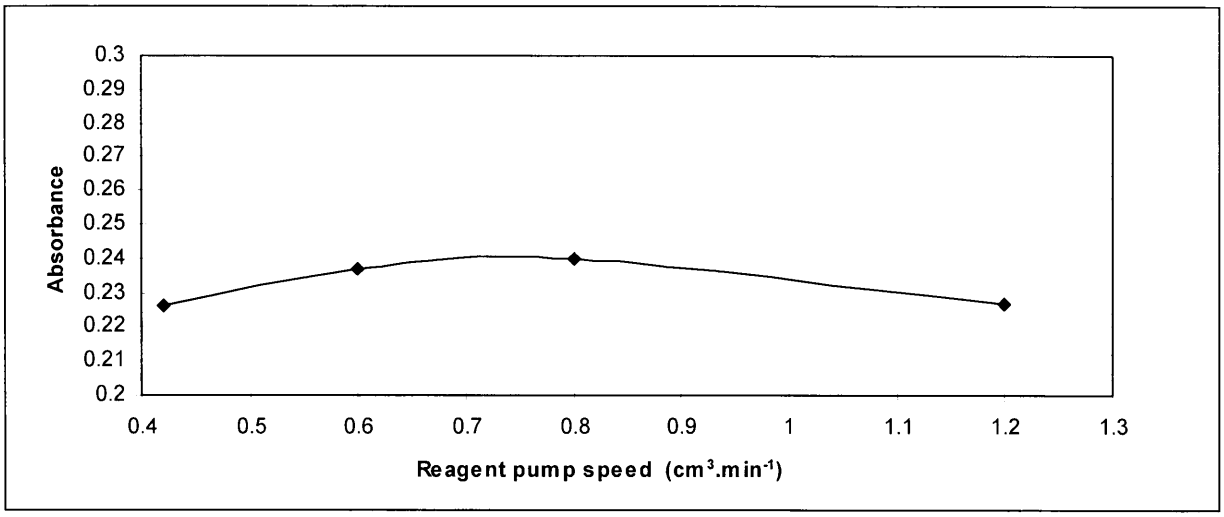

Figure 6.31: Absorbance as a function of reagent pump speed

6.3.2 Preliminary optimization of the chemical factors

Three different wetting agents were investigated and the results are given in figure 6.32. Ethanol was chosen as the best wetting agent since it gave higher peak heights than the other two wetting agents, a lower blank and a graph that was more linear than the graph obtained from sodium laurel sulphate.

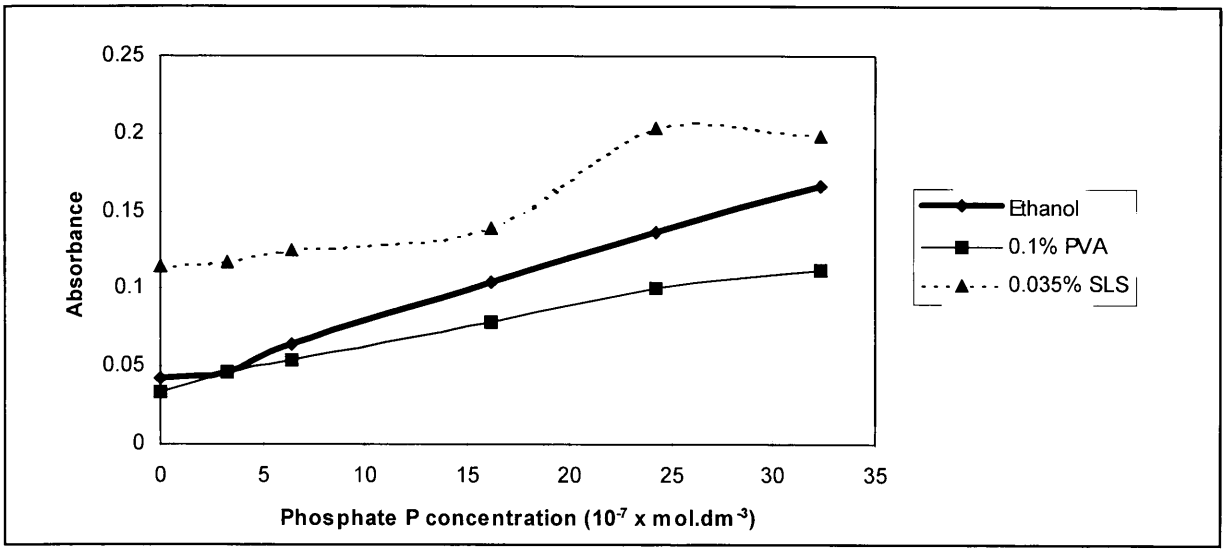

Figure 6.32: Comparison of three wetting agents.

The amount of ethanol in the reagent must be 25 % (V/V) for the best results. The effect of ethanol concentration on peak height is shown in figure 6.33.

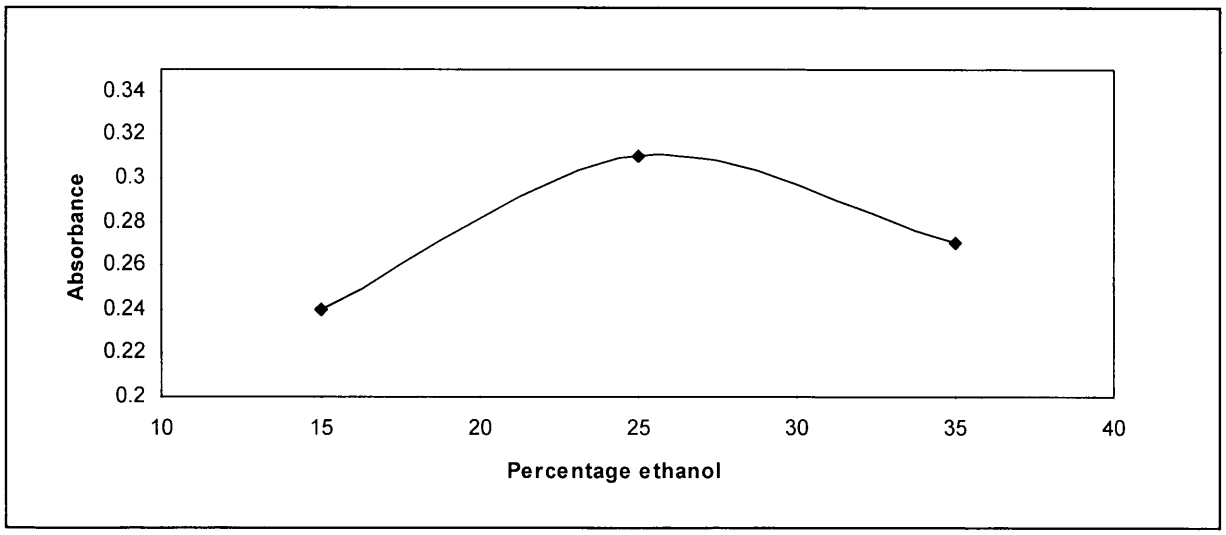

Figure 6.33: Effect of ethanol concentration on peak height

The higher the malachite green concentration the more linear the graph became and the less sensitive the method was at low phosphate concentrations. Figure 6.34 shows

the relationship between malachite green concentration and absorbance.

Increased molybdate - concentration resulted in higher signals and greater sensitivity. Figure 6.35 illustrates the relationships between molybdenum concentration, phosphate concentration and absorbance.

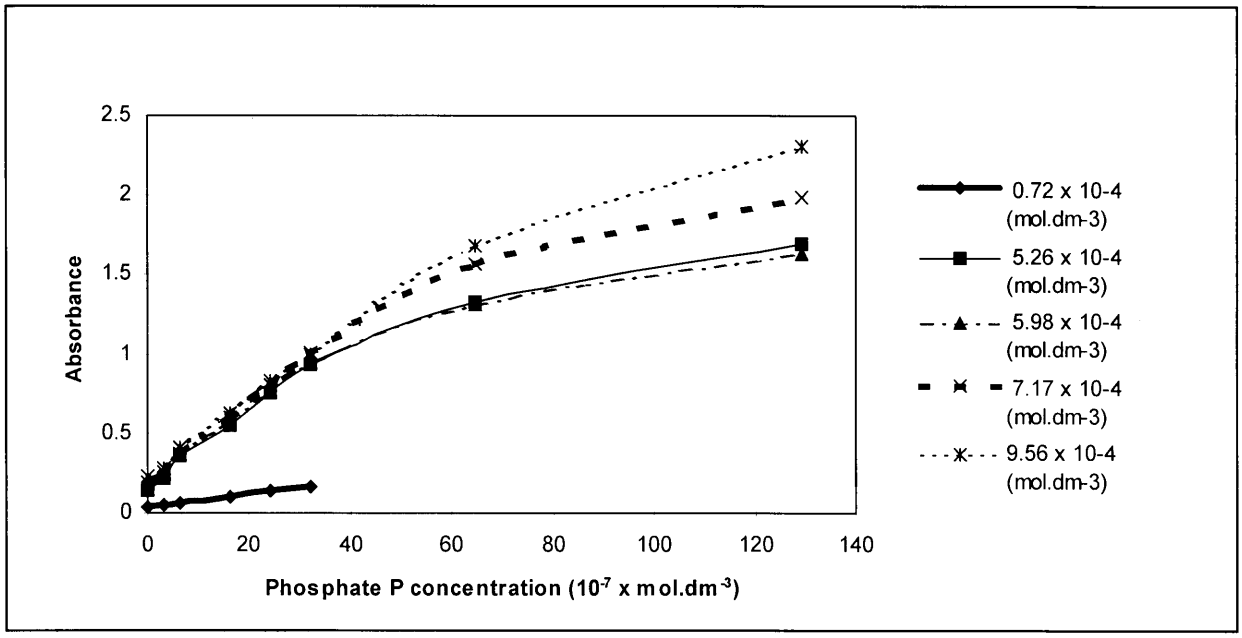

Figure 6.34: Relationship between malachite green concentration and absorbance.

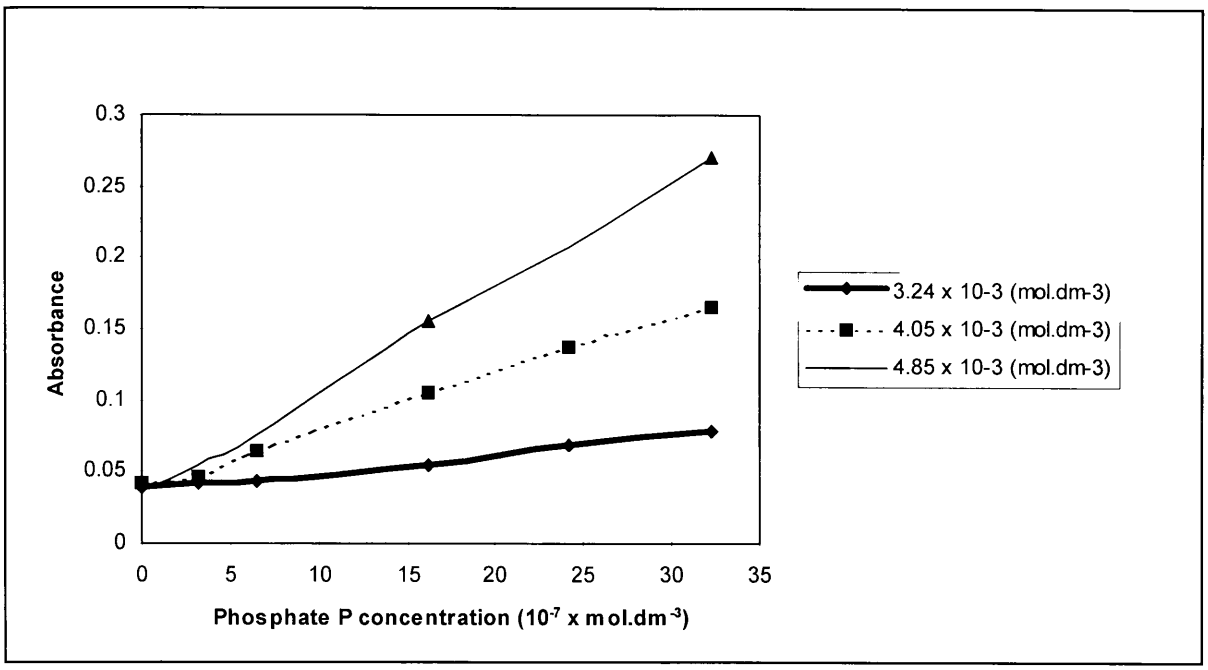

Figure 6.35: Relationship between molybdenum concentration, phosphate concentration and absorbance

Increased H_2SO_4 concentration lead to higher absorbance and an increased range over which the graph was linear. Figure 6.36 shows the absorbance as a function of H_2SO_4 concentration.

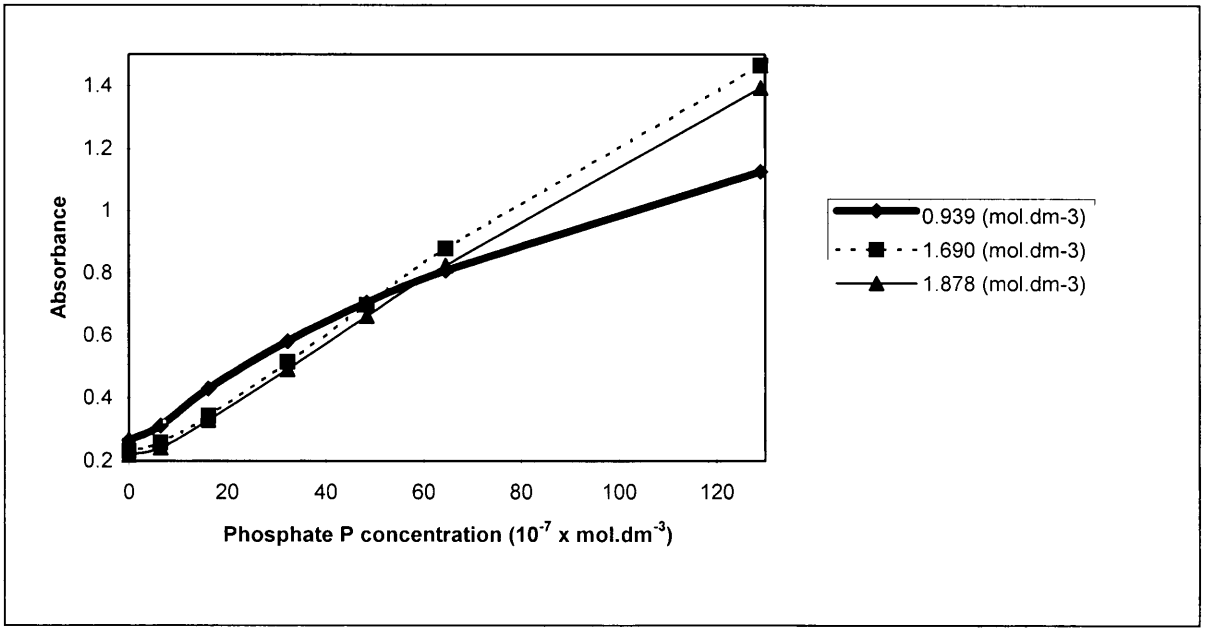

Figure 6.36: Absorbance as a function of H_2SO_4 concentration and phosphate concentration

Malachite green, molybdate - ion and H_2SO_4 were all optimised during simplex optimization.

A slightly acidic carrier stream gave better responses than one containing simply distilled water. The carrier stream contained H_2SO_4 in the concentration 0.1315 mol. dm^{-3}.

6.3.3 The simplex optimization

The simplex optimization was twice restarted due to changes in the interface. The eight previous best response co - ordinates were used to form the corner points of the new original simplex.

Table 6.8 shows the co - ordinates of the original simplex and the boarder values of the factors. Table 6.9 shows the simplex optimization.

Table 6.8 The co - ordinates of the original simplex and the boarder values of the factors

	Nu	C[$(NH_4)Mo_7O_{24}.4\ H_2O$] mol.dm^{-3} x 10^{-1}	C(MALACHITE GREEN) mol.dm^{-3} x 10^{-4}	C(H_2SO_4) mol.dm^{-3}	LOOP VOLUME x 10^{-6} dm^3	COIL LENGTH m	PUMP SPEED CARRIER cm^3.min^{-1}	PUMP SPEED REAGENT cm^3.min^{-1}	RESPONSE ABSORBANCE
minimum		0.03236	0.8563	0.5635	20	0.20	0.20	0.01	
maximum		0.1456	4.303	2.066	400	5.00	5.00	3.80	
	1	0.06068	1.674	1.390	340	1.30	3.50	0.74	0.1961
	2	0.06618	2.113	1.315	312	1.00	3.06	0.53	0.1953
	3	0.05664	1.913	1.334	290	0.70	3.00	0.42	0.1650
	4	0.08576	2.921	1.315	298	1.14	3.30	0.64	0.2094
	5	0.07800	2.596	1.345	268	0.87	3.27	0.52	0.1921
	6	0.07201	2.907	1.349	310	0.92	3.13	0.51	0.1980
	7	0.07169	2.439	1.360	308	0.90	3.10	0.48	0.1938
	8	0.06861	2.247	1.352	291	0.94	3.20	0.55	0.1935

Table 6.9 The simplex optimization

TYPE OF SYMPLEX MOVEMENT	C[$(NH_4)_6$ $Mo_7O_{24}.4\ H_2O$] mol.dm^{-3} x 10^{-1}	C(MALACHITE GREEN) mol.dm^{-3} x 10^{-4}	C(H_2SO_4) mol.dm^{-3}	LOOP VOLUME x 10^{-6} dm^3	COIL LENGTH m	PUMP SPEED CARRIER $cm^3.min^{-1}$	PUMP SPEED REAGENT $cm^3.min^{-1}$	RESPONSE ABSORBANCE
1ST	0.08706	2.768	1.360	318	1.32	3.49	0.71	0.2100
	0.1023	3.194	1.371	332	1.63	3.67	0.86	0.2203
2ND SM	0.07266	2.257	1.356	358	1.37	3.29	0.70	0.2002
3RD SM	0.08318	2.606	1.349	354	1.42	3.39	0.72	0.2087
	0.08334	2.462	1.337	350	1.61	3.57	0.86	0.2032
5TH SM	0.09386	2.888	1.390	357	1.68	3.75	0.92	0.2027
6TH SM	0.1087	3.677	1.315	334	1.49	3.38	0.75	0.2132
7TH SM *	0.1079	3.328	1.349	371	2.03	3.83	1.05	0.2221
	0.1259	3.792	1.349	401	2.59	4.17	1.31	0.2080
	0.1174	3.768	1.337	327	1.78	3.82	0.96	0.2170
	0.1029	3.385	1.288	319	1.47	3.38	0.75	0.1900

Simplex optimization was stopped because there appeared to be no significant increase in response. Factor optimization was done with the seventh simplex move as the starting point, the corner point marked with an asterisk.

6.3.4 The factor optimization

Factor optimization of the coil length is depicted in figure 6.37. From the graph it could be seen that there was a broad maximum but that the shorter coil length (1.63 m) gave a slightly higher peak height than the longer coil length found to be the optimum in the simplex optimization.

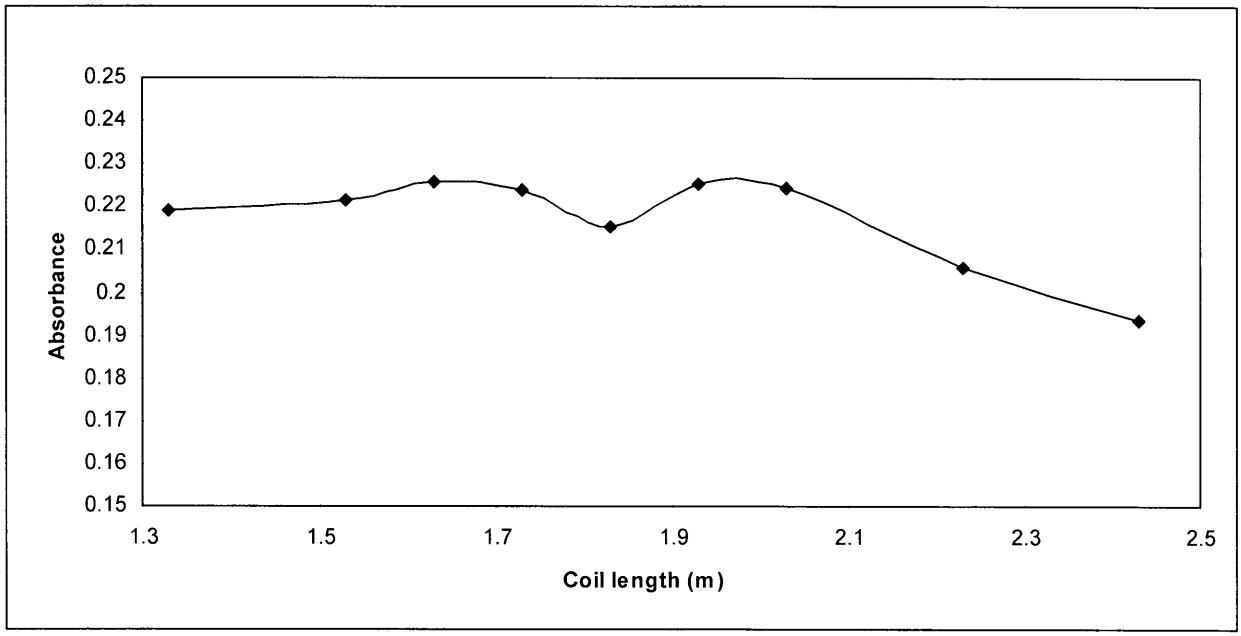

Figure 6.37: Factor optimization of coil length.

Loop volumes of 345 x 10^{-6} dm^3 and higher did not have a very great influence on the response. The differences seen were probably not significant. 393 x 10^{-6} dm^3

was chosen since it gave a slightly higher response than the simplex optimised loop volume of 371 x 10^{-6} dm^3. The effect of loop volume on response is illustrated in figure 6.38.

Figure 6.39 illustrates the response as a function of the pump speed of the carrier stream. There was no significant difference in the response for a pump speed of

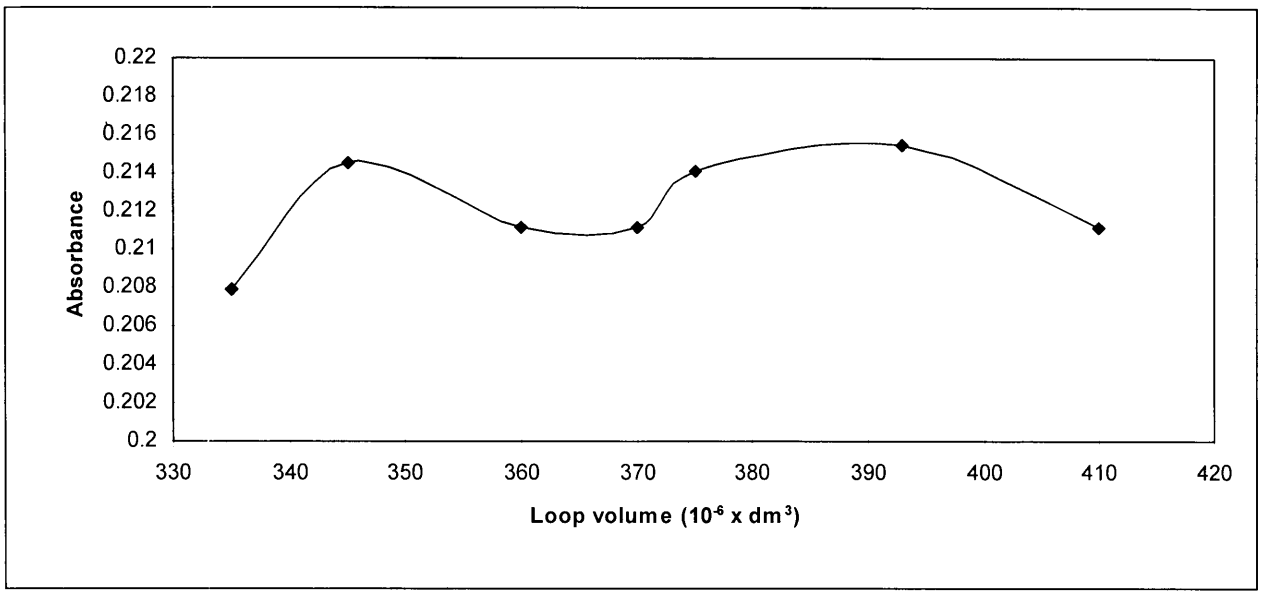

Figure 6.38: The effect of loop volume on response.

2.90 to 3.83 $cm^3.min^{-1}$. The pump speed optimised during simplex optimization namely 3.83 $cm^3.min^{-1}$ gave a lower baseline - to - baseline time and was therefore chosen to be used during the evaluation of the method.

Factor optimization of the pump speed of the reagent showed that a lower pump speed of 0.80 $cm^3.min^{-1}$ gave a better response than the simplex optimised value

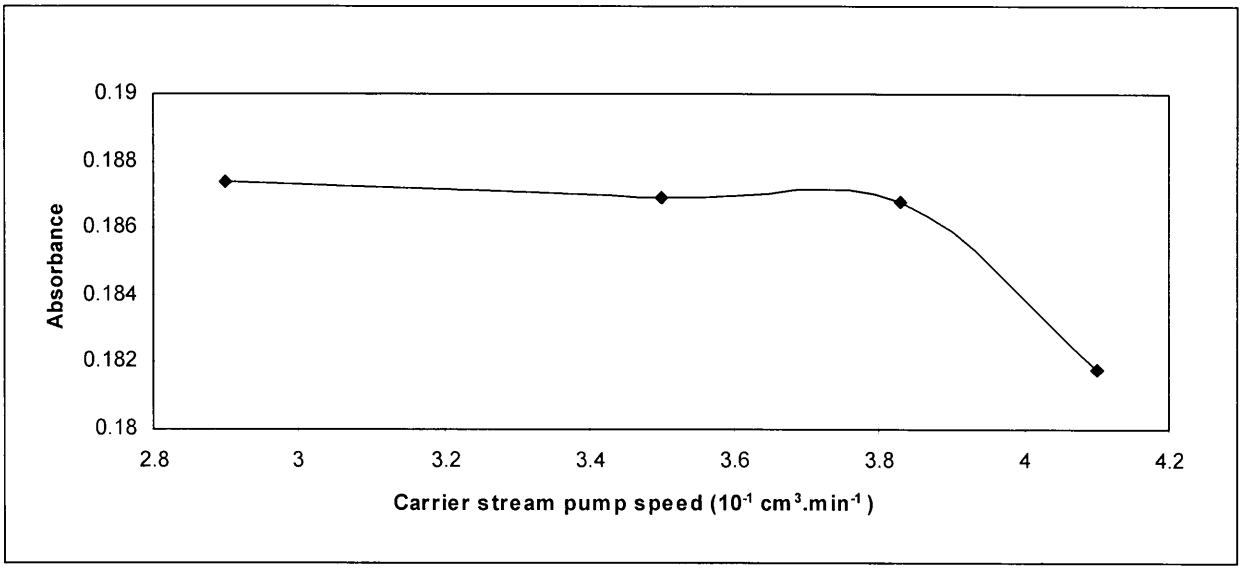

Figure 6.39: Response as a function of carrier stream pump speed.

of 1.05 $cm^3.min^{-1}$. This is illustrated in figure 6.40. It would appear as if this simplex optimization did not reach the true optimum.

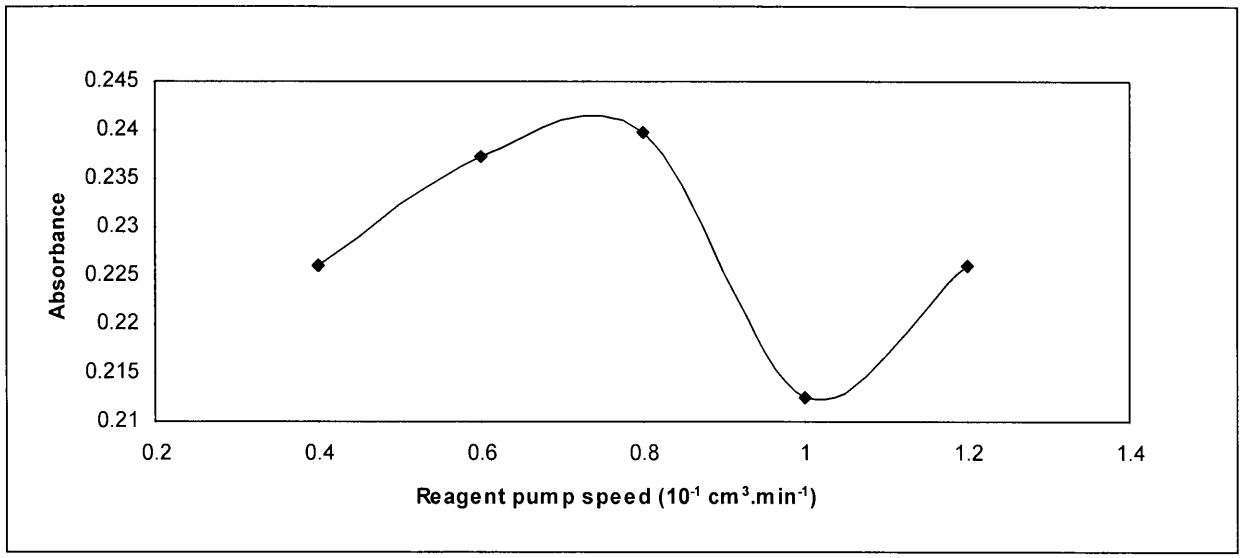

Figure 6.40: Absorbance as a function of reagent pump speed

Absorbance as a function of the H_2SO_4 - concentration in the reagent is given in

figure 6.42. It showed that a lower acid concentration (1.3148 mol.dm^{-3}) than the concentration found to be the optimum value in the simplex optimization (1.349 mol.dm^{-3}), was more favourable. This also helped strengthen the idea that the optimum conditions were not found during this simplex optimization.

The malachite green concentration that was found to be the optimum in the simplex optimization was also found to be the optimum during factor optimization. The influence of the malachite green concentration on the absorbance is illustrated in figure 6.42.

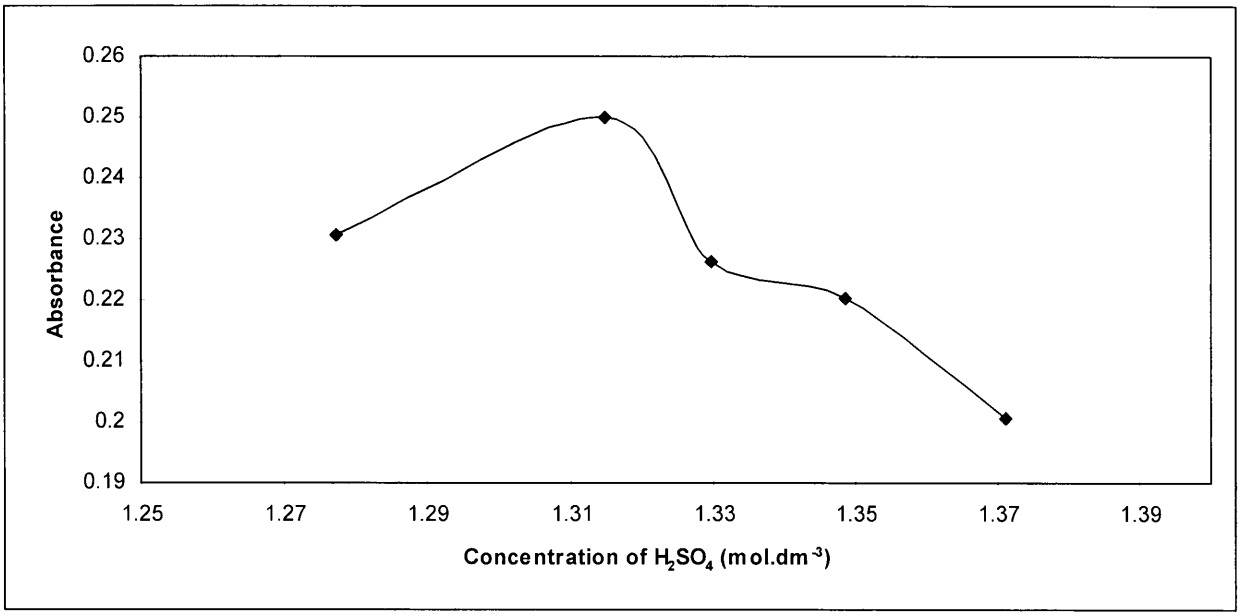

Figure 6.41: Absorbance as a function of H_2SO_4 concentration.

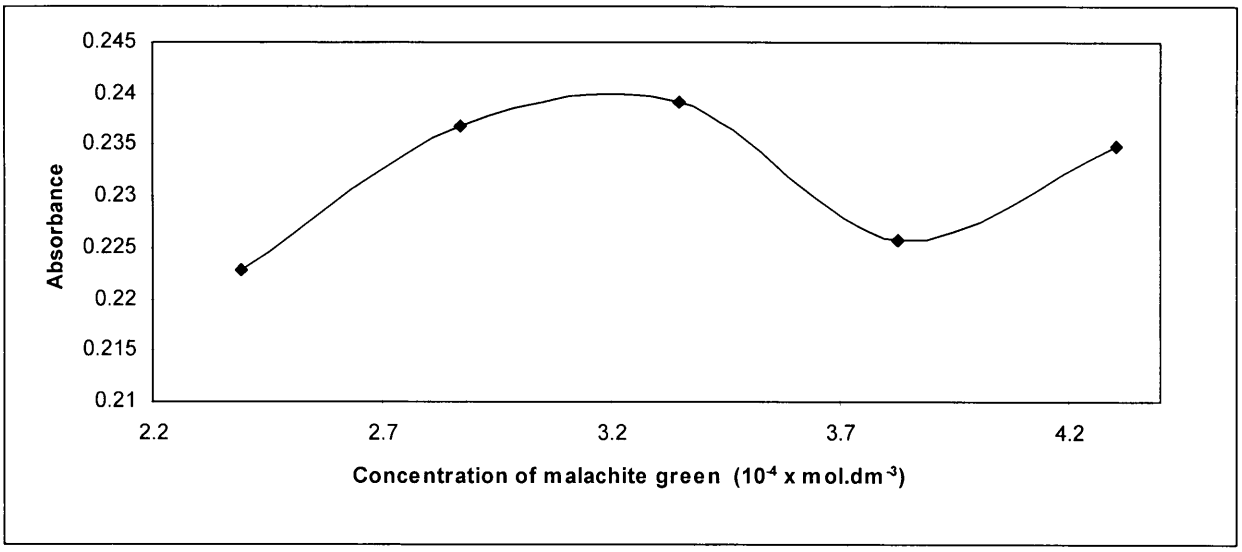

Figure 6.42: Influence of malachite green concentration on absorbance.

During factor optimization it was found that the absorbance continued to increase with increasing molybdate - concentration, but that after a certain level of molybdate concentration the repeatability became unacceptably poor. A slightly higher concentration than the simplex optimised value was chosen. This concentration was 0.01392 mol.dm^{-3}. This information is depicted in figure 6.43.

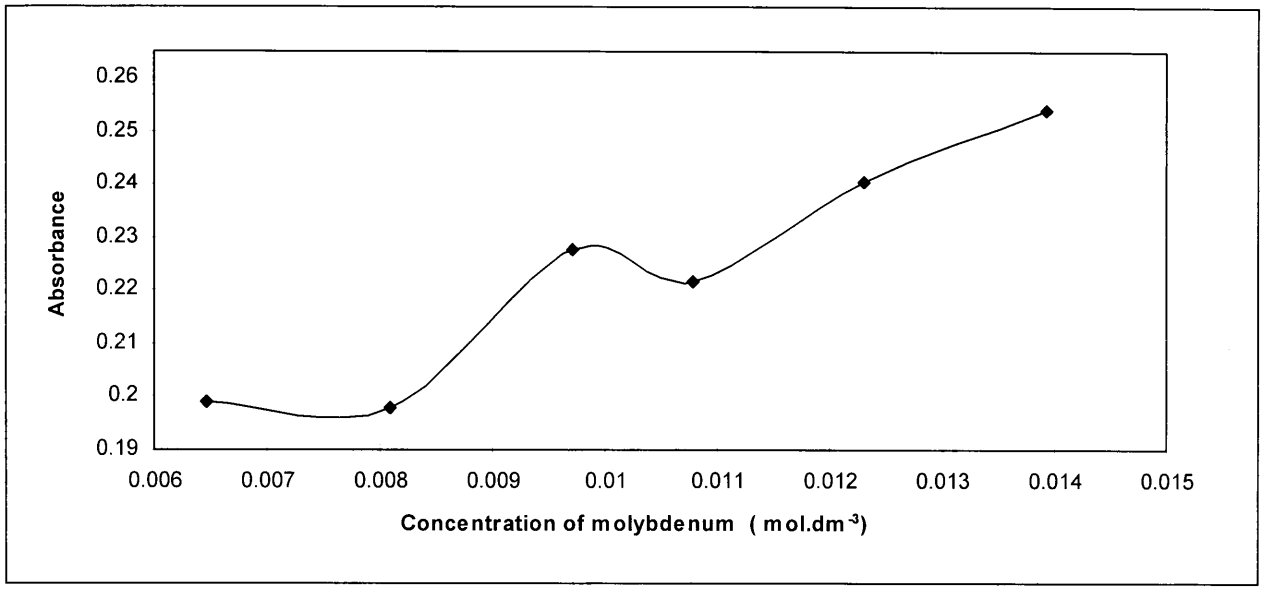

Figure 6.43: Absorbance as a function of molybdenum concentration.

It seems that neither simplex optimization, nor factor optimization could improve the response to a great extent. It also appears that simplex optimization did not find the optimum co - ordinates, since factor optimization changed the values of the co-ordinates of all but two of the factors. A table of the values of some of the factors is given in Table 6.9 and a diagram of the final flow injection system is given in figure 6.44.

Table 6.9 The optimised values for some of the factors

FACTOR	CHARACTERISTICS
SAMPLE LOOP VOLUME	393×10^{-6} dm^3
TEMPERATURE	50°C
C (MALACHITE GREEN)	3.347×10^{-4} mol.dm^{-3}
C $(NH_4)_6 Mo_7O_{24}.4 H_2O$)	0.01392 mol.dm^{-3}
C (H_2SO_4) IN REAGENT	1.3148 mol.dm^{-3}
C (H_2SO_4) IN CARRIER	0.1409 mol.dm^{-3}

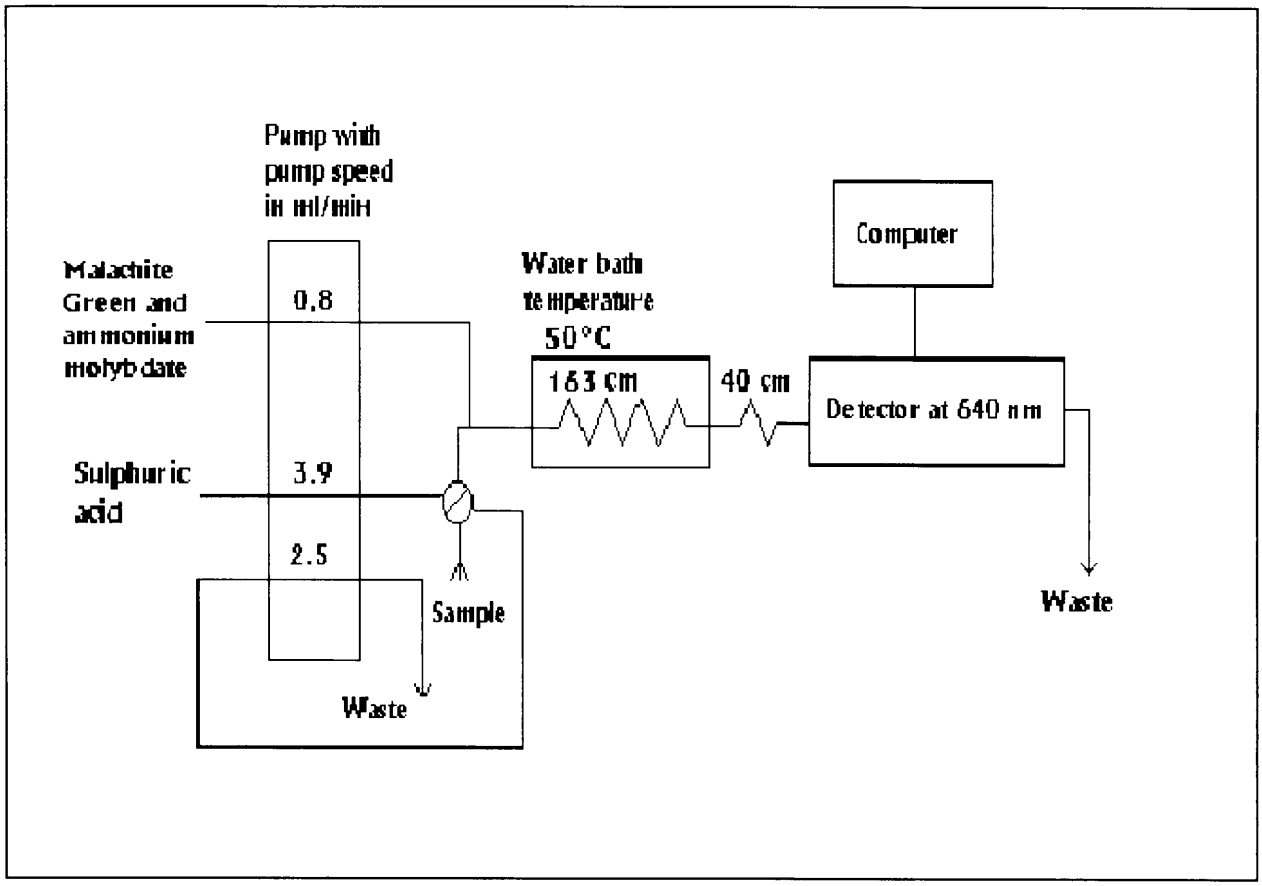

Figure 6.44 The final flow injection system

6.3.5 The evaluation

The method was linear up to 3.229 x 10^{-6} mol.dm^{-3} P (100 mg.kg^{-1} P). The correlation coefficient (r^2) of the graph was 0.9999 and the equation describing the function was y = 351106.4x + 0.4277. Figure 6.45 show the absorbance as a function of the phosphate - P concentration.

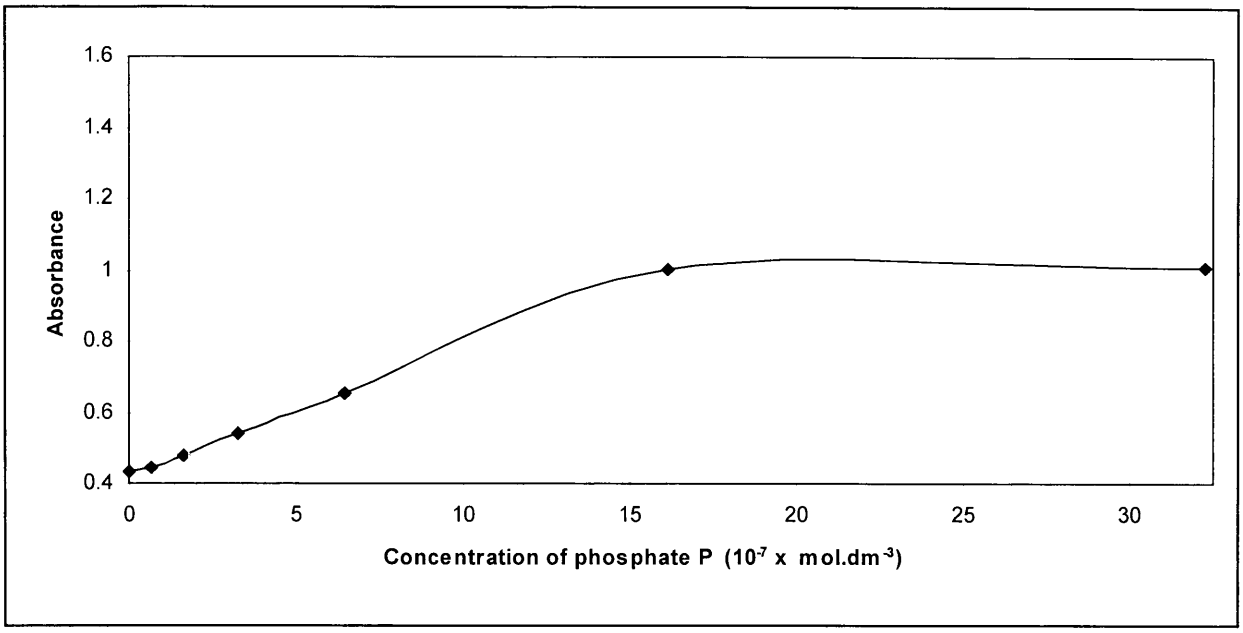

Figure 6.45: Absorbance as a function of the phosphate - P concentration.

The recovery of phosphate - P on unfiltered bore hole water (which had to be diluted fourfold with distilled water to fall within the linear range of this method) for 3.229×10^{-7} mol.dm^{-3} P (10 mg.kg^{-1} P) was 98.1 %. There is no detectable carry - over in this method. The repeatability of the method for a phosphate - P concentration of 6.457×10^{-7} mol. dm^{-3} is $\pm$ 2.2×10^{-8} mol.dm^{-3}. The detection limit of this method is 7.9×10^{-8} mol.dm^{-3} P (2.4 mg.kg^{-1} P). The sample throughput is 80 samples per hour.

Figure 6.46 shows the interference effect of the ion $P_2O_7^{4-}$ on the phosphate analysis. It was clear that the conditions of this method resulted in almost complete hydrolysis of the $P_2O_7^{4-}$ - ion. Hg (II) had no effect on phosphate analysis when using this method. Very low (3.5) and very high (10.5) pH - values had a positive

interference effect on phosphate - analysis. Water samples from boilers could have

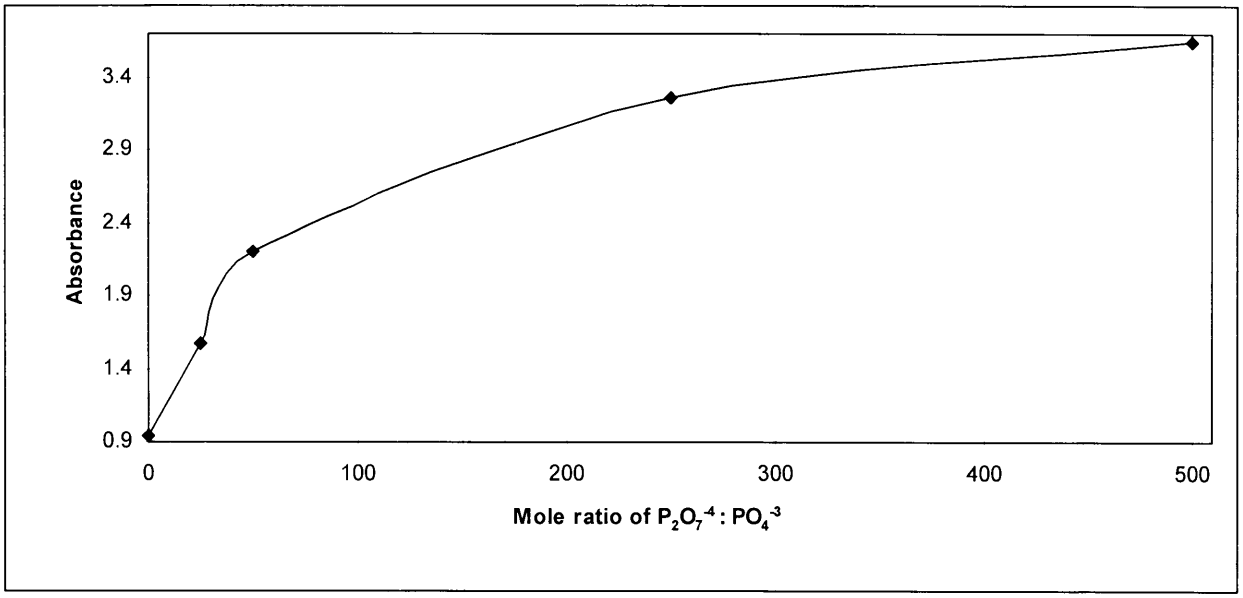

Figure 6.46: The interference effect of the $P_2O_7^{4-}$ ion on the phosphate analysis.

such high pH values and waste water samples from factories could have such low pH values. The pH of these samples would have to be adjusted before analysis with this method could be undertaken.

6.4 Bibliography

1. Ruzicka J, Hansen EH (1988) **Flow injection analysis, Second Edition.** John Wiley. New York.
2. Personal communication with Prof. JF van Staden. University of Pretoria, Department of Chemistry.
3. Painton CC, Mottola HA (1981) **Anal Chim. Acta. 53:** 1713
4. Painton CC, Mottola HA (1984) **Anal Chim. Acta. 158:** 67
5. Vanderslice JT, Stewart KK, Rosenfeld AG, Higgs DJ (1981) **Talanta. 28:** 11

CHAPTER 7

CONCLUSION

It were possible to develop simple, inexpensive methods for the determination of phosphates in water with the aid of flow injection analysis and modified simplex optimization. The detection limits for two of the three methods obtained were lower or close to the detection limits of similar methods obtained from the literature that were not optimised with simplex optimization [1,2]. However the detection limits were not lower than methods obtained from the literature that involved preconcentration or solvent extraction or made use of special apparatus like LCC's or ICP's.

Modified simplex optimization proved easy to work with and functional even though it was clear that it did not obtain the optimum conditions in one of the methods. It is possible that for an optimization with so many variables optimization was stopped too soon or that more contractions and expansions of the simplex was necessary to be able to obtain the optimum. Using only one characteristic like detection limit to optimise might mean that other things like linearity was compromised on. It might also mean that in order not to

compromise on a factor like linearity some of the field won by the modified simplex optimisation must be given up again.

Polyphosphate interfered with all three methods to a great extent. This means that in order to determine only orthophosphate with these methods a separation of the species would have to be made beforehand with an apparatus like an ion - chromatograph.

Modified simplex optimization and flow injection analysis are both useful and powerful tools in the development of new methods for routine analysis, but it must be borne in mind that if not used correctly they might fail in their purpose all together.

7.1 Bibliography

1. Janse TAHM, Van der Wiel PFA, Kateman G (1983) **Anal. Chim. Acta.** 155: 89
2. Tecator 1983 ASN 60-01/83